A vehicle dynamics model for torque vectoring during a turn.

Anusha Mangal

A thesis

submitted in partial fulfillment of the

requirements for the degree of

Master of Science

University of Washington

2018

Committee:

Brian Fabien, Chair

Swayer Fuller

Ashish Banerjee

Program Authorized to Offer Degree:

Mechanical Engineering

University of Washington

Abstract

A vehicle dynamics model for torque vectoring during a turn.

Anusha Mangal

Chair of the Supervisory Committee:
Dr. Brian Fabien
Department of Mechanical Engineering

The focus of this research work is to develop a comprehensive vehicle dynamics model which addresses the coupling between longitudinal, lateral and vertical dynamics. Besides providing information about the translational and rotational variables, both under transient and steady state condition, it also aims to track changes in Euler angles with time which are used in most of the navigation algorithms. This research work strives to be a substantial improvement over the classical and much referred Bicycle Model for lateral dynamics by addressing coupled nature of translational and rotational dynamics; includes the effect of aerodynamics; considers non–linear nature of tire mechanics; has suspension modeling; accounts for lateral and longitudinal load transfers and last but not the least is able to simulate transient dynamics too and informs about other states of vehicles assumed constant or neglected in the former model.

CONTENTS

LIST OF FIGURES

ACKNOWLEDGEMENTS

I would like to extend sincere gratitude to my thesis chair, mentor and advisor Professor Fabien. He is one of those rare teachers who give a student many chances to prove themselves before analyzing them completely. It is hard to find a Professor who gives such critical insights, valuable feedbacks but at the same time does not curb the freedom of a student to explore and then consecutively learn. His sound knowledge of dynamic modeling of systems in general and vehicles in particular has been very helpful for completing my thesis in a form I had always dreamt of. Apart from supporting me academically, he was also, a strong pillar of emotional support, always motivating me to give my best. Without his enthusiastic support and wise words, I wouldn't have been able to complete my thesis, is not an overstatement.

I would also like to convey my regards and heartfelt indebtedness to Prof Swayer Fuller and Prof Ashish Banerjee for serving as my review committee members despite their busy schedule and also for promptly answering to my requests on such a short notice.

I am highly obliged to Miss Laura Prange, who too was a student under Dr. Brian Fabien and had successfully completed a thesis on Vehicle Dynamics in the year 2017. She is a huge support. This acknowledgement would remain incomplete without a sincere mention of the EcoCar3 Team. My teammates have been very cooperative and helped me out whenever I ask for it. I would like to appreciate the UW staff, my program academic advisor Wanwisa Kislang for always answering my queries. Last but not the least a kind and special mention for my family and friends.

DEDICATION

I dedicate this thesis to my brother and best friend Ishan Mangal.

Chapter 1. INTRODUCTION

1.1 BACKGROUND

Electric Vehicles were invented back in Nineteenth Century but gained popularity recently. This can be attributed to the growing concern for the environment and willingness to study and develop clean and sustainable technologies. This was further accelerated because of the ever increasing oil prices clubbed with an increased access to electricity. Development of light batteries having less charging time and more storage capacity is real breakthrough in this direction (Husain, 2003). Many vehicles manufactures, today, are exploring this field and strive to design and manufacture electric vehicles that are more stable and controllable not to mention more efficient too. Some of these electric vehicles just like the Eco-Car at University of Washington, Seattle are employing electric motors on the driven wheels to drive the car forward. This requires the knowledge of torque to be supplied to these motors for different driving maneuvers and conditions. Naturally, there is a need for mathematical models which can simulate the dynamics of the vehicle under study, encompassing all the influencing factors and their outputs. There exist mathematical models for dynamics of cars as such but they are either customized for the vehicle under study or are not very comprehensive. When a proper mathematical model doesn't exist one cannot come up with a good control algorithm which in turn deteriorates the run time performance of the vehicle. This research aims to develop a mathematical model which incorporates the physics and dynamics of the working of a vehicle as accurately as possible and includes as many governing factors as it can to simulate the behavior of the car. The second step then is to develop a control strategy to enhance the present performance and monitor the inputs and outputs to the system especially the torque to be distributed between the inner and outer wheels of the car while taking a turn keeping in mind the different scenarios under which a car may operate.

Why Electric Torque Vectoring is required?

The conventional cars have mechanical differentials which are used to give the inner and outer wheels of a vehicle different torque values during a turning maneuver. This distribution is necessary because the outer and inner wheels move at different speeds during a turn. The mechanical differential allows for equal torque for straight paths and unequal torque for curved paths. However, they do not always distribute torque in an ideal manner. If the road conditions are icy or otherwise undesirable, torque distribution from the mechanical differential could cause the vehicle to behave erratically (Jazar, 2008). With independent electric motors, torque vectoring becomes an important method to improve vehicle handling. Due to the improvement of both motor design and control technology, modern configurations can be motorized wheels, which means wheels are connected to the motors (Kato and Sawase, 2011) Considering that the torque/rotation-speed curve of an electric motor is almost perfectly adapted to the resistance-torque/speed curve of an electric vehicle, the conventional heavy gearbox can be superseded by an electronic differential (ED). With this approach, not only the overall mass is reduced, but also the performance of the EV improves significantly due to the fast response time of the electric motors. An electronic differential can control each of the wheel speeds to satisfy the motion requirements when the EV encounters different conditions, such as curvilinear trajectory or a lane change.

Why Electric Torque Vectoring is preferred?

There are various methods of controlling the torque values given to each wheel in the process of torque vectoring but the Eco Car uses an electrical one. Consider a vehicle with two electric motors which drive two rear wheels independently. In order to move in a straight-line path, there needs to be a controls algorithm to send signals between the motors and make the wheels move in harmony. This system has several advantages. Although the system may seem unstable at first, it has the capability to be more stable than a traditional vehicle with a mechanical differential. For example, road surface sensors can be added to the front of the test vehicle to allow the electric vehicle to sense a change in road condition and relay the information to a controls algorithm, which can give the rear wheels independent responses. This can cause the system to follow a more accurate path. An additional factor in favor of an electric torque vectoring system is that frictional clutches can be avoided, and less energy will be wasted as heat (Wong, 2008). This will also avoid heavy gear box reducing the weight of the vehicle.

Why Vehicle Dynamic Model is required?

A comprehensive vehicle dynamic model is required to understand different facets of vehicle performance which have a large impact in different scenarios. These facets or performance characteristics are listed next.

1. Passenger Safety

This aspect addresses the safety of the vehicle occupants from the perspective of dynamics rather than improving crash resistance. It helps in analyzing how a vehicle behaves when it takes a turn and brakes or accelerates and inform about the over/under steer characteristics of the car.

2. Passenger Comfort (Ride Characteristics)

Passenger comfort is dictated by the ride quality of the vehicle which is in turn affected by subsystems which affect vertical dynamics such as suspension vibration damping features and degree of chassis vertical pitch.

Also, tolerable longitudinal/lateral acceleration levels are included in this characterization.

3. Improved Driver-Vehicle Interaction (Handling)

Qualitative and quantitative study of stability and control quality together with robust feedback mechanisms dictate this performance parameter.

.

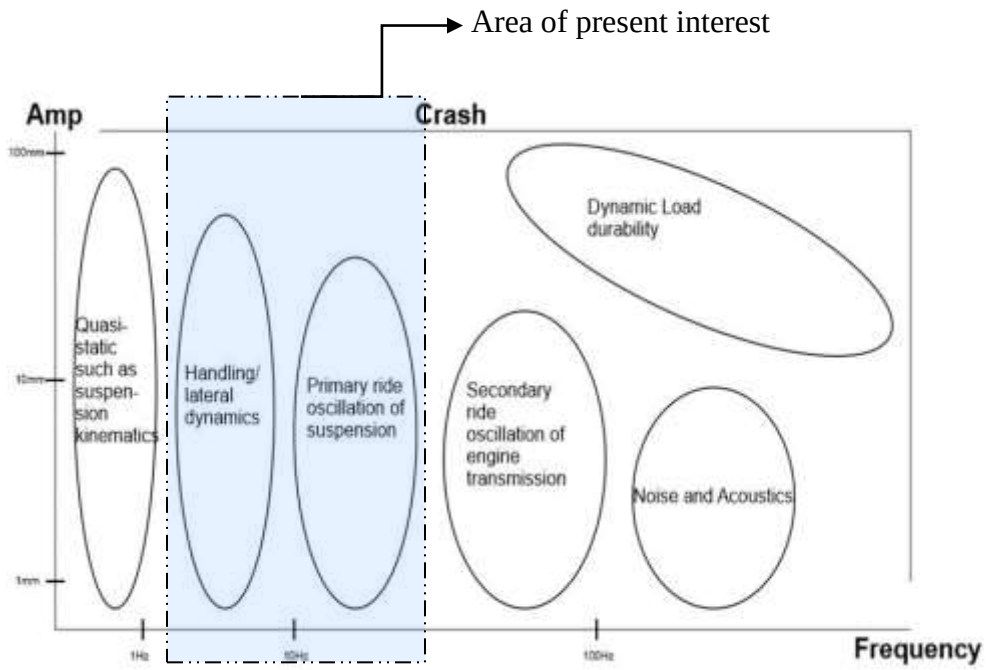

Figure 1.1: The classification of dynamic parameters of a vehicle w.r.t. frequency of the oscillations and their amplitude.

The above figure shows and highlights the area of interest of the thesis. The figure plots the states of vehicle against the amplitude and frequency of oscillations of those variables. All the states of present interest included in the thesis. These states or variables help in characterizing the ride characteristics or handling parameters and are highlighted as shown.

1.2 SCOPE

The existing vehicle dynamics models in the contemporary literature provide an excellent background work for the given thesis (Martino, 2005). The models studied give a firsthand insight in the dynamics of the vehicle and capture many important parameters to be considered. With the help of these models the dynamics of a vehicle can be understood to a great extent and the work done by previous researchers in analyzing these models is indeed commendable. This thesis work is intended to build over the work done till date and add improvisations to it. Many factors can still be incorporated in these models to make them more comprehensive and accurate so that they imitate the real life scenarios to a greater accuracy. The proposed plan is to start eliminating the assumptions and work towards modeling the dynamics till a mathematical model with desired accuracy is achieved.

Two-Wheel Model or the Bicycle Model

The simplest way to model a vehicle is to assume that the two front tires behave roughly the same and condense the effect of the two tires into one modeled tire. The rear tires can be treated in a similar fashion. This gives a vehicle with one tire in the front and one in the rear. However, this model is based on many assumptions listed below:

Assumptions in the Two Wheel Model

- No rolling considered.
- Suspension mechanics not accounted for.
- Does not consider the effect of aerodynamic forces.
- Model assumes that a constant forward velocity is maintained by the vehicle.
- Model assumes tires behave linearly.
- No lateral/longitudinal load transfer accounted for.

Four-Wheel Model

This model considers all the four wheels of the car and also the slip angles at these wheels individually.

Assumptions in the Four Wheel Model

- No Rolling Considered.
- Suspension mechanics not accounted for.
- Aerodynamic forces are considered but a fixed aerodynamic coefficient is used for calculation.
- Longitudinal dynamics is studied here but the effect of longitudinal dynamics is not considered in the lateral direction. In other words the model is decoupled.
- Model assumes tires behave linearly.
- No lateral/longitudinal load transfer accounted for.

Two Wheel Model with Roll

Vehicle roll is considered in this model but other assumptions of the two wheel and four wheel model still need to be studied.

These assumptions have to removed and therefore lay the foundation of work to be done in this thesis.

(I) For instance, say, suspension modeling and its incorporation in the mathematical model can be one of the initial steps to come up with an improvised version of the models previously studied. We know that in reality, suspension is extremely important in determining how the car will behave and makes a big impact on rider comfort and hence has to be considered.

(II) Similarly, tire modeling also needs to be included. It is in fact, one of the most difficult elements to add to a vehicle model, because the interaction between the road surface and the tire involve many factors such as roughness, tire pressure, contact surface, tire type, and many more. But the importance of including it in the mathematical model supersedes the level of difficulty to

be encountered in modeling it and hence has to be incorporated. It is imperative to know the regions in which a linear tire model may be accepted or not accepted. If analytical tire modeling can be included then the model will be of far more use to researchers and vehicle dynamists.

(III) The aerodynamics has to be modeled and proper determination of coefficients of drag have to be determined. A general aerodynamic coefficient cannot be used. Suppose the vehicle has certain sideslip, then the difference in drag on the left and right hand side can result in a moment and produce a yaw. All these factors have to be accounted for.

(IV) While turning there is a transient phase when the car decelerates and corners followed by a steady state of just cornering which is again lead by a transient phase wherein the vehicle accelerates and comes out of the corner. In the Bicycle Model, it is assumed that the longitudinal speed does not change while cornering, which is not what happens in real life. These transient states have to be studied and modeled because the dynamics in longitudinal and lateral direction is coupled and interdependent.

(V) Another perspective to the above models can be gained by considering the effect of rolling in a four wheel model. A bicycle model is analyzed for rolling dynamics but how this phenomenon is manifested in a four wheel car is something to think about.

1.3 JUSTIFICATION FOR THE RESEARCH WORK UNDERTAKEN

A natural question that needs to be addressed before proceeding any further is whether the work is novel and if yes what is its practical applicability and usage value. Indeed, there are many mathematical models for vehicle dynamics out there in literature. But as explained in the previous sections they are based on several assumptions to make the model simpler. Even if analytical modeling of the physics is possible, the inputs to system need to be determined and sometimes they are not easily measurable because of lack of resources and technological infeasibility. But there are software like CARSIM available in the market which give in-depth information about various parameters which implies there are algorithms existing for sure. Is the work still justified? This is a valid question and needs to be answered.

Yes, the work is justified because of two main reasons. First of all, there might be proprietary models available to the concerned industry people but are not published in literature and are not readily available. Secondly, even though the software is giving us the right results we don't know the algorithm behind it. Therefore, this work would be able to bridge that gap and would inform students, academicians and industrials alike. Also, the purpose of undertaking this thesis was to perform torque vectoring for the independent motors running the wheels. The software would give results pertinent to a particular input scenario but would not be directly helpful in building a control algorithm if we don't have the dynamic modeling. This research work also has educational applications and helped the author understand a lot about tire and vehicle mechanics which would not have been possible to such a great extent had there been sole dependency on software only. Hopefully it will help others too in a similar fashion.

1.4 OUTLINE

The thesis starts with the background and the scope of the work done. These have been addressed in the first two sections of ‘Introduction’. The next chapter ‘Literature Theory’ is intended to give a beginner in vehicle dynamics an abridged source to get started on and covers the basic physics and makes him/her abreast of the jargons used in the field. The physics behind decoupled longitudinal & lateral dynamics has been focused on and lays the foundation for comparatively complex vehicle dynamic models. The next section focuses on perturbation theory which forms one of the most crucial aspect of this thesis work. Tire models to be included with vehicle models have also been covered in some detail. Following this is the chapter ‘Methodology’ which explains the structure of the built algorithm in great detail and the generated results too. The results are verified from simulation on CARSIM and match appreciably. The chapter ‘Conclusions and Discussions’ provide the necessary closure to the work together with the future scope of the undertaken project.

Chapter 2. THEORETICAL FRAMEWORK

2.1 STRUCTURE OF A VEHICLE DYNAMIC MODEL

Any vehicle dynamic model, regardless of its accuracy, comprehensiveness and robustness should have certain features which decide its usage and application scenarios. These are mentioned below:

1. Inputs to be provided
    - Steering Angle
    - Steering Rate
    - Acceleration/Braking Pedal Force
2. The Output/ Variables or Response.
    - Acceleration
    - Velocity
    - Braking Distance
3. Feedback Algorithm for the driver.
4. The quantification of effects of the response on the comfort level of the occupants demands that mathematical model should capture maximum driving dynamics.

2.2 PERFORMANCE METRICS

Knowledge of how a vehicle performs during cornering or acceleration and braking is of great importance. Stability and control in steady state condition or transient conditions are also needed to characterize the performance of the vehicle. ISO defined tests such as the Single Lane Change, Double Lane Change, Pulse Test/Pulse Steer and Constant Radius Cornering help in characterizing the inputs for the built mathematical model (Milliken, 1995). This can enable us to study the dynamics by

simulating the mathematical model for straight-line –tracking, maneuverability, self-steering-behavior and oscillations et cetera.

2.3 AXIS SYSTEM

In order to quantify the motion of the system under consideration (here a vehicle) we need to define degrees of freedom as well as the frame with respect to which they would be measured and frames in which they can be represented. An inertial frame is a frame with no acceleration. Newton's Laws of Motion are valid only in an inertial frame. That is, if we want to apply Newton's Second Law of Motion to a moving body with respect to an axis fixed on it, we would get erroneous results. Therefore, we need a fixed frame of reference or a reference moving at a constant velocity having no acceleration. However, measuring DOF with respect to an axis system fixed to the body preferably at its' center of mass and hence moving with it is far easier from the point of practical measurements (Gillespie, 1992). Therefore, there are two axis system used in cases of rigid bodies under motion, Body Fixed Axis and Inertial Frame of Reference. The three DOF for translational motion and three DOF for rotational motion are with respect to the body fixed axis as shown in the figure. However, if we want to apply Newton's Law of motion we need to have an inertial frame of reference which is usually a right handed axis system fixed on ground. The DOF of freedom are represented in this frame. The concept of Euler angles is introduced to measure the rotational motion with respect to this inertial frame where the rotation along X axis of the inertial frame is termed as Phi-Φ, rotation along Y axis as Theta- θ and finally rotation along the Z axis is termed as Shi-Ψ.

Vehicle Axis System/Body Fixed Axis

A vehicle axis system has to be defined to account for the 6 DOF of the vehicle. There are three translational degree of freedom associated with the X, Y and Z axis. Also, there are three rotational degree of freedom associated with these axes. They are named as follows for convenience of understanding and reference:

1. Linear Velocities
    - X Axis: Longitudinal
    - Y Axis: Lateral
    - Z Axis: Vertical

2. Angular Velocities
    - X Axis : Roll
    - Y Axis: Pitch
    - Z Axis : Yaw

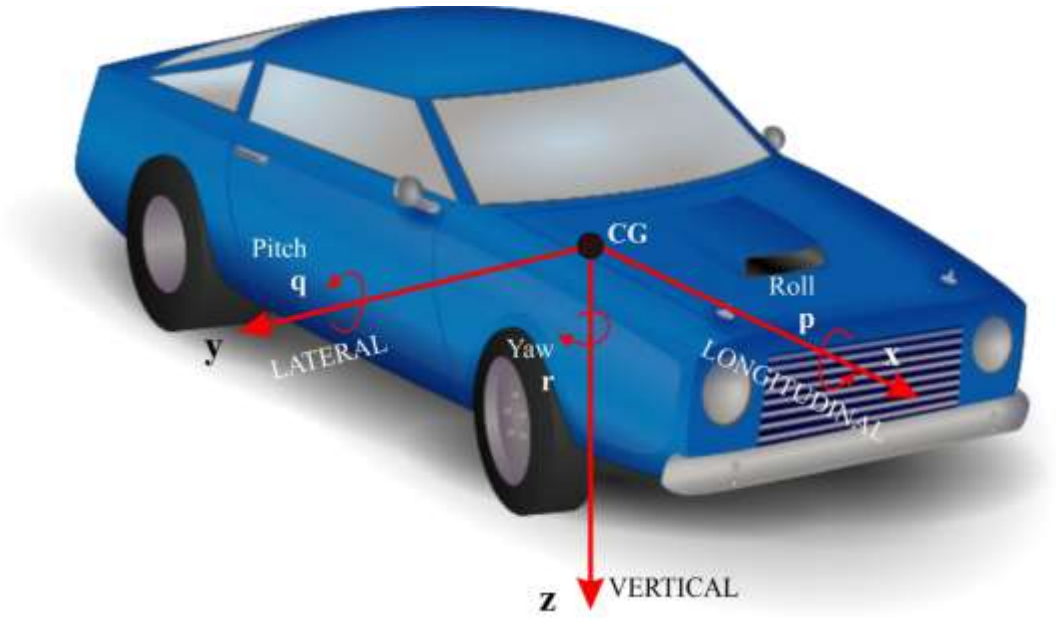

Figure 2.1: Vehicle Axis System

Inertial Reference Frame/Fixed Reference Frame

The three Euler angles are measured with respect to the three axes of the fixed frame where the rotation along X axis of the inertial frame is termed as Phi-Φ, rotation along Y axis as Theta- θ and finally rotation along the Z axis is termed as Shi-ψ as mentioned above.

Now, let us assume that the dynamics of the vehicle is decoupled in the three directions. This helps in simplifying the problem to a great degree and provides a basic insight in the mechanics of the system. To begin with, let us model the dynamics of the vehicle or automobile in the X direction/Longitudinal dynamics.

2.4 LONGITUDINAL DYNAMICS

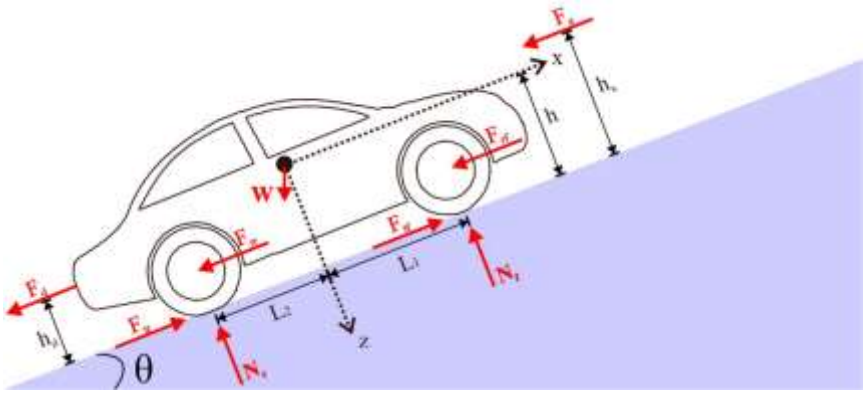

Figure 2.2: Forces acting on the vehicle

The above figure represents a vehicle of weight "*W*" on a road of gradient theta (θ). The forces acting on this vehicle are shown in red color and listed below:

Forces under consideration:

1) Aerodynamic Drag
2) Toeing Force from the attached vehicle.

3) Traction Force developed on the basis of Rear Wheel Drive/Four Wheel Drive/Four Wheel Drive.

4) Rolling Resistance on the four wheels.

5) Gravitational Force Component.

6) Ground Reaction at the rear and front wheels.

Before diving further into the longitudinal dynamics let us first understand what does Rolling Resistance mean? It isn't the frictional resistance to a rolling tire rather it is produced due to nature of the tire material (Dixon, 1996). Tires are made of elastomers and elastomers have a unique property: Visco-elasticity. Any material can be categorized into elastic, visco-elastic or plastic material. Elastic material can be modeled as a spring. Visco-elastic material can be modeled as a spring and a dashpot. Plastic material can be modeled as a spring and frictional element. These models can be used to characterize the material behavior and write constitutive stress-strain relationships to be used in the mathematical model. In a visco-elastic material, loading and unloading curves are not the same as in elastic material. The strain eventually comes to zero but after a certain period of time. The portion of graph between the loading and unloading curve gives the energy lost in the process. This is known as hysteresis.

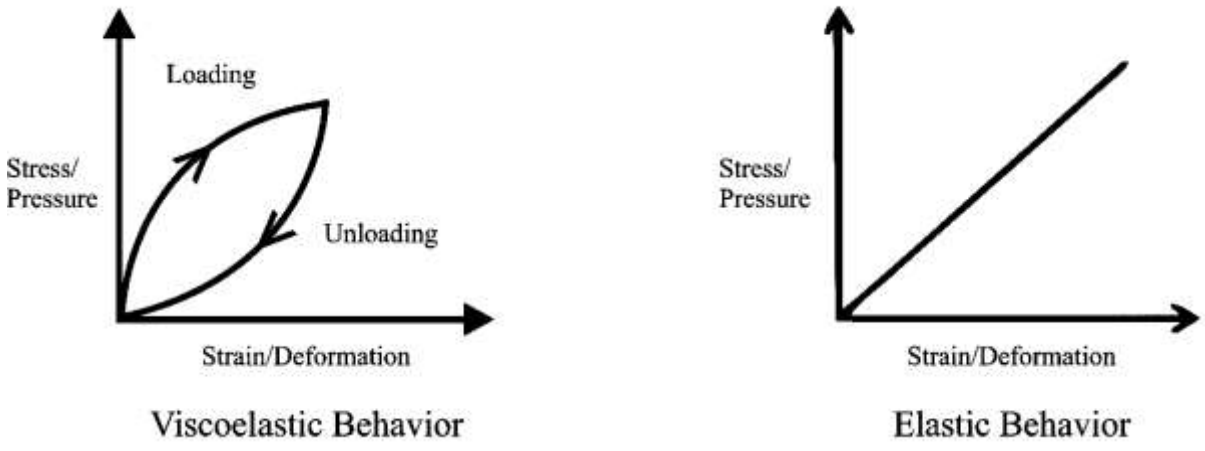

Figure 2.3: Hysteresis loss in viscous-elastic materials

We are considering pneumatic tires. Tires carcass has many threads made of visco-elastic rubber which undergo loading and unloading cycle as the tire rolls. Because of this loading/unloading cycle there is a hysteresis loss. The power of the engine compensates for the loss and this phenomenon is termed as the rolling resistance.

Contact patch of tire is formed due to interaction with the road. Ideally the contact pressure at the tire –road interface should be uniform and equal to the inflation pressure of the tires but it isn't because of bending of side walls of the pneumatic tires and rolling resistance. It is also not necessary that contact patch is formed only when tire rolls. Contact patch is formed when the vehicle is stationary too and has even and symmetrical pressure distribution.

2.5 INFLATION PRESSURE AND BENDING OF SIDE WALLS OF A TIRE

Tire has many grooves on its surface and these grooves are not supported. Local bending because of inflation pressure occurs and these grooves hence sack. Contact patch pressure is affected by these local bending forces. The other factor in uneven contact patch pressure distribution is the tire sidewall. Under pressure the sidewall also bends. Bending moment produced in these tire walls therefore affect the pressure on the contact patch edges. The contact pressure which we will consider here is because of compression of the tire threads. Numbers of threads are involved at various compressive positions. However, when the tire is rolling and one block of thread is considered, that block goes to a maximum compression and then gets released. During unloading, hysteresis develops in these blocks. While at the time of loading, for the same strain, the stress produced is higher than the unloading path leading to unsymmetrical pressure distribution. As a result the curve shifts and becomes skewed. This results in a moment which opposes vehicle motion and is considered to be a force against the forward motion of the vehicle termed as rolling resistance.

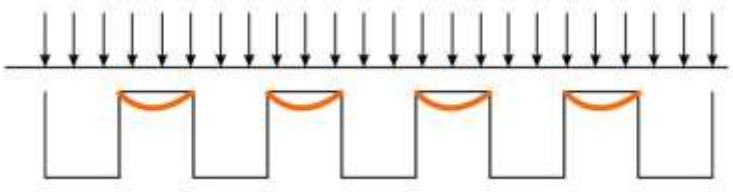

Figure2.4: Bending of the side walls due to the tire inflation pressure

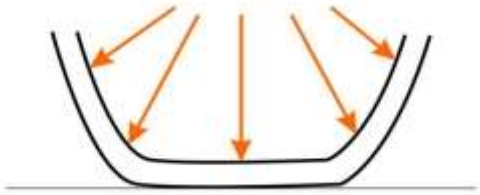

Figure 2.5: Tire inflation pressure on the side walls of the tire.

Rolling Resistance comes out of a force which supports weight. Hence, Rolling Resistance Force

$$= W * Fr \qquad 2.1$$

Here Fr is the rolling resistance coefficient. Also, rolling resistance aids braking. The above figures depict the effect of inflation pressure and resultant bending of the tire walls. Now suppose that the tire is rotating anticlockwise. The threads will get compressed up to a maximum point and then would start getting released. However, as explained above the strain does not go to zero and therefore the curve depicting stress/load is skewed towards the left side. This can be simplified into a force which is offset from the center. Because of this eccentricity a moment will be produced in the opposite direction of rotation (here the clockwise direction). The whole setup can therefore be represented as the normal load acting at the center of the wheel and a horizontal force in the direction which would produce the same effect as the moment by the skewed normal force

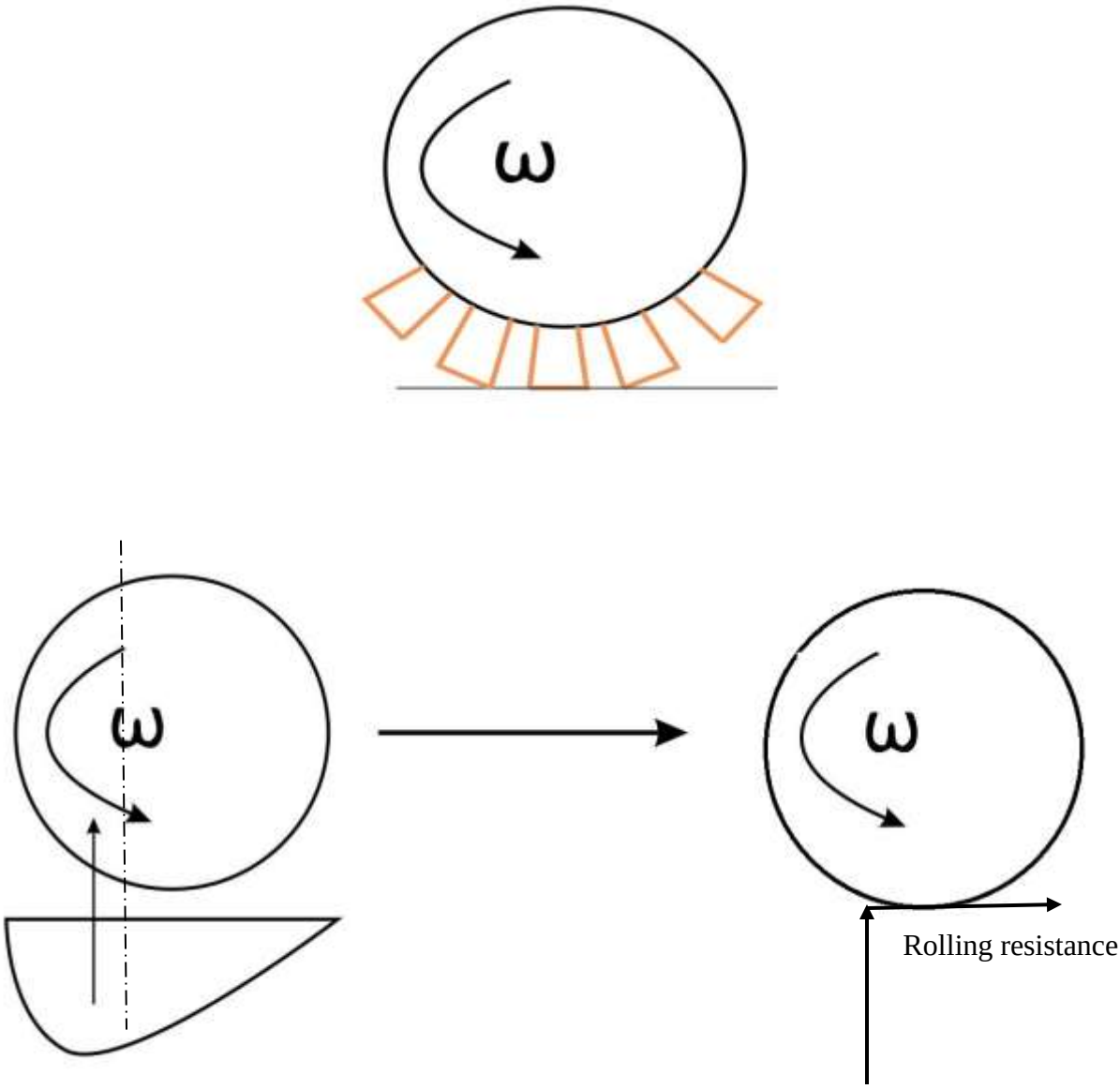

Figure 2.6: Tire rotating in anticlockwise direction and the resultant force originating.

2.6 TIRE SLIP AND SLIP ANGLE

The direction of tire travel is not always aligned with the wheel plane (Sakai, 1981). The angle between the wheel travel and the wheel plane or the longitudinal direction is called slip angle. The figure below shows the angle between direction of wheel travel and the wheel plane which actually is the slip angle. Slip angle is necessary to generate the lateral force. Longitudinal force is created because of slip and this is a sort of misnomer. These concepts are explained in next few sections.

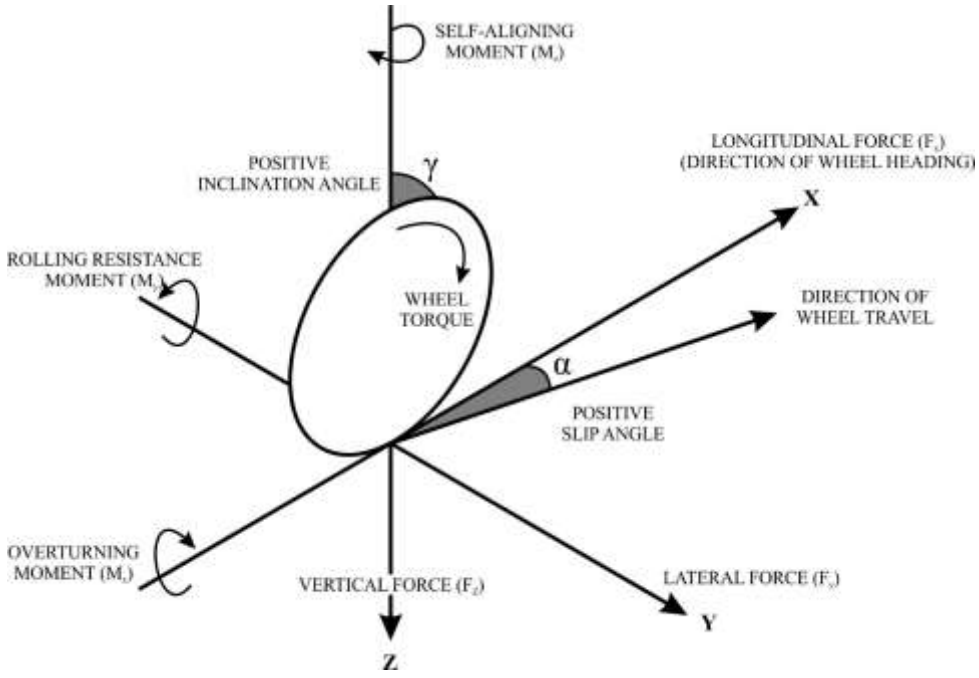

Figure 2.7: Forces and Moments on their respective axis of action

How are these forces or moments developed?

Figure 2.7: Structure of visco-elastic materials

The elastic behavior of these elastomers is very different from that of metal. A metal has elastic properties by the virtue of lattice deformation. Elastomers' elasticity can be attributed to entropy. When an elastomeric molecule is stretched, its entropy decreases and the reverse is also true. Hence elastomers can be modeled as springs. When these long chain molecules are pulled, they start interacting with nearby molecules. This gives a dashpot effect.

Two factors become important in this interaction mechanism

- Frequency
- Temperature

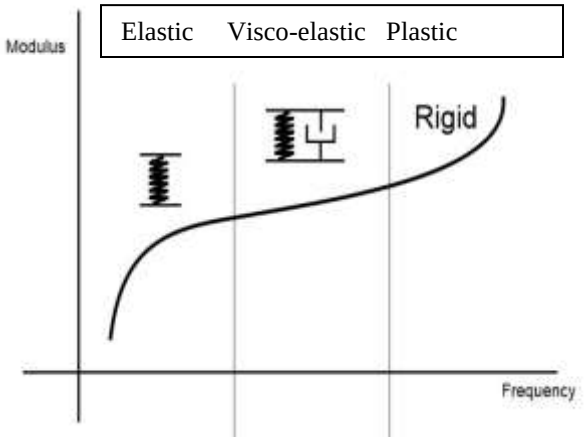

Figure 2.8: Behavior of different materials with change in frequency

At very low frequency, the chain of molecules has the time to react to forces. When force is released it has time to come back to its original configuration. Hence at low frequency it behaves as a spring. When frequency increases then this interaction between molecules increases giving the dashpot effect. The chains of molecules do not have time to return back to its original configuration and hence will behave very stiffly. The effect of temperature is opposite to that of frequency (Sakai, 1981).

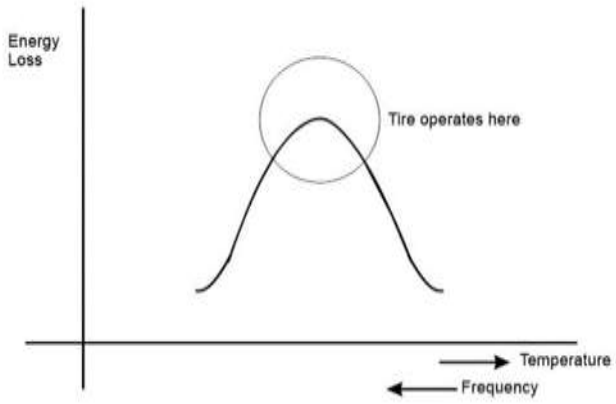

Figure 2.9: Magnitude of energy lost in hysteresis with change in frequency/temperature

2.7 TYPES OF RADIUS IN A ROLLING TIRE

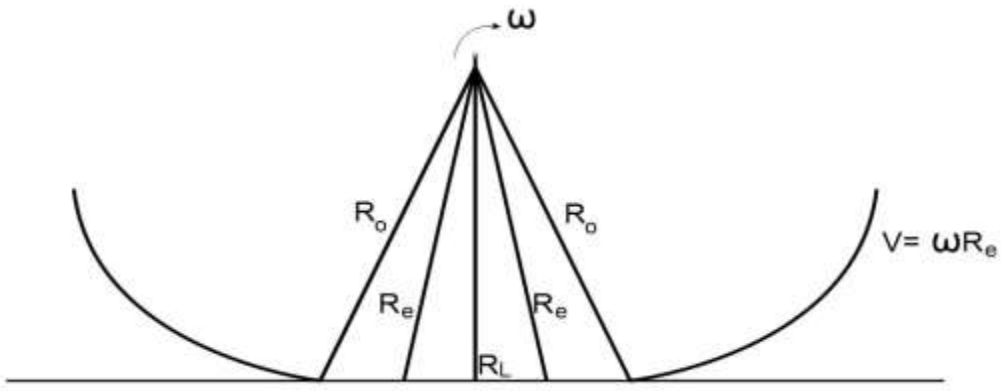

Figure 2.10: Different Radius Zones in a loaded rolling tire

There are three types of radius in a rolling tire:

1. Free radius
2. Loaded radius
3. Effective radius of rolling

As we know the tire supports the weight of the vehicle. This weight will compress the tire and the radius of the tire after loading is called the loaded radius or R_L. The original radius of the tire or the unloaded radius is R_O. The effective radius of rolling is given by the expression 'Effective radius = $\omega * R_e$.The relation between these three radius is quantified as $R_O > R_e > R_L$. Suppose the tire starts compressing at a given point on its circumference, gets compressed to a maximum level and then the tire comes out of compression through rolling. The radius at the point on circumference where it starts getting compressed is R_O and where it comes out of compression would again be R_O. The radius at the center would be R_L and somewhere in between we would have the effective radius of rolling R_e. The four different regions because of this change in radius along the circumference of the tire carcass in shown in the figure above. The first region where the speed of thread on the tire would be greater than the velocity of ground or $\omega * R_e$ would cause a slip in the backward direction and hence a force in positive x direction. For the second region where the speed of thread on the tire carcass would be smaller than the speed of ground would cause the ground to exert a force in the negative x direction on the tire and so on. This boils down to a simple working principle that without slip there is no friction and with no friction there isn't any grip. Here slip means the difference in tangential velocity of the threads and the ground. It's an oxymoron. Unless there is no slip, there is no deformation (no difference in tangential velocity and ground velocity) and no force is generated in the straight bristle. This is the case of micro slip responsible for the grip of the tire.

Free rolling is neither braking nor accelerating. Rolling resistance acts even during free rolling and has to be compensated. We are not applying other longitudinal force. When thread goes over the contact patch apart from normal force there is this longitudinal force acting too because of tire deformation. This results in uneven contact pressure distribution.

Grip of a tire is a result of frictional resistance to its motion. This grip is caused by:

- Elastomeric material (Hysteresis)
- Interaction between road and the tire (Adhesion)

Roads have two types of undulations:

- Macro
- Micro (few microns to 100 microns)

Two forces are exerted on the tire (Only Longitudinal Dynamics is considered)

- Normal
- Traction/Braking or longitudinal forces

Two phenomena happen between the road and tire material:

- Hysteresis (macro phenomena)
- Molecular adhesion (micro phenomena)

Adhesive Mechanism

1. Long Chain molecules get attached to the surface by forming Vander Waal bonds
2. When subjected to a force these bonds break.
3. There is continuous joining and breaking of these bonds leading to series of stick and slip phenomena.

Hysteresis Mechanism

1. When rubber piece is subjected to loading and unloading, it results in hysteresis.
2. Because of the resultant force the block in contact slips down and becomes unloaded and may load again.
3. This frequency of loading and unloading because of macro undulations results in hysteresis loss.
4. The frequency of stick and slip because of macro undulations is less than that of adhesion.

5. Friction works to result in energy loss and oppose motion. Both hysteresis and adhesion have the same effect and friction in case of automobiles can thus be attributed to these two mechanisms.

Therefore,

Friction = Friction due to adhesion + Friction due to hysteresis

Traction or braking longitudinal force occurs by pulling and pushing of threads. There is friction force due to normal pressure. There is competition between the longitudinal force due to stretching and that due to friction. This is the phenomena of macro slip. The region where the longitudinal force is not able to overcome this friction force is the sticking region of the contact patch and the other is the sliding region. Let us consider a simple case of sudden brake application, wherein the wheel will lock. But the vehicle will still be moving. Thread elastomers will get extended because the portion of the thread attached to the carcass are at zero velocity but those attached to the ground are still in movement. The braking force is produced because of this stretching. Same is the case of acceleration. Longitudinal force development can be understood by brush model. The contact patch can be divided into two regions: Region where tire sticks to the ground and the region where tangential forces exceed the friction and slides. By slide here we mean macro slip. This model explains how longitudinal force is developed and how it can be mathematically framed. Total Longitudinal Force = Force in the sticking plus the force in the sliding region. The tire models would be covered in greater detail in the lateral sections.

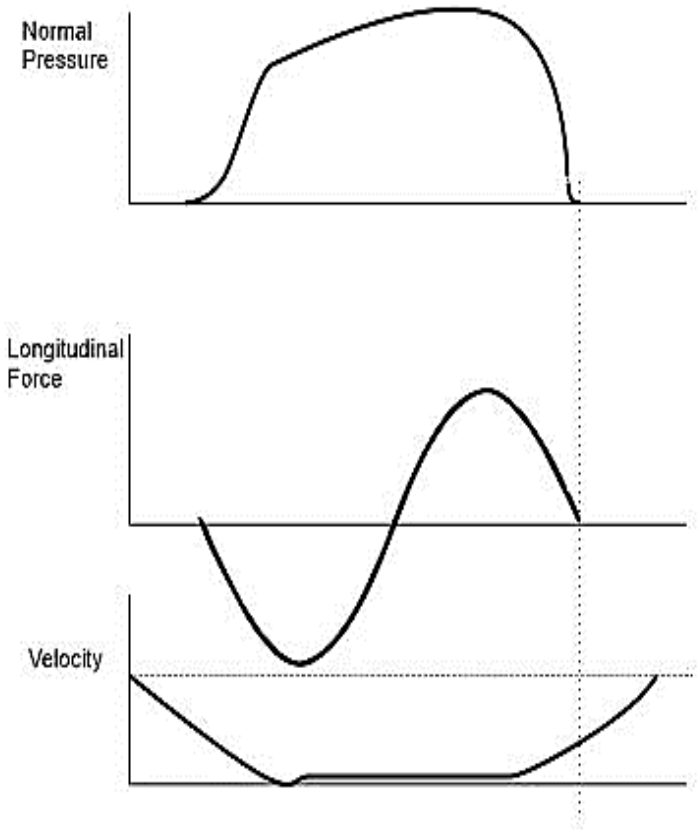

Figure 2.11: Distribution of forces and relative velocity of the tire threads and the ground in the contact patch during micro slip

2.8 MATHEMATICAL MODELING OF VEHICLE DYNAMICS

As stated in the previous section, the mathematical modeling of vehicle dynamics can help in preliminary design and analysis of vehicle configuration, structure and performance. This section helps in building simple decoupled models for the longitudinal, lateral and vertical directions to give the reader a better understanding and make him/her think in the desired direction. Let us first try to understand Longitudinal Dynamics.

2.9 LONGITUDINAL DYNAMICS REVISITED

The body fixed X axis direction is termed as the longitudinal direction and this subsection helps in formulating the dynamics of the vehicle in the said direction. Before proceeding with the mathematical model the notations for various terms used are given below:

Notations

1. F_f, F_r are the traction forces on the front and real wheels repsectively
2. R_a is the aerodynamic resistance
3. R_r is the rolling resistance arsing due to viscoelasticity of tires
4. $Wsin\theta$ is the component of weight W along the direction of travel. Here θ Is the slope of the uphill.
5. R_d is the toeing force by the vehicle attached at the backside.

Applying Newton's Second Law of Motion in the longitudinal direction gives us:

$$F_{Total} = F_f + F_r - R_a - R_r - Wsin\theta - \cancel{R_d} \quad (2.2)$$

Zero Toeing Force/No trailer

Let W_f and W_r be the weight distribution on the front and the rear wheels of the vehicle with wheel base *l*. The distance of the center of mass from the front wheel axle is l_1 and that from the rear is l_2. The height of the COM from the ground is *h*. The acceleration of the vehicle is *a.*

Weight Distribution between the front and rear wheels during acceleration

Applying the moment balance equation about the rear wheel at point B as shown in the figure 2.2 results into:

$$W_f * l + R_a * h + Wsin\theta * h + \frac{W}{g} * a * h - Wcos\theta * l_2 = 0 \quad (2.3)$$

$$W_f = \frac{1}{l}(Wcos\theta * l_2 - R_a * h - Wsin\theta * h - \frac{W}{g} * a * h) \quad (2.4)$$

Similarly the moment balance equation about the front wheel at point A results into:

$$W_r = \frac{1}{l}(Wcos\theta * l_1 + R_a * h + Wsin\theta * h + \frac{W}{g} * a * h) \quad 2.5$$

Theta being the slope of the road will usually be very small and therefore the equation reduces to:

$$W_f = \frac{Wcos\theta * l_2}{l} - \frac{h}{l}(R_a + Wsin\theta + \frac{W}{g} * a) \quad 2.6$$

Simplifying the equations further and taking the total tractive force to be *F:*

$$W_f = \frac{W * l_2}{l} - \frac{h}{l}(F - R_r) \quad 2.7$$

$$W_f = \frac{W * l_2}{l} - \frac{h}{l}(F - f_r * W) \quad 2.8$$

And

$$W_r = \frac{W * l_1}{l} + \frac{h}{l}(R_a + Wsin\theta + \frac{W}{g} * a) \quad 2.9$$

$$W_r = \frac{W * l_1}{l} + \frac{h}{l}(F - f_r * W) \quad 2.10$$

Limit on Traction Force F

For a front wheel drive, maximum traction force will result when the all the friction force is used to provide traction. We know, friction force is just the friction coefficient times the weight and this can be equated to the maximum traction force.

$$(F\_\max)_f = \mu * W_f = \mu * \frac{W}{l} * \frac{(l_2 + f_r * h)}{(1 + \frac{\mu h}{l})} \quad 2.11$$

Similarly, in a rear wheel drive

$$(F\_\max)_r = \mu * W_r \quad 2.12$$

Weight Distribution between the front and rear wheels during Deceleration

Just like the moment balance equations obtained in the case of acceleration, we can calculate the weight distribution when the vehicle is decelerating.

$$W_f = \frac{W * l_2}{l} + \frac{h}{l}(F_b + R_r) \quad 2.13$$

$$W_r = \frac{W * l_1}{l} - \frac{h}{l}(F_b + R_r) \quad 2.14$$

Here F_b is the total braking force. Also, k_{bf}+ k_{br} =1 which basically means if k_{bf} is more than k_{br} a greater proportion of the braking force is applied on the front wheels and vice versa.

$$(F\_\max)_{bf} = \mu * W_f = k_{bf} * F_b \quad 2.15$$

$$(F\_\max)_{br} = \mu * W_r = k_{br} * F_b \quad 2.16$$

Ideal braking will ensure all the friction force available on the front and rear wheels provide braking force which leads to the following formulation:

$$\frac{l_2 + h(\mu + f_r)}{l_1 - h(\mu + f_r)} = \frac{k_{bf}}{k_{br}} \quad 2.17$$

2.10 LATERAL DYNAMICS

Continuing the dynamic modeling in lateral direction would be our next step. The following are the notations for terms used in the mathematical modeling of lateral dynamics (Martino, 2005)

i, j, k – unit vectors

u, v, w – linear velocities along the body fixed axes

Here, u is the longitudinal velocity, v is the lateral velocity and w is the vertical velocity.

p, q, r – angular velocities along the body fixed axes

Here, p is the roll velocity or roll rate, q is the pitch velocity and pitch rate and r is the yaw rate or yaw velocity.

The force vector is simply stated as:

$$F = F_x i + F_y j + F_z k \quad 2.18$$

The moment vector τ would be:

$$\tau = Li + Mj + Nk \quad 2.19$$

Linear momentum is denoted by P = mv

While the angular momentum is denoted by H = [I]{ω}; I being the inertia matrix and ω is the angular velocity vector.

$$I = \begin{bmatrix} I_{xx} & I_{xy} & I_{xz} \\ I_{yx} & I_{yy} & I_{yz} \\ I_{zx} & I_{zy} & I_{zz} \end{bmatrix} \quad 2.20$$

Newton's Second Law simply states that:

$$F = \frac{dP}{dt} \text{ and } \tau = \frac{dH}{dt} \quad 2.21$$

Also, Transport Theorem in mechanics gives us the below formulation

$$\frac{dA}{dt}|_{Inertial\_Frame} = \frac{dA}{dt}|_{Body\_Frame} + \omega \times A. \quad 2.22$$

Here A is any vector quantity.

Hence,

$$\frac{dA}{dt}|_{Inertial\_Frame} = \begin{matrix} \dot{A}_x + (qA_z - rA_y) \\ \dot{A}_y + (rA_x - pA_z) \\ \dot{A}_z + (pA_y - qA_x) \end{matrix} \quad 2.23$$

In the same line of thought,

$$\begin{Bmatrix} F_x \\ F_y \\ F_z \end{Bmatrix} = \mathrm{m} \begin{bmatrix} \dot{u} + & (qw - rv) \\ \dot{v} + & (ru - pw) \\ \dot{w} + & (pv - qu) \end{bmatrix} \quad 2.24$$

$$\begin{Bmatrix} L \\ M \\ N \end{Bmatrix} = \begin{bmatrix} \mathrm{I}_{xx}\dot{p} & \mathrm{I}_{xy}\dot{q} & \mathrm{I}_{xz}\dot{r} \\ \mathrm{I}_{yx}\dot{p} & \mathrm{I}_{yy}\dot{q} & \mathrm{I}_{yz}\dot{r} \\ \mathrm{I}_{zx}\dot{p} & \mathrm{I}_{zy}\dot{q} & \mathrm{I}_{zz}\dot{r} \end{bmatrix} + \begin{Bmatrix} qH_z - rH_y \\ rH_x - pH_z \\ pH_y - qH_x \end{Bmatrix} \quad 2.25$$

Force in Y direction and moment produced in z direction (yaw) produced because of this force is of interest to us when studying Lateral Dynamics. The classical and much referred Bicycle Model gives insight into the same through a very simplified model. The next section covers the Bicycle Model and lays foundation for the complex modeling in this thesis and other literature too.

2.11 Simplified Model- Bicycle Model

This simplified model, Bicycle Model (Blundell and Damian, 2004) condenses the two front wheels into a single wheel and the two rear wheels into a single rear wheel and hence the name. As stated earlier, we are concerned about the velocity in the Y direction and Yaw rate about Z axis when discussing lateral dynamics. Assuming that the vertical velocity *w* is very small and that the longitudinal velocity *u* is constant during the cornering maneuver simplifies the modeling and mathematics involved. Also, the pitch rate q and the roll rate q are considered to very negligible. This makes the dynamics decoupled and simpler. Moreover, F_{yf} and F_{yr} give the lateral force or the force in the Y direction originating at the two wheels while *a* and *b* are the distance between the COM and the front axle and rear axle respectively. Applying Newton's Laws gives us:

$$I_{zz}\dot{r} = aF_{yf} - bF_{yr} \quad 2.26$$

$$m(\dot{v} + ru) = F_{yf} + F_{yr} \quad (2.27)$$

Let us define vehicle side slip angle as β. δ is the steering angle given to the front wheels (This is not the hand steering wheel angle). The slip angles at the front and rear wheels are given by α_f and α_r respectively.

Now, tan (β) = $\frac{v}{u}$

$$\alpha_f = -\left(\delta - \frac{ar + v}{u}\right) = -\delta + \frac{a}{R} + \beta \quad (2.28)$$

$$\alpha_r = \frac{v - br}{u} = \beta - \frac{b}{R} \quad (2.29)$$

Therefore,

$$\delta = \frac{L}{R} - \alpha_f + \alpha_r \quad (2.30)$$

Using a simple tire model to calculate the tire forces results into:

$$F_{yf} = -C_{\alpha f}\alpha_f \quad (2.31)$$

$$F_{yr} = -C_{\alpha r}\alpha_r \quad (2.32)$$

$$F_y = F_{yf} + F_{yr} = -C_{\alpha f}\alpha_f - C_{\alpha r}\alpha_r \quad (2.33)$$

Here $C_{\alpha f}$ and $C_{\alpha r}$ are the front and rear wheel stiffness respectively.

Hence,

$$F_y = \left(-\frac{a}{u}C_{\alpha f} + \frac{b}{u}C_{\alpha r}\right)r - \left(C_{\alpha f} + C_{\alpha r}\right)\beta + (C_{\alpha f})\delta \quad (2.34)$$

$$M_z = -\left(-\frac{a^2}{u}C_{\alpha f} + \frac{b^2}{u}C_{\alpha r}\right)r - \left(C_{\alpha f} - C_{\alpha r}\right)\beta + (C_{\alpha f})\delta \quad (2.35)$$

2.12 STATE SPACE FORM

$$\dot{x} = Ax + Bu$$

$$\begin{bmatrix}\dot{v}\\ \dot{r}\end{bmatrix} = \begin{bmatrix} -\frac{(C_{\alpha f} + C_{\alpha r})}{mu} & -\frac{(aC_{\alpha f} - bC_{\alpha r})}{mu} - u \\ -\frac{(aC_{\alpha f} - bC_{\alpha r})}{Iu} & -\frac{(a^2C_{\alpha f} + b^2C_{\alpha r})}{Iu} \end{bmatrix} \times \begin{bmatrix}v\\ r\end{bmatrix} + \begin{bmatrix}\frac{C_{\alpha f}}{m}\\ \frac{aC_{\alpha f}}{I}\end{bmatrix} \times [\delta] \quad 2.36$$

2.13 STABILITY OF THE STATE SPACE FORM

Since the values of system parameters are unknown here, the Eigen values are not directly calculated for estimating the stability of the system. Rather, Routh Stability Criteria is applied to develop a condition, which if satisfied under a given scenario, will ensure that the system is stable (Karnopp and Donald, 2008).

Mathematically, the non-trivial solution of the system can be found when Det (s*[I]-A) = 0 (This is the characteristic equation of the system). The above characteristic equation can be expressed as:

$$a_0 s^2 + a_1 s^1 + a_2 s^0 = 0 \quad 2.37$$

By Routh criteria, for this system to be stable, all the coefficients should be positive, i.e.

$$a_0,\ a_1 \,\&\, a_2 > 0 \quad 2.38$$

Evaluating $a_0,\ a_1 \,\&\, a_2$ for the above system and normalizing it we obtain,

$$a_0 = 1 \quad 2.39$$

$$a_1 = -(a_{11} + a_{22}) \quad 2.40$$

$$a_2 = -(a_{11}a_{22} - a_{12}a_{21}) \quad 2.41$$

Where, $A = \begin{bmatrix} a_{11} & a_{12} \\ a_{21} & a_{22} \end{bmatrix}$

From the given A matrix, we obtain,

$$\boldsymbol{a_0 = 1} \tag{2.42}$$

$$\boldsymbol{a_1 = \left(\frac{(C_{\alpha f} + C_{\alpha r})}{mu} + \frac{(a^2 C_{\alpha f} + b^2 C_{\alpha r})}{Iu}\right)} \tag{2.43}$$

$$a_2 = -\left(\frac{(C_{\alpha f} + C_{\alpha r})}{mu} * \frac{(a^2 C_{\alpha f} + b^2 C_{\alpha r})}{Iu} - \frac{(aC_{\alpha f} - bC_{\alpha r})}{Iu} * \left(\frac{(aC_{\alpha f} - bC_{\alpha} \right.\right. \tag{2.44}$$

$$= \frac{a^2 * C_{\alpha f} * C_{\alpha r} + b^2 * C_{\alpha f} * C_{\alpha r} + 2 * a * b * C_{\alpha f} * C_{\alpha r}}{mIu^2} + \frac{bC_{\alpha r} - aC_{\alpha f}}{I}$$

$$= \boldsymbol{\frac{C_{\alpha f} * C_{\alpha r} * l^2}{mIu^2} + \frac{bC_{\alpha r} - aC_{\alpha f}}{I}}$$

It is possible that the second term of the above expression, '$\boldsymbol{\frac{bC_{\alpha r} - aC_{\alpha f}}{I}}$', may be negative depending on the values of stiffness and distance of the COM from the axles. As long as $bC_{\alpha r} > aC_{\alpha f}$, the system is stable but if it is otherwise then there is a possibility that system turns unstable.

When,

$bC_{\alpha r} > aC_{\alpha f}$, Under-steer Condition

$bC_{\alpha r} < aC_{\alpha f}$, Over-steer Condition

$bC_{\alpha r} = aC_{\alpha f}$, Neutral-steer Condition

After some manipulation;

$$a_2 = \frac{1}{mIu^2}\left[1 + \frac{(bC_{\alpha r} - aC_{\alpha f})mu^2}{C_{\alpha f} * C_{\alpha r} * l^2}\right] * C_{\alpha f} * C_{\alpha r} * l^2 \tag{2.45}$$

For stability;

$$\left[1 + \frac{(bC_{\alpha r} - aC_{\alpha f})mu^2}{C_{\alpha f} * C_{\alpha r} * l^2}\right] > 0$$

$$1 + ku^2 > 0$$

Where $K = \frac{(bC_{\alpha r} - aC_{\alpha f})m}{C_{\alpha f} * C_{\alpha r} * l^2}$ is called as the under-steer gradient.

When K is negative;

$$u = \sqrt{-\frac{1}{K}} \quad 2.46$$

This is the velocity at which the system changes from understeer to oversteer and is known as the critical velocity. Also note that K is a vehicle parameter.

Returning back to the governing equations;

$$I_{zz}\dot{r} = aF_{yf} - bF_{yr} \quad 2.47$$

$$m(\dot{v} + ru) = F_{yf} + F_{yr} \quad 2.48$$

If analyzed under steady state;

$$0 = aF_{yf} - bF_{yr} \quad 2.49$$

$$m(ru) = F_{yf} + F_{yr} \quad 2.50$$

Also;

$$\delta = \frac{L}{R} - \alpha_f + \alpha_r \quad 2.51$$

Analyzing the effect of under-steer gradient on δ;

$$m(ru) = F_{yf} + F_{yr} \quad 2.52$$

$$m\left(\frac{u^2}{R}\right) = F_{yf} + F_{yr} \quad 2.53$$

We know the distribution of load between the front and rear tire is given as;

$$W_f = \frac{W}{l} * b \quad 2.54$$

$$W_r = \frac{W}{l} * a \tag{2.55}$$

In a similar fashion;

$$F_{yf} = \frac{F_y}{l} * b = m\left(\frac{u^2}{lR}\right) * b = \frac{W_f}{g} * \frac{u^2}{R} \tag{2.56}$$

$$F_{yr} = \frac{F_y}{l} * a = m\left(\frac{u^2}{lR}\right) * a = \frac{W_r}{g} * \frac{u^2}{R} \tag{2.57}$$

Since,

$$\delta = \frac{L}{R} - \alpha_f + \alpha_r \tag{2.58}$$

$$\delta = \frac{L}{R} + \frac{F_{yf}}{C_{\alpha f}} - \frac{F_{yr}}{C_{\alpha r}} \tag{2.59}$$

$$\delta = \frac{L}{R} + \frac{m\left(\frac{u^2}{lR}\right) * b}{C_{\alpha f}} - \frac{m\left(\frac{u^2}{lR}\right) * a}{C_{\alpha r}} \tag{2.60}$$

$$\delta = \frac{L}{R} + \frac{(bC_{\alpha r} - aC_{\alpha f})m}{C_{\alpha f} * C_{\alpha r} * l} * \frac{u^2}{R} \tag{2.61}$$

Here, $K_2 = \frac{(bC_{\alpha r} - aC_{\alpha f})m}{C_{\alpha f} * C_{\alpha r} * l} * \frac{u^2}{R}$ is another definition of under-steer gradient.

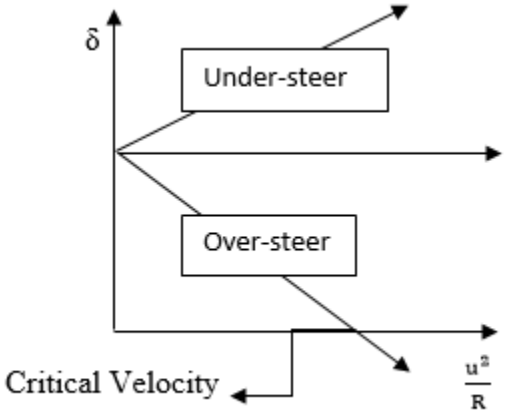

Mathematical Interpretation of the Graph

For cornering with same radius R, if more steering input is required as the speed of the vehicle (u) increases. This is the case when the vehicle is under-steered. On the other hand, if the gradient is negative or the vehicle is over-steered then the steering input decreases with the speed. In this case, for a particular value of $\frac{u^2}{R}$ the steering angle goes down to zero. This means no steering input is required in that particular scenario! If the speed increases further, then δ becomes negative. That is for turning towards right; a left steering input is required. Therefore, the factor $bC_{\alpha r} - aC_{\alpha f}$ plays an important role in vehicle dynamics. Nowadays, many of the vehicles are front wheel driven which means 'a' is smaller when compared to b. This usually results in under-steered vehicles. Vehicle Manufacturers prefer under-steered vehicles as they are more stable than over-steered vehicles. Vehicle Manufacturers prefer slightly under-steered vehicles because it is stable but limit the degree to which the vehicle is under-steered for handling reasons. If it is highly under-steered then the driver will have difficulty in handling the vehicle. Many electric cars are over-steered because they are rear wheel driven making b smaller compared to a. Sport cars are usually over-steered too. This is a preferable characteristic as the scenarios under which these vehicles are used desire high speeds and under-steer might lead to fatal accidents. Also, the steering input demanded from the driver is less and therefore less effort is prioritized over stability.

2.14 PERTURBATION ANALYSIS

Perturbation Analysis is a mathematical method to find approximate solutions to mathematical model. It is used in formulating flight mechanics to a large extent (Schmitz, 2011). This technique hasn't been applied to vehicle dynamics and this thesis is a humble attempt to do so. This section formulates the perturbation equations and a beginner in perturbation analysis is highly advised to read through to understand the vehicle dynamic model built.

Consider an Inertial Reference Frame I fixed to the Earth and V is the Vehicle Fixed Reference Frame. Let us consider an infinitesimal volume dV having position p' with respect to O_I, the Origin of Inertial Frame of Reference. The density of material at this location is $\rho_{v\ and}$ hence the mass is given by

$$dm = \rho_v * dV \tag{2.62}$$

Apart from gravitational forces, only mechanical forces are considered here.
Newton's Law of Motion is applied on this mass.

Linear Momentum and Force relation:

$$\frac{\boldsymbol{d}}{\boldsymbol{dt}}|_{\boldsymbol{I}}\left(\boldsymbol{\rho_v} * \frac{\boldsymbol{dp'}}{\boldsymbol{dt}} * \boldsymbol{dV}\right) = \boldsymbol{\rho_v} * \boldsymbol{g} * \boldsymbol{dV} + \boldsymbol{df_{ext}} \tag{2.63}$$

Angular Momentum and Moment relation:

$$\frac{\boldsymbol{d}}{\boldsymbol{dt}}|_{\boldsymbol{I}}\left(\mathbf{p'} * \boldsymbol{\rho_v} * \frac{\boldsymbol{dp'}}{\boldsymbol{dt}} * \boldsymbol{dV}\right) = \mathbf{p'} * \boldsymbol{\rho_v} * \boldsymbol{g} * \boldsymbol{dV} + \mathbf{p'} * \boldsymbol{df_{ext}} \tag{2.64}$$

Integrating the above expressions **over all the infinitesimal volumes** $\boldsymbol{dV}$ in the vehicle,

$$\int_{\boldsymbol{vol}} \frac{\boldsymbol{d}}{\boldsymbol{dt}}|_{\boldsymbol{I}}\left(\boldsymbol{\rho_v} * \frac{\boldsymbol{dp'}}{\boldsymbol{dt}} * \boldsymbol{dV}\right) = \int_{\boldsymbol{vol}} \boldsymbol{\rho_v} * \boldsymbol{g} * \boldsymbol{dV} + \int_{\boldsymbol{vol}} \boldsymbol{df_{ext}} \tag{2.65}$$

$$\int_{\boldsymbol{vol}} \frac{\boldsymbol{d}}{\boldsymbol{dt}}|_{\boldsymbol{I}}\left(\mathbf{p'} * \boldsymbol{\rho_v} * \frac{\boldsymbol{dp'}}{\boldsymbol{dt}} * \boldsymbol{dV}\right) = \int_{\mathbf{vol}} \mathbf{p'} * \boldsymbol{\rho_v} * \boldsymbol{g} * \boldsymbol{dV} + \int_{\boldsymbol{vol}} \mathbf{p'} * \boldsymbol{df_{ext}} \tag{2.66}$$

All internal forces in the vehicle material will be assumed in equilibrium so the only net forces on the vehicle must act on the surface of the vehicle. This yields the two fundamental equations of motion.

$$\int_{vol} \frac{\boldsymbol{d}}{\boldsymbol{dt}}|_I \left(\boldsymbol{\rho_v} * \frac{\boldsymbol{dp'}}{\boldsymbol{dt}} * \boldsymbol{dV}\right) = \int_{vol} \boldsymbol{\rho_v} * \boldsymbol{g} * \boldsymbol{dV} + \int_{\boldsymbol{Surface}} \boldsymbol{df_{ext}} \tag{2.67}$$

$$\int_{vol} \frac{\boldsymbol{d}}{\boldsymbol{dt}}|_I \left(\mathbf{p'} * \boldsymbol{\rho_v} * \frac{\boldsymbol{dp'}}{\boldsymbol{dt}} * \boldsymbol{dV}\right) = \int_{\mathbf{vol}} \mathbf{p'} * \boldsymbol{\rho_v} * \boldsymbol{g} * \boldsymbol{dV} + \int_{\boldsymbol{Surface}} \mathbf{p'} * \boldsymbol{df_{ext}} \tag{2.68}$$

and hence are not in the most useful form. The aim is to obtain these equations relative to the vehicle fixed frame.

Now,

$$p' = p_v + p \tag{2.69}$$

Here, p is the position of dV relative to the origin of Vehicle Fixed Reference Frame V or O_v.

Also, the instantaneous mass of vehicle, *m*, is,

$$\int_{\boldsymbol{vol}} \boldsymbol{\rho_v} * \boldsymbol{dV} = \boldsymbol{m} \tag{2.70}$$

Define the origin of Vehicle Fixed Frame O_v or at the instantaneous center of mass *cm* of the vehicle which is also the center of gravity as here g is assumed to be constant.

First moment of the vehicle about the inertial origin can be therefore given by the following equation

$$\int_{\mathbf{vol}} \boldsymbol{\rho_v} * \mathbf{p'} * \boldsymbol{dV} = \int_{\mathbf{vol}} \boldsymbol{\rho_v} * \mathbf{p_v} * \boldsymbol{dV} + \int_{\mathbf{vol}} \boldsymbol{\rho_v} * \mathbf{p} * \boldsymbol{dV} = \boldsymbol{m}\mathbf{p_v} + \int_{\mathbf{vol}} \boldsymbol{\rho_v} * \mathbf{p} * \boldsymbol{dV} \tag{2.71}$$

But the first moment about center of mass is zero,

$$\int_{\mathbf{vol}} \boldsymbol{\rho_v} * \mathbf{p'} * \boldsymbol{dV} = \int_{\mathbf{vol}} \boldsymbol{\rho_v} * \mathbf{p_v} * \boldsymbol{dV} + \int_{\mathbf{vol}} \boldsymbol{\rho_v} * \mathbf{p} * \boldsymbol{dV} \qquad 2.72$$

$$= \boldsymbol{m}\mathbf{p_v} + \cancelto{\mathbf{0}}{\int_{\mathbf{vol}} \boldsymbol{\rho_v} * \mathbf{p} * \boldsymbol{dV}}$$

$$\mathbf{p_v} = \frac{\int_{\mathbf{vol}} \boldsymbol{\rho_v} * \mathbf{p'} * \boldsymbol{dV}}{m} \qquad 2.73$$

$$\int_{vol} \frac{\boldsymbol{d}}{\boldsymbol{dt}}|_{\boldsymbol{I}} \left(\boldsymbol{\rho_v} * \frac{\boldsymbol{dp'}}{\boldsymbol{dt}}|_I * \boldsymbol{dV}\right) = \int_{vol} \frac{\boldsymbol{d}}{\boldsymbol{dt}}|_{\boldsymbol{I}} \left(\boldsymbol{\rho_v} * \frac{\boldsymbol{dp_v}}{\boldsymbol{dt}}|_I * \boldsymbol{dV}\right) + \int_{vol} \frac{\boldsymbol{d}}{\boldsymbol{dt}}|_{\boldsymbol{I}} \left(\boldsymbol{\rho_v} * \frac{\boldsymbol{dp}}{\boldsymbol{dt}}|_I * \boldsymbol{dV}\right) \qquad 2.74$$

Therefore, the inertial position of the center of mass of the vehicle is,

But,

$$\int_{vol} \frac{\boldsymbol{d}}{\boldsymbol{dt}}|_{\boldsymbol{I}} \left(\boldsymbol{\rho_v} * \frac{\boldsymbol{dp_v}}{\boldsymbol{dt}}|_I * \boldsymbol{dV}\right) = \frac{\boldsymbol{d}}{\boldsymbol{dt}}|_{\boldsymbol{I}} \left(\frac{\boldsymbol{dp_v}}{\boldsymbol{dt}}|_I \int_{vol} (\boldsymbol{\rho_v} * \boldsymbol{dV})\right) = \frac{\boldsymbol{d}}{\boldsymbol{dt}}|_{\boldsymbol{I}} (m * \frac{\boldsymbol{dp_v}}{\boldsymbol{dt}}|_I) \qquad 2.76$$

$$\frac{\boldsymbol{dp}}{\boldsymbol{dt}}|_I = \frac{\boldsymbol{dp}}{\boldsymbol{dt}}|_V + \omega_{V,I} \times p \qquad 2.75$$

Substituting it in the integral yields,

$$\int_{vol} \frac{\boldsymbol{d}}{\boldsymbol{dt}}|_{\boldsymbol{I}} \left(\boldsymbol{\rho_v} * \frac{\boldsymbol{dp}}{\boldsymbol{dt}}|_I * \boldsymbol{dV}\right) = \int_{vol} \frac{\boldsymbol{d}}{\boldsymbol{dt}}|_{\boldsymbol{I}} \left(\boldsymbol{\rho_v} * \frac{\boldsymbol{dp}}{\boldsymbol{dt}}|_V * \boldsymbol{dV}\right) + \int_{vol} \frac{\boldsymbol{d}}{\boldsymbol{dt}}|_{\boldsymbol{I}} (\boldsymbol{\rho_v} * (\omega_{V,I} \times p) * \boldsymbol{dV}) \qquad 2.77$$

Vehicle is rigid, hence this term is zero!

The last integral can be manipulated as follows,

$$\int_{vol} \frac{\boldsymbol{d}}{\boldsymbol{dt}}|_{\boldsymbol{I}} (\boldsymbol{\rho_v} * (\omega_{V,I} \times p) * \boldsymbol{dV}) \qquad 2.78$$

$$= \frac{\boldsymbol{d}\omega_{V,I}}{\boldsymbol{dt}}|_{\boldsymbol{I}} \times \int_{vol} (\boldsymbol{\rho_v} * p * \boldsymbol{dV}) + \omega_{V,I} \times \int_{vol} \frac{\boldsymbol{d}}{\boldsymbol{dt}}|_{\boldsymbol{I}} (\boldsymbol{\rho_v} * p * \boldsymbol{dV})$$

$$= \frac{\boldsymbol{d}\omega_{V,I}}{\boldsymbol{dt}}|_{\boldsymbol{I}} \times \int_{\boldsymbol{vol}} (\boldsymbol{\rho_v} * p * \boldsymbol{dV}) + \omega_{V,I} \times (\int_{\boldsymbol{vol}} \frac{\boldsymbol{d}}{\boldsymbol{dt}}|_{\boldsymbol{V}} (\boldsymbol{\rho_v} * p * \boldsymbol{dV}) + \omega_{V,I} \times \int_{\boldsymbol{vol}} (\boldsymbol{\rho_v} * p * \boldsymbol{dV})$$

$$= 0$$

Similar manipulation can be carried out for rotational equations of motion leading to:

$$\frac{\boldsymbol{d}}{\boldsymbol{dt}}|_{\boldsymbol{I}} \left(\boldsymbol{m} * \frac{\boldsymbol{dp_v}}{\boldsymbol{dt}}|_{\boldsymbol{I}} \right) = \boldsymbol{m} * \frac{\boldsymbol{dV_v}}{\boldsymbol{dt}}|_{\boldsymbol{I}} = \boldsymbol{mg} + \boldsymbol{F_{ext}} \quad 2.79$$

$$\int_{\boldsymbol{vol}} \boldsymbol{p} \times (\boldsymbol{\rho_v}(\left(\frac{\boldsymbol{d\omega_{V,I}}}{\boldsymbol{dt}}|_{\boldsymbol{I}} \times \boldsymbol{p} \right) + \boldsymbol{\omega_{V,I}} \times (\boldsymbol{\omega_{V,I}} \times \boldsymbol{p}))\boldsymbol{dV}) = \boldsymbol{M} \quad 2.80$$

Scalar Equations of Motion

$$\frac{\boldsymbol{dp_V}}{\boldsymbol{dt}} = V_V = Ui_V + Vj_V + Wk_V \quad 2.81$$

$$\boldsymbol{p} = xi_V + yj_V + zk_V$$

$$\boldsymbol{g} = g_x i_V + g_y j_V + g_z k_V$$

$$\boldsymbol{\omega_{V,I}} = Pi_V + Qj_V + Rk_V$$

$$\boldsymbol{F} = F_x i_V + F_y j_V + F_z k_V$$

$$\mathbf{M} = Li_V + Mj_V + Nk_V$$

Direction Cosine Matrix

The transformation matrix from earth to vehicle frame can be given by:

$$T_{E-V}(\emptyset, \theta, \Psi) = \begin{bmatrix} 1 & 0 & 0 \\ 0 & cos\emptyset & sin\emptyset \\ 0 & -sin\emptyset & cos\emptyset \end{bmatrix} \begin{bmatrix} cos\theta & 0 & -sin\theta \\ 0 & 1 & 0 \\ sin\theta & 0 & cos\theta \end{bmatrix} \begin{bmatrix} cos\Psi & sin\Psi & 0 \\ -sin\Psi & cos\Psi & 0 \\ 0 & 0 & 1 \end{bmatrix} \quad 2.82$$

Translational Equations of Motion

$$\frac{\boldsymbol{d}}{\boldsymbol{dt}}|_{\boldsymbol{I}} \left(\boldsymbol{m} * \frac{\boldsymbol{dp_v}}{\boldsymbol{dt}}|_{\boldsymbol{I}} \right) = \boldsymbol{m} * \frac{\boldsymbol{dV_v}}{\boldsymbol{dt}}|_{\boldsymbol{I}} = \boldsymbol{mg} + \boldsymbol{F_{ext}} = \boldsymbol{m}(\frac{\boldsymbol{dV_v}}{\boldsymbol{dt}}|_{\boldsymbol{V}} + \boldsymbol{\omega_{V,I}} \times \boldsymbol{V_v}) \quad 2.83$$

$$m(\dot{U} + QW - VR) = mg_x + F_x \quad (2.84)$$
$$m(\dot{V} + RU - PW) = mg_y + F_y$$
$$m(\dot{W} + PV - QU) = mg_z + F_z$$

Or

$$m(\dot{U} + QW - VR) = -mgsin\theta + F_x$$
$$m(\dot{V} + RU - PW) = mgcos\theta sin\emptyset + F_y$$
$$m(\dot{W} + PV - QU) = mgcos\theta cos\emptyset + F_z$$

Rotational Equations of Motion

$$\int_{\boldsymbol{vol}} \boldsymbol{p} \times (\boldsymbol{\rho_v}(\left(\frac{\boldsymbol{d\omega_{V,I}}}{\boldsymbol{dt}}|_I \times \boldsymbol{p}\right) + \boldsymbol{\omega_{V,I}} \times (\boldsymbol{\omega_{V,I}} \times \boldsymbol{p}))\boldsymbol{dV}) = \mathbf{M} \quad (2.85)$$

$$\frac{\boldsymbol{d\omega_{V,I}}}{\boldsymbol{dt}}|_I = \frac{\boldsymbol{d\omega_{V,I}}}{\boldsymbol{dt}}|_V + \boldsymbol{\omega_{V,I}} \times \boldsymbol{\omega_{V,I}} = \frac{\boldsymbol{d\omega_{V,I}}}{\boldsymbol{dt}}|_V \quad (2.86)$$

$$= \dot{P}i_V + \dot{Q}j_V + \dot{R}k_V$$

Vector Triple Product Identity

$$a \times b \times c = b(a.c) - c(a.b)$$
$$p \times (\left(\left(\frac{d\omega_{V,I}}{dt}|_I \times p\right) + \omega_{V,I} \times \left(\omega_{V,I} \times p\right)\right) \quad (2.87)$$

$$= \frac{d\omega_{V,I}}{dt}|_V (p.p) - p\left(p.\frac{d\omega_{V,I}}{dt}|_V\right) + p \times \omega_{V,I}(\omega_{V,I}.p) - p \times p(\omega_{V,I}.\omega_{V,I})$$

Cross product of two parallel vectors is zero

$$p.p = x^2 + y^2 + z^2 \quad (2.88)$$

$$p.\omega_{V,I} = Px + Qy + Rz \quad (2.89)$$

$$p.\frac{d\omega_{V,I}}{dt}|_V = \dot{P}x + \dot{Q}y + \dot{R}z \tag{2.90}$$

Also,

$$I_{xx} = \int_{vol}(y^2 + z^2)\,\boldsymbol{\rho_v}\,\boldsymbol{dV} I_{xy} = \int_{vol} xy\,\boldsymbol{\rho_v}\,\boldsymbol{dV} \tag{2.91}$$

$$I_{yy} = \int_{vol}(x^2 + z^2)\,\boldsymbol{\rho_v}\,\boldsymbol{dV} I_{yz} = \int_{vol} yz\,\boldsymbol{\rho_v}\,\boldsymbol{dV}$$

$$I_{zz} = \int_{vol}(x^2 + y^2)\,\boldsymbol{\rho_v}\,\boldsymbol{dV} I_{xz} = \int_{vol} xz\,\boldsymbol{\rho_v}\,\boldsymbol{dV}$$

$$\int_{\boldsymbol{vol}} \boldsymbol{p} \times (\boldsymbol{\rho_v}(\left(\frac{\boldsymbol{d\omega_{V,I}}}{\boldsymbol{dt}}|_{\boldsymbol{I}} \times \boldsymbol{p}\right) + \boldsymbol{\omega_{V,I}} \times (\boldsymbol{\omega_{V,I}} \times \boldsymbol{p}))\boldsymbol{dV}) \tag{2.92}$$

$$= (I_{xx}\dot{P} - I_{xz}\left(\dot{R} + PQ\right) - I_{yz}(Q^2 - R^2) - I_{xy}\left(\dot{Q} - RP\right) + \left(I_{zz} - I_{yy}\right)RQ)i_V$$

$$+\left(I_{yy}\dot{Q} + (I_{xx} - I_{zz})PR - I_{xy}\left(\dot{P} + QR\right) - I_{yz}\left(\dot{R} - PQ\right) + I_{xz}(P^2 - R^2)\right)j_V$$

$$+(I_{zz}\dot{R} - I_{xz}\left(\dot{P} - QR\right) - I_{xy}(P^2 - Q^2) - I_{yz}\left(\dot{Q} + RP\right) + (I_{yy} - I_{xx})PQ)k_v$$

Hence;

$$(I_{xx}\dot{P} - I_{xz}\left(\dot{R} + PQ\right) - I_{yz}(Q^2 - R^2) - I_{xy}\left(\dot{Q} - RP\right) + \left(I_{zz} - I_{yy}\right)RQ) = L \tag{2.93}$$

$$\left(I_{yy}\dot{Q} + (I_{xx} - I_{zz})PR - I_{xy}\left(\dot{P} + QR\right) - I_{yz}\left(\dot{R} - PQ\right) + I_{xz}(P^2 - R^2)\right) = M$$

$$\left(I_{zz}\dot{R} - I_{xz}\left(\dot{P} - QR\right) - I_{xy}(P^2 - Q^2) - I_{yz}\left(\dot{Q} + RP\right) + \left(I_{yy} - I_{xx}\right)PQ\right) = N$$

$$\boldsymbol{\omega_{V,I}} = \dot{\emptyset} i_V + \dot{\theta} j_V + \dot{\Psi} k_I \tag{2.94}$$

$$\boldsymbol{\omega_{V,I}} = P i_V + Q j_V + R k_V \tag{2.95}$$

Now;

$$j_2 = cos\emptyset j_V - sin\emptyset k_V \tag{2.96}$$

Also;

$$k_I = -sin\theta i_V + sin\emptyset cos\theta j_V + cos\emptyset cos\theta k_V \tag{2.97}$$

This gives;

$$P = \dot{\emptyset} - \dot{\Psi}sin\theta \tag{2.98}$$

$$Q = \dot{\theta}cos\emptyset + \dot{\Psi}cos\theta sin\emptyset$$

$$R = \dot{\Psi}cos\theta cos\emptyset - \dot{\theta}sin\emptyset$$

Or;

$$\dot{\emptyset} = P + Qsin\emptyset tan\theta + Rcos\emptyset tan\theta \tag{2.99}$$

$$\dot{\theta} = Qcos\emptyset - Rsin\emptyset$$

$$\dot{\Psi} = (Qsin\emptyset + Rcos\emptyset)sec\theta$$

$$V_V = Ui_V + Vj_V + Wk_V = [U\ V\ W]\begin{Bmatrix} i_V \\ j_V \\ k_V \end{Bmatrix} \tag{2.100}$$

$$V_V = [\dot{X}_I \dot{Y}_I - \dot{h}_I]\begin{Bmatrix} i_I \\ j_I \\ k_I \end{Bmatrix} \tag{2.101}$$

$$T_{E-V}(\emptyset,\theta,\Psi) = \begin{bmatrix} 1 & 0 & 0 \\ 0 & cos\emptyset & sin\emptyset \\ 0 & -sin\emptyset & cos\emptyset \end{bmatrix}\begin{bmatrix} cos\theta & 0 & -sin\theta \\ 0 & 1 & 0 \\ sin\theta & 0 & cos\theta \end{bmatrix}\begin{bmatrix} cos\Psi & sin\Psi & 0 \\ -sin\Psi & cos\Psi & 0 \\ 0 & 0 & 1 \end{bmatrix} \tag{2.102}$$

$$\begin{Bmatrix} i_V \\ j_V \\ k_V \end{Bmatrix} = T_{E-V}(\emptyset,\theta,\Psi)\begin{Bmatrix} i_E \\ j_E \\ k_E \end{Bmatrix} = T_{I-V}(\emptyset,\theta,\Psi)\begin{Bmatrix} i_I \\ j_I \\ k_I \end{Bmatrix} \tag{2.103}$$

$$\begin{bmatrix} \dot{X}_I \\ \dot{Y}_I \\ -\dot{h}_I \end{bmatrix} = {T_{I-V}}^T(\emptyset,\theta,\Psi)\begin{bmatrix} U \\ V \\ W \end{bmatrix} \tag{2.104}$$

$$\dot{X}_I = Ucos\theta cos\Psi + V(sin\emptyset sin\theta cos\Psi - cos\emptyset sin\Psi) + W(cos\emptyset sin\theta cos\Psi + sin\emptyset sin\Psi) \tag{2.105}$$

$$\dot{Y}_I = Ucos\theta sin\Psi + V(sin\emptyset sin\theta sin\Psi + cos\emptyset cos\Psi) + W(cos\emptyset sin\theta sin\Psi - sin\emptyset cos\Psi)$$

$$\dot{h}_I = Usin\theta - Vsin\emptyset cos\theta - Wcos\emptyset cos$$

2.15 REFERENCE AND PERTURBATION EQUATIONS

$U=U_0+u$	$V=V_0+v$	$W=W_0+w$
$P=P_0+p$	$Q=Q_0+q$	$R=R_0+r$
$\Theta=\Theta_0+\theta$	$\Phi=\Phi_0+\varphi$	$\Psi=\Psi_0+\Psi$
$F_x=F_{x0}+f_x$	$F_y=F_{y0}+f_y$	$F_z=F_{z0}+f_z$
$L=L_0+l$	$M=M_0+m$	$N=N_0+n$

$$m\big((U_0\dot{+}\dot{u})+(Q_0W_0+Q_0w+W_0q+wq)-(V_0R_0+V_0r+R_0v+rv\big) \qquad 2.106$$

$$=-mg\sin(\theta_0+\theta)+F_{x0}+f_x$$

$$m\big((\dot{V_0}+\dot{v})+(R_0U_0+R_0u+U_0r+ru)-(P_0W_0+P_0w+W_0p+pw)\big)$$

$$=mgcos(\theta_0+\theta)\sin(\Phi_0+\emptyset)+F_{y0}+f_y$$

$$m\Big(\big(\dot{W_0}+\dot{w}\big)+(P_0V_0+P_0v+V_op+pv)-(Q_0U_0+Q_0u+U_0q+qu\Big)$$

$$=mgcos(\theta_0+\theta)cos(\Phi_0+\emptyset)+F_{z0}+f_z$$

Also;

$$\sin(\theta_0+\theta)=sin\theta_0cos\theta+cos\theta_0sin\theta$$

$$\cos(\theta_0+\theta)=cos\theta_0cos\theta-sin\theta_0sin\theta$$

$$m\big((U_0\dot{+}\dot{u})+(Q_0W_0+Q_0w+W_0q+wq)-(V_0R_0+V_0r+R_0v+rv \qquad 2.107$$

$$=-mg(sin\theta_0cos\theta+cos\theta_0sin\theta)+F_{x0}+f_x$$

$$m\big((\dot{V_0}+\dot{v})+(R_0U_0+R_0u+U_0r+ru)-(P_0W_0+P_0w+W_0p+pw)\big)$$

$$=mg(cos\theta_0cos\theta-sin\theta_0sin\theta)(sin\emptyset_0cos\emptyset+cos\emptyset_0sin\emptyset)+F_{y0}+f_y$$

$$m\Big(\big(\dot{W_0}+\dot{w}\big)+(P_0V_0+P_0v+V_op+pv)-(Q_0U_0+Q_0u+U_0q+qu\Big)$$

$$=mg(cos\theta_0cos\theta-sin\theta_0sin\theta)(cos\Phi_0cos\emptyset-sin\Phi_0sin\emptyset)+F_{z0}+f_z$$

Small Perturbation Assumption

If the perturbations are small the following assumptions and simplifications can be safely made:

Products of Perturbation Quantities ~ 0

Sin (perturbation angle) ~ perturbation angle

Cos (perturbation angle) ~ **1**

Under these assumptions:

$$m\big((U_0 \dot{+} \dot{u}) + (Q_0W_0 + Q_0w + W_0q) - (V_0R_0 + V_0r + R_0v\big) \qquad 2.108$$

$$= -mg(sin\theta_0 + cos\theta_0\Theta) + F_{x0} + f_x$$

$$m\big((V_0 \dot{+} \dot{v}) + (R_0U_0 + R_0u + U_0r) - (P_0W_0 + P_0w + W_0p\big)$$

$$= mg(cos\theta_0 - sin\theta_0\Theta)(sin\Phi_0 + cos\Phi_0\emptyset) + F_{y0} + f_y$$

$$m\left(\left(\dot{W}_0 + \dot{w}\right) + (P_0V_0 + P_0v + V_op) - (Q_0U_0 + Q_0u + U_0q\right)$$

$$= mg(cos\theta_0 - sin\theta_0\Theta)(cos\Phi_0 - sin\Phi_0\emptyset) + F_{z0} + f_z$$

Reference Equations:

$$m\big(\dot{U}_0 + Q_0W_0 - V_0R_0\big) = -mgsin\theta_0 + F_{x0} \qquad 2.109$$

$$m\big(\dot{V}_0 + R_0U_0 - P_0W_0\big) = mgcos\theta_0 sin\Phi_0 + F_{y0}$$

$$m\big(\dot{W}_0 + P_0V_0 - Q_0U_0\big) = mgcos\theta_0 cos\Phi_0 + F_{z0}$$

Perturbation Equations:

$$m(\dot{u} + (Q_0w + W_0q) - (V_0r + R_0v)) = -mgcos\theta_0\Theta + f_x \qquad 2.110$$

$$m(\dot{v} + (R_0u + U_0r) - (P_0w + W_0p)) = -mgsin\theta_0 sin\Phi_0\Theta + mgcos\theta_0 cos\Phi_0\emptyset) + f_y$$

$$m(\dot{w} + (P_0v + V_op) - (Q_0u + U_0q)) = -mg(cos\theta_0 sin\Phi_0\emptyset + sin\theta_0 cos\Phi_0\Theta) + f_z$$

Similarly,

Reference Equations for rotational rates are given as under:

$$I_{xx}\dot{P}_0 - I_{xz}\left(\dot{R}_0 + P_0Q_0\right) + \left(I_{zz} - I_{yy}\right)R_0Q_0 = L_0 \qquad 2.111$$

$$I_{yy}\dot{Q}_0 + (I_{xx} - I_{zz})P_0R_0 + I_{xz}\left({P_0}^2 - {R_0}^2\right) = M_0$$

$$I_{zz}\dot{R}_0 - I_{xz}\left(\dot{P}_0 - Q_0R_0\right) + \left(I_{yy} - I_{xx}\right)P_0Q_0 = N_0$$

$$\dot{\phi} = p + tan\Theta_0(sin\Phi_0 q + cos\Phi_0 r + (\mathrm{Q}_0 cos\Phi_0 - \mathrm{R}_0 sin\Phi_0)\phi) \qquad 2.112$$
$$+ (\mathrm{Q}_0 sin\Phi_0 + \mathrm{R}_0 cos\Phi_0 + (\dot{\Phi}_0 - \mathrm{P}_0)tan\Theta_0)\theta$$
$$\dot{\theta} = cos\Phi_0 q - sin\Phi_0 r - (\mathrm{Q}_0 sin\Phi_0 + \mathrm{R}_0 cos\Phi_0)\phi$$
$$\dot{\psi} = \dot{\Psi}_0\, tan\Theta_0\, \theta + (sin\Phi_0 q + cos\Phi_0 r - (\mathrm{R}_0 sin\Phi_0 - \mathrm{Q}_0 cos\Phi_0)\phi)/cos\Theta_0$$

$$I_{xx}\dot{p} - I_{xz}(\dot{r} + (\mathrm{Q}_0 p + \mathrm{P}_0 q)) + (I_{zz} - I_{yy})(\mathrm{R}_0 q + Q_0 r) = \mathrm{l}_A \qquad 2.113$$

$$I_{yy}\dot{q} + (I_{xx} - I_{zz})(\mathrm{R}_0 p + P_0 r) + 2I_{xz}(\mathrm{P}_0 p + R_0 r) = \mathrm{m}_A$$
$$I_{zz}\dot{r} - I_{xz}(\dot{p} - (\mathrm{R}_0 q + Q_0 r)) + (I_{yy} - I_{xx})\,(\mathrm{Q}_0 p + \mathrm{P}_0 q) = \mathrm{n}_A$$

$$\mathrm{P}_0 = \dot{\Phi}_0 + \dot{\Psi}_0 sin\Theta_0 \qquad 2.114$$

$$\mathrm{Q}_0 = \dot{\Theta}_0 cos\Phi_0 + \dot{\Psi}_0 sin\Phi_0 cos\Theta_0$$
$$\mathrm{R}_0 = -\dot{\Theta}_0 sin\Phi_0 + \dot{\Psi}_0 cos\Phi_0 cos\Theta_0$$

$$\dot{\Phi}_0 = \mathrm{P}_0 + \mathrm{Q}_0 sin\Phi_0 tan\Theta_0 + \mathrm{R}_0 cos\Phi_0 tan\Theta_0 \qquad 2.115$$

$$\dot{\Theta}_0 = \mathrm{Q}_0 cos\Phi_0 - \mathrm{R}_0 sin\Phi_0$$
$$\dot{\Psi}_0 = (\mathrm{Q}_0 sin\Phi_0 + \mathrm{R}_0 cos\Phi_0)sec\Theta_0$$

$$p = \dot{\phi} - \dot{\Psi}_0 cos\Theta_0\theta - sin\Theta_0\dot{\psi} \qquad 2.116$$

$$q = cos\Phi_0\dot{\theta} - \dot{\Theta}_0 sin\Phi_0\phi + \dot{\Psi}_0(cos\Phi_0 cos\Theta_0\phi - sin\Phi_0 sin\Theta_0\theta) + sin\Phi_0 cos\Theta_0\dot{\psi}$$
$$r = cos\Phi_0 cos\Theta_0\dot{\psi} - \dot{\Theta}_0 cos\Phi_0\phi - sin\Phi_0\dot{\theta} - \dot{\Psi}_0(sin\Phi_0 cos\Theta_0\phi + cos\Phi_0 sin\Theta_0\theta)$$

2.16 MATH MODEL ASSEMBLY AND DRIVE SIMULATION

Perturbation Equations for Translational Dynamics

$$m(\dot{u} + (Q_0 w + W_0 q) - (V_0 r + R_0 v)) = -mgcos\theta_0 \Theta + f_x \qquad 2.117$$

$$m(\dot{v} + (R_0 u + U_0 r) - (P_0 w + W_0 p)) = -mgsin\theta_0 sin\Phi_0 \Theta + mgcos\theta_0 cos\Phi_0 \emptyset) + f_y$$

$$m(\dot{w} + (P_0 v + V_o p) - (Q_0 u + U_0 q)) = -mg(cos\theta_0 sin\Phi_0 \emptyset + sin\theta_0 cos\Phi_0 \Theta) + f_z$$

Dividing by vehicle mass m and rearranging the terms we have;

$$\dot{u} = (V_0 r + R_0 v) - (Q_0 w + W_0 q) - gcos\theta_0 \Theta + \frac{f_x}{m} \qquad 2.118$$

$$\dot{v} = (P_0 w + W_0 p) - (R_0 u + U_0 r) + g(cos\theta_0 cos\Phi_0 \emptyset - sin\theta_0 sin\Phi_0 \Theta) + \frac{f_y}{m}$$

$$\dot{w} = (Q_0 u + U_0 q) - (P_0 v + V_o p) - g(cos\theta_0 sin\Phi_0 \emptyset + sin\theta_0 cos\Phi_0 \Theta) + \frac{f_z}{m}$$

Also recall that;

$$V_V = U i_V + V j_V + W k_V \qquad 2.119$$

Hence;

$$\delta V_V = u i_V + v j_V + w k_V = [u\ v\ w] \begin{Bmatrix} i_V \\ j_V \\ k_V \end{Bmatrix} \qquad 2.120$$

Perturbation Equations for Rotational Dynamics

$$\dot{p} - \frac{I_{xz}\dot{r}}{I_{xx}} = \frac{1}{I_{xx}}(I_{xz}(\mathrm{Q}_0 p + \mathrm{P}_0 q) + (I_{yy} - I_{zz})(\mathrm{R}_0 q + Q_0 r) + \mathrm{l}_A) \qquad 2.121$$

$$\dot{q} = \frac{1}{I_{yy}}((I_{zz} - I_{xx})(\mathrm{R}_0 p + P_0 r) + 2I_{xz}(R_0 r - \mathrm{P}_0 p) + \mathrm{m}_A)$$

$$\dot{r} - \frac{I_{xz}}{I_{zz}}\dot{p} = \frac{1}{I_{zz}}(-I_{xz}(\mathrm{R}_0 q + Q_0 r) + (I_{xx} - I_{yy})(\mathrm{Q}_0 p + \mathrm{P}_0 q) + \mathrm{n}_A)$$

Also;

$$\delta\boldsymbol{\omega}_{\boldsymbol{V,I}} = pi_V + qj_V + rk_V = [p\ q\ r]\begin{Bmatrix} i_V \\ j_V \\ k_V \end{Bmatrix} \tag{2.122}$$

$$\begin{bmatrix} 1 & -\frac{I_{xz}}{I_{xx}} \\ -\frac{I_{xz}}{I_{zz}} & 1 \end{bmatrix}\begin{Bmatrix} \dot{p} \\ \dot{r} \end{Bmatrix} = \begin{bmatrix} \frac{1}{I_{xx}}(I_{xz}(\mathrm{Q}_0 p + \mathrm{P}_0 q) + (I_{yy} - I_{zz})(\mathrm{R}_0 q + Q_0 r) + \mathrm{l}_A) \\ \frac{1}{I_{zz}}(-I_{xz}(\mathrm{R}_0 q + Q_0 r) + (I_{xx} - I_{yy})(\mathrm{Q}_0 p + \mathrm{P}_0 q) + \mathrm{n}_A) \end{bmatrix} \tag{2.123}$$

By inverting the leading coefficient matrix we get the decoupled perturbation equations for rotational dynamics;

$$\begin{Bmatrix} \dot{p} \\ \dot{r} \end{Bmatrix} = \frac{1}{1 - \frac{{I_{xz}}^2}{I_{xx}I_{zz}}}\begin{bmatrix} 1 & \frac{I_{xz}}{I_{xx}} \\ \frac{I_{xz}}{I_{zz}} & 1 \end{bmatrix}\begin{bmatrix} \frac{1}{I_{xx}}(I_{xz}(\mathrm{Q}_0 p + \mathrm{P}_0 q) + (I_{yy} - I_{zz})(\mathrm{R}_0 q + Q_0 r) + \mathrm{l}_A) \\ \frac{1}{I_{zz}}(-I_{xz}(\mathrm{R}_0 q + Q_0 r) + (I_{xx} - I_{yy})(\mathrm{Q}_0 p + \mathrm{P}_0 q) + \mathrm{n}_A) \end{bmatrix} \tag{2.124}$$

Apart from six equations governing Translational and Rotational Dynamics we have three Kinematic Relations too.

$$\dot{\phi} = p + tan\Theta_0(sin\Phi_0 q + cos\Phi_0 r + (\mathrm{Q}_0 cos\Phi_0 - \mathrm{R}_0 sin\Phi_0)\phi) \tag{2.125}$$
$$+(\mathrm{Q}_0 sin\Phi_0 + \mathrm{R}_0 cos\Phi_0 + (\dot{\Phi}_0 - \mathrm{P}_0) tan\Theta_0)\theta$$
$$\dot{\theta} = cos\Phi_0 q - sin\Phi_0 r - (\mathrm{Q}_0 sin\Phi_0 + \mathrm{R}_0 cos\Phi_0)\phi$$
$$\dot{\psi} = \dot{\Psi}_0\, tan\Theta_0\, \theta + (sin\Phi_0 q + cos\Phi_0 r - (\mathrm{R}_0 sin\Phi_0 - \mathrm{Q}_0 cos\Phi_0)\phi)/cos\Theta_0$$

We also need equations to track vehicle position in an earth fixed reference frame;

$$\dot{X}_I = Ucos\theta cos\Psi + V(sin\emptyset sin\theta cos\Psi - cos\emptyset sin\Psi) + W(cos\emptyset sin\theta cos\Psi + sin\emptyset sin\Psi) \tag{2.126}$$

$$\dot{Y}_I = Ucos\theta sin\Psi + V(sin\emptyset sin\theta sin\Psi + cos\emptyset cos\Psi) + W(cos\emptyset sin\theta sin\Psi - sin\emptyset cos\Psi)$$

$$\dot{h}_I = Usin\theta - Vsin\emptyset cos\theta - Wcos\emptyset cos\theta$$

Writing the above equations using direction cosine matrixes;

$$\begin{bmatrix} \dot{X}_I \\ \dot{Y}_I \\ -\dot{h}_I \end{bmatrix} = T_{I-V}{}^{T}(\emptyset, \theta, \Psi) \begin{bmatrix} U \\ V \\ W \end{bmatrix} \qquad 2.127$$

Making the necessary substitutions, using he trigonometric identities and making small perturbation assumptions we have;

$$\begin{bmatrix} \dot{x}_I \\ \dot{y}_I \\ -\dot{h}_I \end{bmatrix} = \left(\begin{bmatrix} -sin\Psi_0\Psi & -cos\Psi_0\Psi & 0 \\ -sin\Psi & -sin\Psi_0\Psi & 0 \\ cos\Psi_0\Psi & 0 & 0 \end{bmatrix} \begin{bmatrix} cos\theta_0 & 0 & -sin\theta_0 \\ 0 & 1 & 0 \\ sin\theta_0 & 0 & cos\theta_0 \end{bmatrix} \begin{bmatrix} 1 & 0 & 0 \\ 0 & cos\emptyset_0 & -sin\emptyset_0 \\ 0 & sin\emptyset_0 & cos\emptyset_0 \end{bmatrix} \right. \qquad 2.128$$

$$+ \begin{bmatrix} cos\Psi_0 & -sin\Psi_0 & 0 \\ sin\Psi_0 & cos\Psi_0 & 0 \\ 0 & 0 & 1 \end{bmatrix} \begin{bmatrix} -sin\theta_0\theta & 0 & cos\theta_0\theta \\ 0 & 0 & 0 \\ -cos\theta_0\theta & 0 & -sin\theta_0\theta \end{bmatrix} \begin{bmatrix} 1 & 0 & 0 \\ 0 & cos\emptyset_0 & -sin\emptyset_0 \\ 0 & sin\emptyset_0 & cos\emptyset_0 \end{bmatrix}$$

$$\left. + \begin{bmatrix} cos\Psi_0 & -sin\Psi_0 & 0 \\ sin\Psi_0 & cos\Psi_0 & 0 \\ 0 & 0 & 1 \end{bmatrix} \begin{bmatrix} cos\theta_0 & 0 & -sin\theta_0 \\ 0 & 1 & 0 \\ sin\theta_0 & 0 & cos\theta_0 \end{bmatrix} \begin{bmatrix} 0 & 0 & 0 \\ 0 & sin\emptyset_0\emptyset & -cos\emptyset_0\emptyset \\ 0 & cos\emptyset_0\emptyset & -sin\emptyset_0\emptyset \end{bmatrix} \right) \begin{Bmatrix} U \\ V \\ W \end{Bmatrix}$$

$$+ \begin{bmatrix} cos\Psi_0 & -sin\Psi_0 & 0 \\ sin\Psi_0 & cos\Psi_0 & 0 \\ 0 & 0 & 1 \end{bmatrix} \begin{bmatrix} cos\theta_0 & 0 & -sin\theta_0 \\ 0 & 1 & 0 \\ sin\theta_0 & 0 & cos\theta_0 \end{bmatrix} \begin{bmatrix} 1 & 0 & 0 \\ 0 & cos\emptyset_0 & -sin\emptyset_0 \\ 0 & sin\emptyset_0 & cos\emptyset_0 \end{bmatrix} \begin{Bmatrix} u \\ v \\ w \end{Bmatrix}$$

The perturbation equations derived above are linear in perturbation variables thought they don't seem so. Coefficients of these variables include vehicle mass and inertia which are assumed to be constant plus the terms evaluated at reference drive condition. These terms are constant when evaluating a given reference condition.

2.17 Numerical Simulation for Linear Models

Our system from the perturbation equations can be modeled in a more generic form, the state space form as given below:

$$\dot{\boldsymbol{x}} = \boldsymbol{Ax} + \boldsymbol{Bu};$$

$$\boldsymbol{y} = \boldsymbol{Cx} + \boldsymbol{Du}$$

However, we haven't calculated the force and moment perturbations. Therefore the state space form cannot be fully outlined here. The modeling of force and moment perturbations is carried out in detail in later sections.

2.18 TIRE MODELS

Tire mathematical models are very important to estimate the longitudinal and lateral tire forces being developed because of tire slip and slip angles respectively. But this is easier said than done because of a plethora of reasons (Sleeper, 1980). The tire force generating capacity is dependent on numerous tire's physical parameters like pneumatic pressure and nature of tire material as well as operating conditions such as the surface on which it is running, the longitudinal speed, temperature and the load on the tire too. Moreover, there isn't any exact analytical expression for the relation between these parameters and force generation. Tire models used in vehicle dynamics simulation and tire related research rely basically on curve fitted experimental data and empirical adjustments of theoretical models. The complexity of tire mechanics has limited the development of a complete and reasonable analytical force theory.

One of the much used and referred tire model in vehicle dynamics literature and otherwise is the Tire Brush Model by Pacejka (Rajamani, 2006) which is explained in detail in the next section to give a flavor of how such models are formulated and make reader abreast of the concepts involved.

2.19 TIRE BRUSH MODEL BY PACEJKA

The longitudinal stiffness of the tire bristles is given by C_{px} per unit length (say mm). Now given that the wheel is moving with an angular speed of Omega ($\boldsymbol{\omega}$) in the clockwise direction which means that the circumferential longitudinal speed of the carcass thread is $\boldsymbol{\omega} * \boldsymbol{r_e}$where $\boldsymbol{r_e}$is the effective rolling radius of the tire in motion. The ground can be thought of moving with the same speed in the opposite direction that of the vehicle i.e. in the backward direction. Now suppose that the driver applies

some braking torque. This means that the carcass thread moves at a slower speed where it is attached to the tire and at a greater speed where it is attached to the ground. The ground because of this relative motion would try to oppose the motion and pull the thread with it in the backward direction. This effect would be prevalent on all the tire carcass threads the resultant of which is a force in the backward direction which provides the desired braking to the car. Similarly is the working of the tire when a accelerating torque is applied to the wheels. Now this would lead to the threads pulling the vehicle forwards or backwards depending on the accelerating or braking scenarios. The friction force would resist this motion up to some level and then would eventually yield if the pulling force is greater than maximum friction available. That is the tire thread would stick in a particular region and then would eventually slide. That precisely describes the contact patch shape and force distribution.

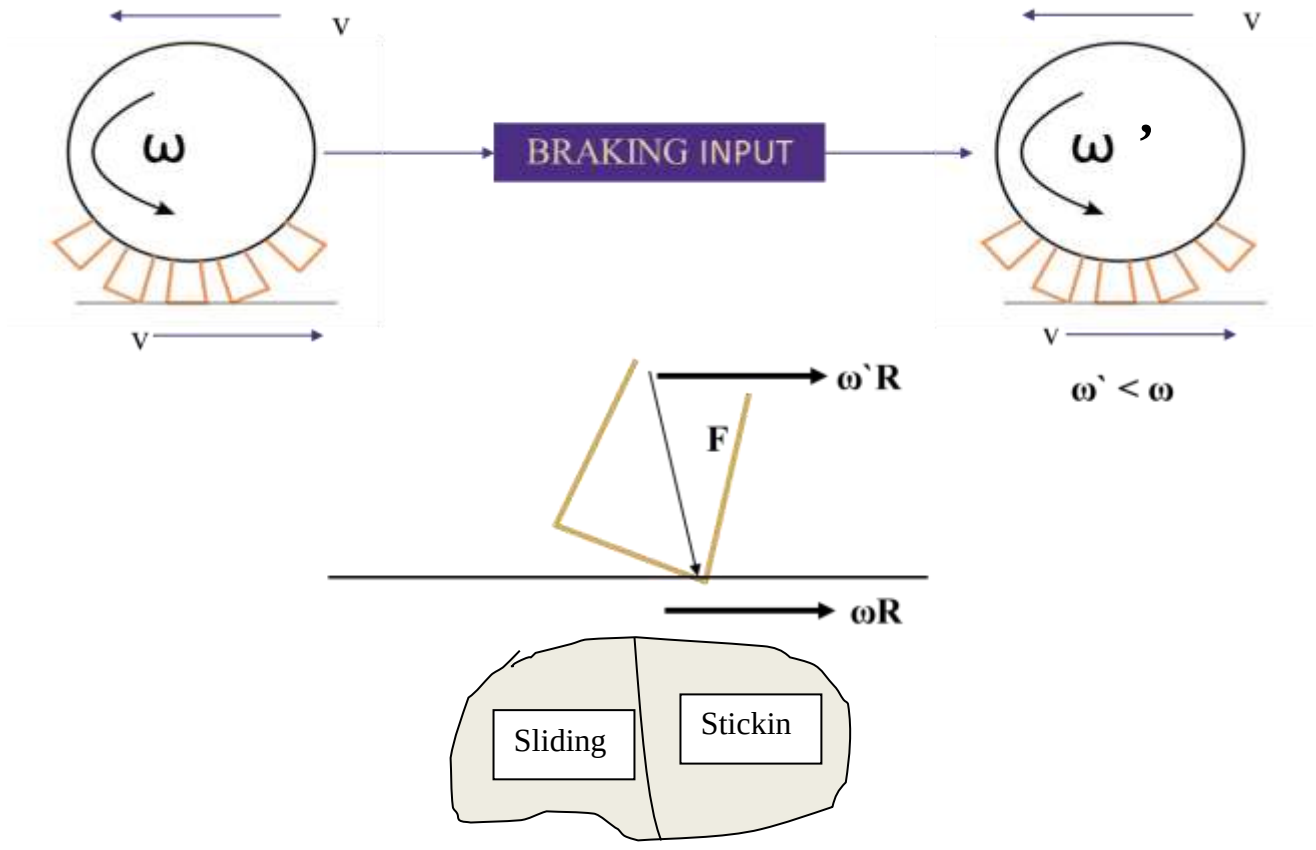

Figure 2.12: A typical tire contact patch

Though the above description qualitatively describes the mechanism of tires providing the desired acceleration or braking to vehicles it does not help in quantitative analysis. The aim is to express the longitudinal force mathematically.

Algorithm to find the Longitudinal Force

1) Calculate the deformation 'u' in the bristle.
2) Calculate the force produced in these bristles i.e. $F = C_{px} * u$
3) Assume a parabolic pressure distribution q_z
4) Find the point at which sliding starts;x_s
5) Total Longitudinal Force = Force in the sticking region +Force in the sliding region

Let us denote the velocity of the tire bristle where it is attached to the carcass as V_{r} and the velocity of the bristle where it is attached to the ground as V_{x}. The difference in these velocities is denoted as V_{sx} which signifies the relative movement of the two ends of the bristles. The mid-length of contact patch is a. Also, x is the distance of this bristle from the origin; the distance travelled by this particular bristle on ground is $(a - x)$ in timeΔt. The deformation of this bristle can simple be found by the relative velocity of the two ends of the bristle times the time intervalΔt.

$$V_{\mathrm{sx}} = V_{\mathrm{x}} - V_r = V_{\mathrm{x}} - \omega R \qquad 2.129$$

$$\Delta t = \frac{(a - x)}{V_r}$$

$$u = -\frac{(a - x)V_{\mathrm{sx}}}{V_r}$$

The next step is to define two physical quantities as below:

Theoretical Slip σ*:* $\frac{-V_{\mathrm{sx}}}{V_r}$

Practical Slip κ*:* $\frac{-V_{\mathrm{sx}}}{V_x}$

$$u = -\frac{(a - x)V_{\mathrm{sx}}}{V_r} = (a - x) * \sigma = \frac{(a - x) * \kappa}{1 + \kappa} \qquad 2.130$$

Also, assuming a parabolic pressure distribution in the contact patch gives us:

$$q_z = \frac{3F_z}{4a}\left(1 - \left(\frac{x}{a}\right)^2\right) \tag{2.131}$$

We know that the force in the bristle is simple stiffness times the deformation produced which simplifies to:

$$q_x = C_{px} * (a - x) * \sigma \tag{2.132}$$

Since we have the normal force, we can calculate the friction forces acting on the bristle. If this friction force is less than the force in the bristle than the bristle will stick to the surface otherwise it would slide over. Mathematically expressing this condition leads to:

When $q_x > or = \mu * q_z$; *then sliding will take place.*

$$q_x = C_{px} * (a - x) * \sigma = \mu * q_z = \mu * \frac{3F_z}{4a}\left(1 - \left(\frac{x}{a}\right)^2\right) \tag{2.133}$$

Define $\theta_x = \frac{2C_{px}a^2}{3\mu F_z}$ and $x_s = a - 2a\lambda$ as the point at which sliding starts.

$$\sigma = \mu * \frac{3F_z}{4C_{px}a^2}\left(\frac{a + x_s}{a}\right) \tag{2.134}$$

$$\sigma = \frac{1}{2\theta_x}\frac{(\boldsymbol{a} + \boldsymbol{a} - 2a\lambda)}{\boldsymbol{a}}$$

$$\sigma = \frac{1}{\theta_x}(\mathbf{1} - \lambda)$$

$Hence; \lambda = 1 - \theta_x\sigma$

Total Longitudinal Force = Force in the sticking region +Force in the sliding region

$$x_s = a - \frac{\mu F_z \omega R}{V_{\mathrm{sx}} C_{px}} \tag{2.135}$$

$$\boldsymbol{F} = \int_a^{a-2a\lambda} V_{\mathrm{sx}} C_{px} \frac{(a - x_c)dx_c}{\omega R} + \int_{a-2a\lambda}^{-a} \mu * q_z \, dx_c \tag{2.136}$$

$$\boldsymbol{F} = 2C_{px}a^2\sigma - \frac{4}{3} * \frac{\left(C_{px}a^2\sigma\right)^2}{\mu * q_z} + \frac{8}{27} * \frac{\left(C_{px}a^2\sigma\right)^3}{(\mu * q_z)^3}$$

The tire model by Pacejka gives a quantitative formulation indeed but some discrepancies are found when the experimental results are compared with the analytical formulation. Some curve fitting techniques have to be used to gain results to be used in research and industry. Nonetheless, it is very useful in understanding the physics behind force generation in tire carcass threads and how to analytically address them. Experimental results for tires are cumbersome both from the point of measurement and also their dependency on so many factors both known and unknown. The idea of this thesis was to build a model for estimation of the states of the vehicle which has a great dependency upon the tire model to be used. Experimentally determining the tire forces every time is difficult and tedious. Moreover, many resources are not available in an academic setup like this which might be available in an industry. This led to reading papers which were as close to analytical modeling of tire as possible. Unfortunately, there are very limited resources in this regard. However, the paper by Mohamed Salaani (Salaani, 2007) on analytical tire forces was very helpful and provided valuable insights. The next subsection explains the idea of the research in as concise and simple terms as possible. Readers who want to understand the paper in a far greater detail can refer the appendix.

The paper by Mohammed Salaani validates a numerical tire model developed by the author. This theoretical model uses physical parameters: lateral and longitudinal stiffness, aligning moment pneumatic trail, overturning moment arm, lateral force relaxation length, and friction properties. These are standard mechanical properties that characterize the force generating capacity of tires. The validation procedure compares the theoretical ground forces and moments with experimental data. Tire data measured on a flat track tire testing machine are used in this validation. It covers the full range of longitudinal, lateral, and combined slips. This model can be applied in vehicle dynamics simulations up to extreme handling maneuvers and can be used to assess the effect of a specific tire's physical property on the performance of vehicle motion and stability. This validated analytical tire model is an important advancement in the field of tire force and moment predictions and puts more emphasis on the mechanics of tire contact rather than curve fitting practices. The dynamic inputs to the model are road wheel kinematic variables and normal load. The kinematic input is composed of longitudinal and lateral slip, and inclination angle with respect to the road surface. The outputs of the model are: longitudinal and lateral ground forces, aligning moment, and overturning moment.

2.20 HANDLING RESPONSE OF A VEHICLE

Performing Laplace transformation on the bicycle model equations gives us:

$$\begin{bmatrix} ms + \frac{(C_{\alpha f} + C_{\alpha r})}{u} & \frac{(aC_{\alpha f} - bC_{\alpha r})}{u} + mu \\ \frac{(aC_{\alpha f} - bC_{\alpha r})}{u} & Is + \frac{(a^2C_{\alpha f} + b^2C_{\alpha r})}{u} \end{bmatrix} \times \begin{bmatrix} v \\ r \end{bmatrix} = \begin{bmatrix} \frac{C_{\alpha f}}{1} \\ \frac{aC_{\alpha f}}{1} \end{bmatrix} \times [\delta] \quad 2.137$$

When a vehicle wants to overtake another vehicle (double lane change) lateral acceleration should intuitively dominate over yaw. However, when vehicle wants to corner, yaw should dominate over lateral acceleration (Sakai, 1981).

Applying Crammers rule;

$$\frac{v}{\delta} = \frac{IC_{\alpha f}s - maC_{\alpha f}u + {(a+b)bC_{\alpha f}C_{\alpha r}}/{u}}{Det(\Delta)} \quad 2.138$$

$$\frac{r}{\delta} = \frac{maC_{\alpha f}s + {(a+b)C_{\alpha f}C_{\alpha r}}/{u}}{Det(\Delta)} \quad 2.139$$

Where $\Delta = \begin{bmatrix} ms + \frac{(C_{\alpha f}+C_{\alpha r})}{u} & \frac{(aC_{\alpha f}-bC_{\alpha r})}{u} + mu \\ \frac{(aC_{\alpha f}-bC_{\alpha r})}{u} & Is + \frac{(a^2C_{\alpha f}+b^2C_{\alpha r})}{u} \end{bmatrix}$

Lateral acceleration Gain =

$$\frac{\dot{v} + ru}{\delta} = \frac{IC_{\alpha f}s^2 + {(a+b)bsC_{\alpha f}C_{\alpha r}}/{u} + (a+b)C_{\alpha f}C_{\alpha r}}{mIs^2 + \left(m\frac{(a^2C_{\alpha f}+b^2C_{\alpha r})}{u} + I\frac{(aC_{\alpha f}+bC_{\alpha r})}{u}\right)s + l^2\frac{C_{\alpha f}C_{\alpha r}(1+ku^2)}{u^2}} \quad 2.140$$

Yaw Gain =

$$\frac{r}{\delta} = \frac{maC_{\alpha f}s + {(a+b)C_{\alpha f}C_{\alpha r}}/{u}}{mIs^2 + \left(m\frac{(a^2C_{\alpha f}+b^2C_{\alpha r})}{u} + I\frac{(aC_{\alpha f}+bC_{\alpha r})}{u}\right)s + l^2\frac{C_{\alpha f}C_{\alpha r}(1+ku^2)}{u^2}} \quad 2.141$$

Steady Sate Gain; s=0;

Yaw Gain =

$$\frac{r}{\delta} = \frac{u}{l(1 + ku^2)} \tag{2.142}$$

Lateral Acceleration Gain =

$$\frac{\dot{v} + ru}{\delta} = \frac{u^2}{l(1 + ku^2)} \tag{2.143}$$

For lateral acceleration; numerator and denominator both has square power of ‘s’ but for yaw; numerator has s to the power one while denominator has s to the power two. At higher frequency, hence, yaw gain will diminish when compared to lateral acceleration gain which will be constant for a given delta. Therefore it is advised to pick up a sensor for lateral acceleration measurement because yaw measurements won’t give any insight. Our ultimate aim is to understand handling in a quantitative fashion. Subjective evaluation of any vehicle is just obtained by driving it and getting the feel of the vehicle under question. However, objective evaluation is more mathematical and analytical. However, both these evaluations are important.

Chapter 3. METHODOLOGY

The previous chapters, sections and subsections were to educate a beginner about various vehicle dynamics terminologies and mechanisms. Being a vast field, there is much more than the given information but the knowledge required to understand and proceed further in the thesis should be sufficient. There are many books and other resources by vehicle dynamists in industries or academia for interested readers and it is highly recommended to browse through them if desired.

This chapter works on the theory outlined in previous sections and forms the main part of the thesis. Having discussed the bicycle model in detail in the previous sections, the reader can conclude that indeed it is a very simple model but takes into account many assumptions which do not hold ground under a real scenario. The bicycle model does not address the coupled effect of longitudinal and vertical dynamics on lateral dynamics. It is incapable of informing about other states of the vehicle such as longitudinal velocity or roll rate. It is based on the assumption of steady state cornering. That is longitudinal velocity is kept constant in calculations. Besides these, it does not include the effect of aerodynamics or suspensions. Moreover, it does not address lateral & longitudinal load transfers during different maneuvers. Also, it assumes constant lateral & longitudinal tire stiffness and is able to handle only a steering input and cannot simulate the dynamics if an acceleration/braking torque is provided. This thesis attempts to overcome and remove these assumptions by modeling the physics behind them to give a more comprehensive and realistic model. Apart from addressing the issues in the bicycle model, the proposed models can handle any reference state of the vehicle and give relevant outputs corresponding to the steer, accelerating/braking torque. Vehicle dynamic modeling being an iterative process, there are two solutions proposed wherein the second solution is more comprehensive than the first one. However, both solutions are appreciable and significant improvements than the existing

models discussed in the introduction. The solution obtained from the first iteration is discussed in the next section. The results of this model is compared with the classical bicycle model. The shortcomings of this algorithm are studied and the author tries to overcome those in the second solution.

3.1 ALGORITHM FOR THE FIRST ITERATIVE MODEL

The first step is to design a vehicle dynamic model involving the physical parameters of the vehicle under consideration. The car model used for simulation of the developed algorithm is Mercedes CLS 63 AMG. The value of physical parameters pertaining to this car model are given in the appendix. The perturbation equations are found out for the three translational and rotational variables. Perturbation equations for Euler angles are also included. The detailed notation for variables included in the below equations can be found out in section "Perturbation Analysis".

Perturbation Equations for Translational Dynamics

$$m(\dot{u} + (Q_0 w + W_0 q) - (V_0 r + R_0 v)) = -mgcos\theta_0 \theta + f_x$$

$$m(\dot{v} + (R_0 u + U_0 r) - (P_0 w + W_0 p)) = -mgsin\theta_0 sin\Phi_0 \theta + mgcos\theta_0 cos\Phi_0 \emptyset) + f_y$$

$$m(\dot{w} + (P_0 v + V_o p) - (Q_0 u + U_0 q)) = -mg(cos\theta_0 sin\Phi_0 \emptyset + sin\theta_0 cos\Phi_0 \theta) + f_z$$

Perturbation Equations for Rotational Dynamics

$$\begin{bmatrix} 1 & -\frac{I_{xz}}{I_{xx}} \\ -\frac{I_{xz}}{I_{zz}} & 1 \end{bmatrix} \begin{Bmatrix} \dot{p} \\ \dot{r} \end{Bmatrix} = \begin{bmatrix} \frac{1}{I_{xx}}(I_{xz}(\mathrm{Q}_0 p + \mathrm{P}_0 q) + (I_{yy} - I_{zz})(\mathrm{R}_0 q + Q_0 r) + \mathrm{l}_A) \\ \frac{1}{I_{zz}}(-I_{xz}(\mathrm{R}_0 q + Q_0 r) + (I_{xx} - I_{yy})(\mathrm{Q}_0 p + \mathrm{P}_0 q) + \mathrm{n}_A) \end{bmatrix}$$

$$\begin{Bmatrix} \dot{p} \\ \dot{r} \end{Bmatrix} = \frac{1}{1 - \frac{{I_{xz}}^2}{I_{xx} I_{zz}}} \begin{bmatrix} 1 & \frac{I_{xz}}{I_{xx}} \\ \frac{I_{xz}}{I_{zz}} & 1 \end{bmatrix} \begin{bmatrix} \frac{1}{I_{xx}}(I_{xz}(\mathrm{Q}_0 p + \mathrm{P}_0 q) + (I_{yy} - I_{zz})(\mathrm{R}_0 q + Q_0 r) + \mathrm{l}_A) \\ \frac{1}{I_{zz}}(-I_{xz}(\mathrm{R}_0 q + Q_0 r) + (I_{xx} - I_{yy})(\mathrm{Q}_0 p + \mathrm{P}_0 q) + \mathrm{n}_A) \end{bmatrix}$$

$$\dot{q} = \frac{1}{I_{yy}}((I_{zz} - I_{xx})(\mathrm{R}_0 p + P_0 r) + 2I_{xz}(R_0 r - \mathrm{P}_0 p) + \mathrm{m}_A)$$

Perturbation Equations for Euler Angles

$$\dot{\phi} = p + tan\Theta_0(sin\Phi_0 q + cos\Phi_0 r + (Q_0 cos\Phi_0 - R_0 sin\Phi_0)\phi) + (Q_0 sin\Phi_0 + R_0 cos\Phi_0 + (\dot{\Phi}_0 - P_0)tan\Theta_0)\theta$$

$$\dot{\theta} = cos\Phi_0 q - sin\Phi_0 r - (Q_0 sin\Phi_0 + R_0 cos\Phi_0)\phi$$

$$\dot{\psi} = \dot{\Psi}_0 tan\Theta_0 \theta + (sin\Phi_0 q + cos\Phi_0 r - (R_0 sin\Phi_0 - Q_0 cos\Phi_0)\phi)/cos\Theta_0$$

The most important task here is to formulate the perturbation forces and moments to apply the above equations. The perturbation forces are f_x, f_y and f_z while the perturbation moments are l_A, n_A and m_A. The perturbation force in the x direction comes from the varying longitudinal slip with each iteration for the four wheels. Considering, that we know this slip we can calculate corresponding forces generated from the given longitudinal tire stiffness. Similarly, the lateral forces can be calculated from the lateral stiffness of the tires times the slip angle. The slip angles are different for all the wheels depending upon the maneuver taken and hard to calculate analytically. However, expressing theses force terms using formulations used in the bicycle models gives a good solution i.e.

$$f_y = \left(-\frac{a}{U}C_{\alpha f} + \frac{b}{U}C_{\alpha r}\right)r - \left(C_{\alpha f} + C_{\alpha r}\right)v/U + (C_{\alpha f})\delta \qquad 3.1$$

Where $C_{\alpha f}$ and $C_{\alpha r}$ values are twice the stiffness of each front and rear tire respectively, a and b are the distance of COM from the front axle and rear axle respectively. The small letters as before denote perturbations while the capital ones represent the reference state values. Also we know, δ is the steering angle of the wheels in radians and not the hand steer angle given by the driver. Since the terms $-\frac{a}{U}C_{\alpha f} + \frac{b}{U}C_{\alpha r}$ and $-\left(C_{\alpha f} + C_{\alpha r}\right)/U$ are bulky and would be repeated they are denoted by variables

'One' and 'Two' in the MATLAB script given in the appendix. Once, the lateral force perturbations are mathematically modelled the next step is derive longitudinal force perturbations in a similar manner.

$$F_{Total} = F_f + F_r - R_a - R_r - Wsin\theta - R_d \quad 3.2$$

0

The rolling resistance does not change much so we neglect it in the perturbation equations. The component of weight contributing to the longitudinal force equation has already been included in the longitudinal perturbation equations above. Also, no toeing force is considered.

The traction/braking force at the four wheels (considering a four wheel drive) can be calculated from the slip and longitudinal tire stiffness. Also, the perturbation in aerodynamic force is accounted for by inclusion of the term Cd*Surface*U*u*Rho where Cd is the aerodynamic coefficient, Surface represents the outer surface area of the car model and Rho represents the air density. The slips are randomly generated at the four wheels and there effect seen on the longitudinal dynamics because we haven't figured out a way to quantify slips from driver inputs till now. No suspension modelling is done in this iteration which basically yields zero perturbation in the vertical forces. The next step is to find the perturbations in moments along the three axes. Let us start with the longitudinal or X axis. The moment along X axis or l_A can be attributed to forces in the Z and Y direction. Since we aren't assuming any perturbation in Z direction for this solution iteration, the moment $l_A$can be a representative of forces in Y direction exclusively. Now the moment is force times distance which the height of the COM from the ground. Mathematically representing the above information boils down into.

$$h * \left(\left(-\frac{a}{U} C_{\alpha f} + \frac{b}{U} C_{\alpha r} \right) r - \left(C_{\alpha f} + C_{\alpha r} \right) {}^{v}/_{U} + \left(C_{\alpha f} \right) \delta \right) \quad 3.3$$

$$= h * \left(One * m * r - Two * m * v + \left(C_{\alpha f} \right) * \delta \right)$$

The moment along Y axis or m_A can be attributed to forces in the Z and X direction. Since we aren't assuming any perturbation in Z direction for this solution iteration, the moment $m_A$can be a representative of forces in X direction exclusively. Now the moment is force times distance which the height of the COM from the ground. Mathematically representing the above information results into$h *$ $C_{LongStiffness} * slip$ for all the four tires.

The moment along Z axis or n_A can be attributed to forces in the X and Y direction. Where the moment arms for forces in the x direction n are decided by the wheel track and the COM location. While the moment arms for the forces in the y direction are calculated by the wheel base and the position of COM. Refer to the schematic diagram of the car shown below.

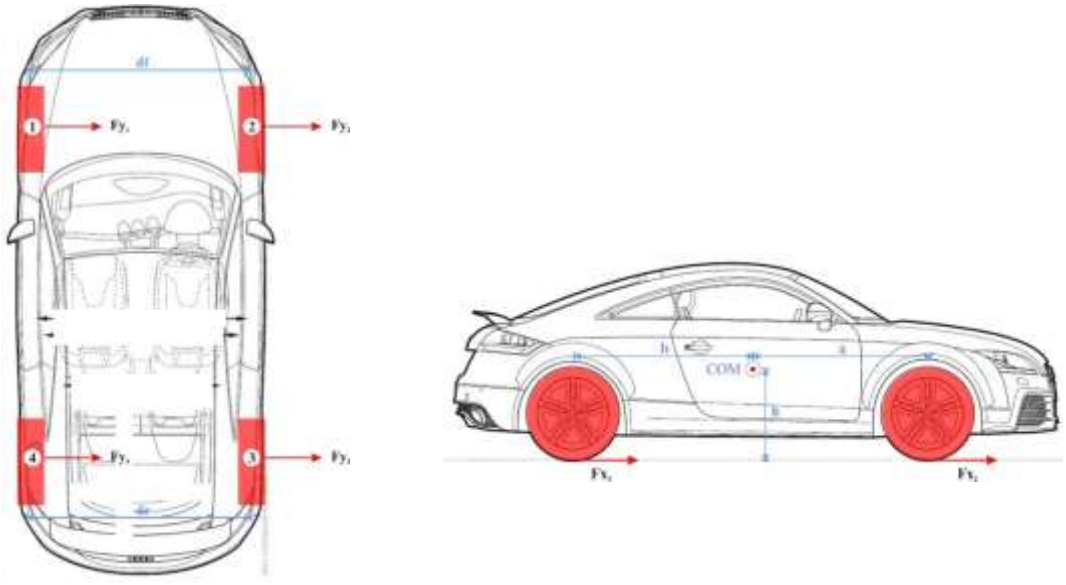

Figure 3.1: Forces along the X and Y axes of the wheels

The tires are numbered in the order of front left, front right, rear right and rear left respectively. The moment equation in the z direction can therefore be formulated as below:

$$N= (a*(F_{y1} + F_{y2}) - b*(F_{y3} + F_{y4}))+ (\frac{df}{2}*(F_{x1} + F_{x4}) - \frac{dr}{2}*(F_{x3} + F_{x2})); \quad 3.4$$

Where, F_{yi} denotes the lateral force on the ith wheel.Similarly F_{xi} denotes the longitudinal force on the ith wheel.

Here we assume that $\frac{df}{2} = \frac{dr}{2}$ i.e. the wheel track in the front and the rear is the same. Now, once we have the moment in all the three directions we can substitute the same in the perturbation equations. The next important task is to separate and arrange these equations in a state space form for simulation. The nine states of the vehicle (x) are [u v w p q r$\emptyset$ θ ψ]. The A matrix or the state space matrix would involve terms pertinent to these states. The B matrix would include terms pertinent to the inputs for this iterative model which is the slip at four wheels and the wheel steering angle. Arranging the terms accordingly leads to a state space form which can be conveniently simulated to track changes in the translational, rotational variable and the Euler angles too with time. The code is given in the appendix for eager readers to develop a deeper insight into modelling. An input of wheel steering angle is given to the model together with random but equal slips at the four wheels to calculate the lateral and longitudinal forces. The bicycle model is simulated for the same steering input and the results are compared and shown in the next section.

3.2 SIMULATION RESULTS FROM THE ALGORITHM FOR THE FIRST ITERATIVE MODEL

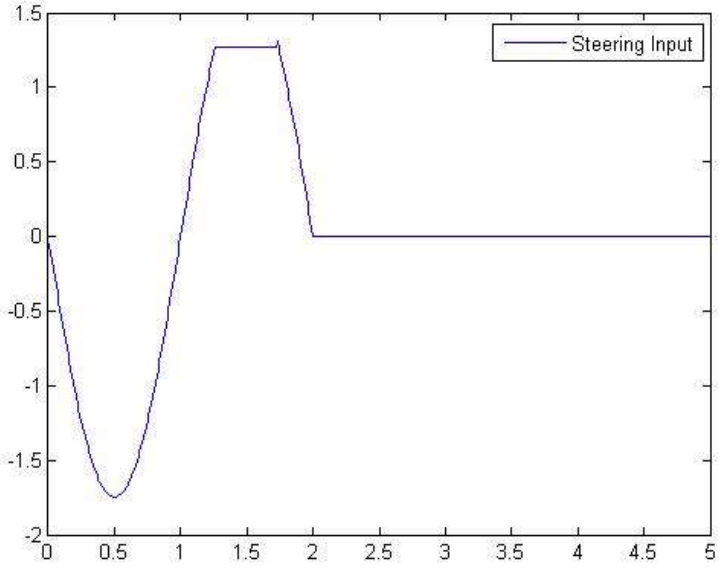

Figure 3.2: Steering input (rad) vs time (s)

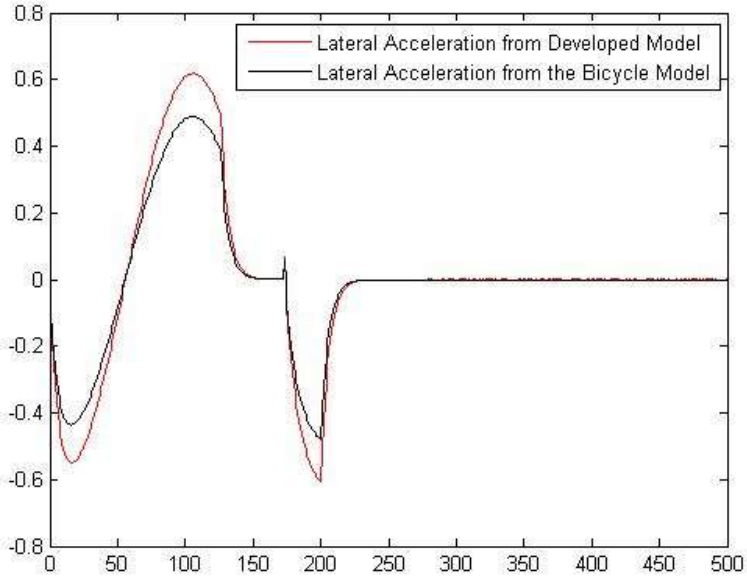

Figure 3.3: Lateral acceleration (/g) vs time (s)

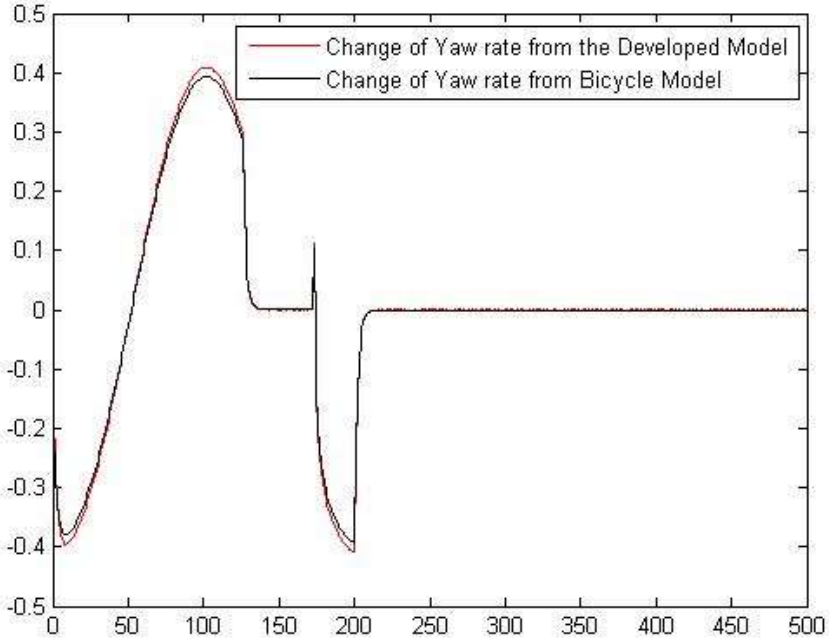

Figure 3.4: Change of Yaw rate (rad/s^2) vs time (s)

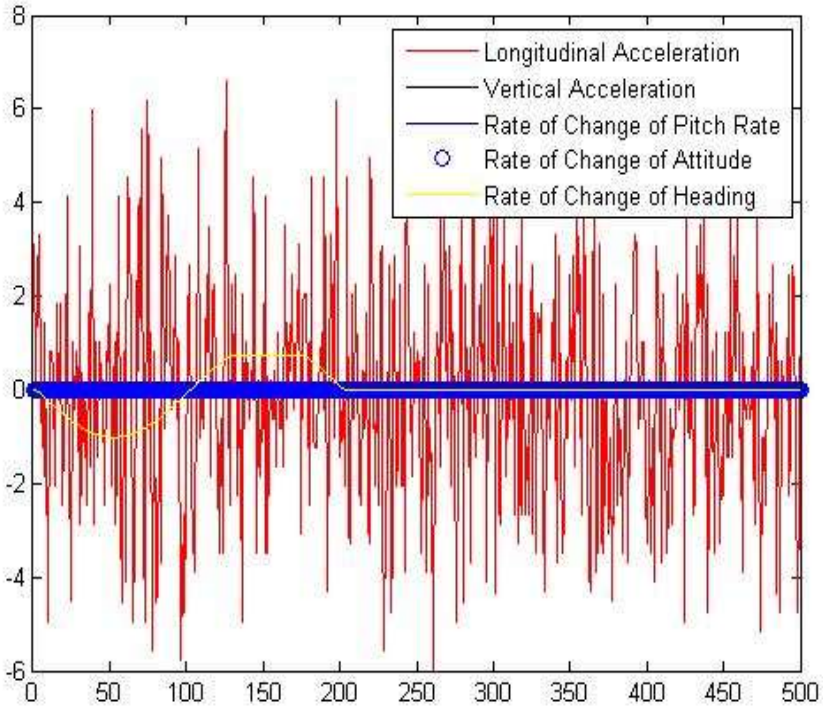

Figure 3.5: Longitudinal acceleration (m/s^2) vs time (s)

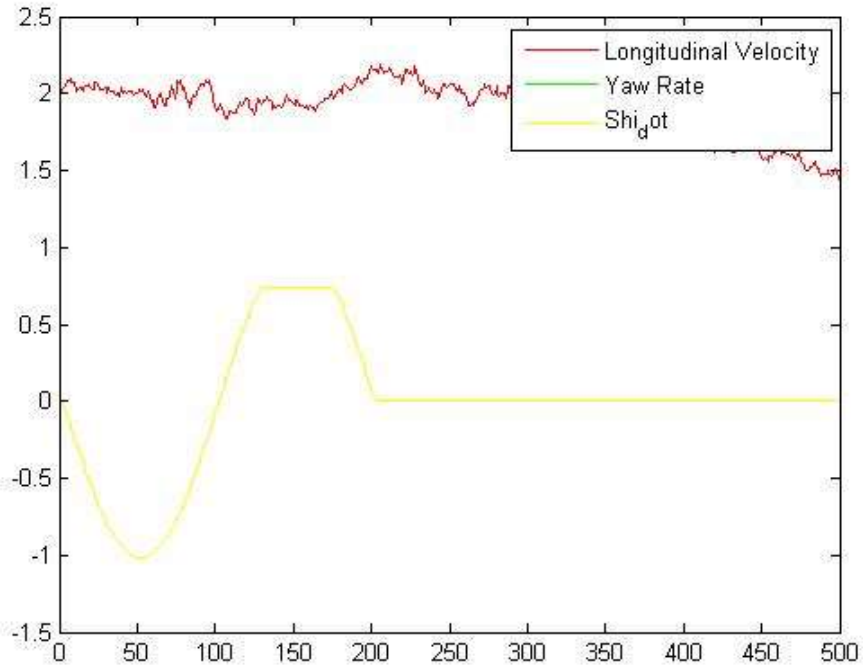

Figure 3.6: Longitudinal velocity (m/s) vs time (s)

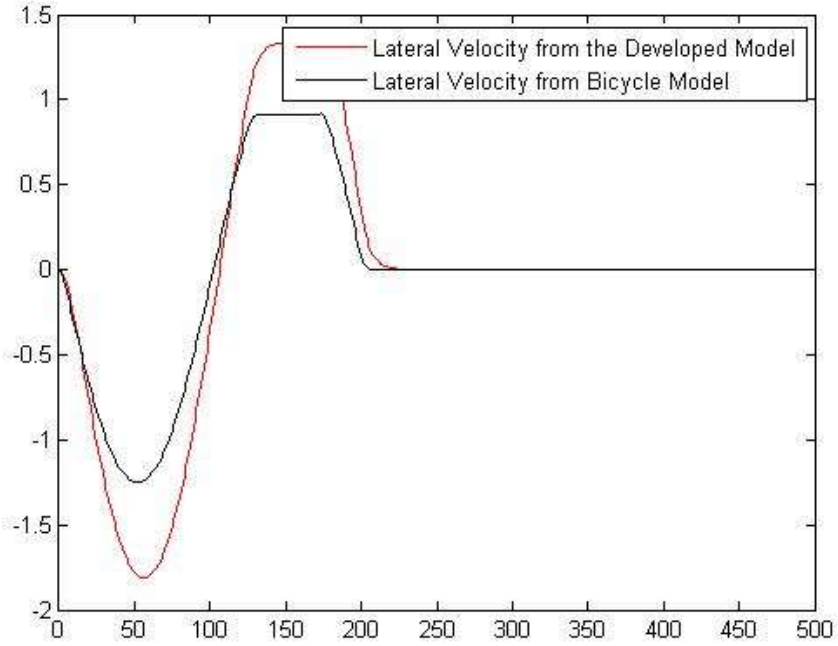

Figure 3.7: Lateral velocity (m/s) vs time (s)

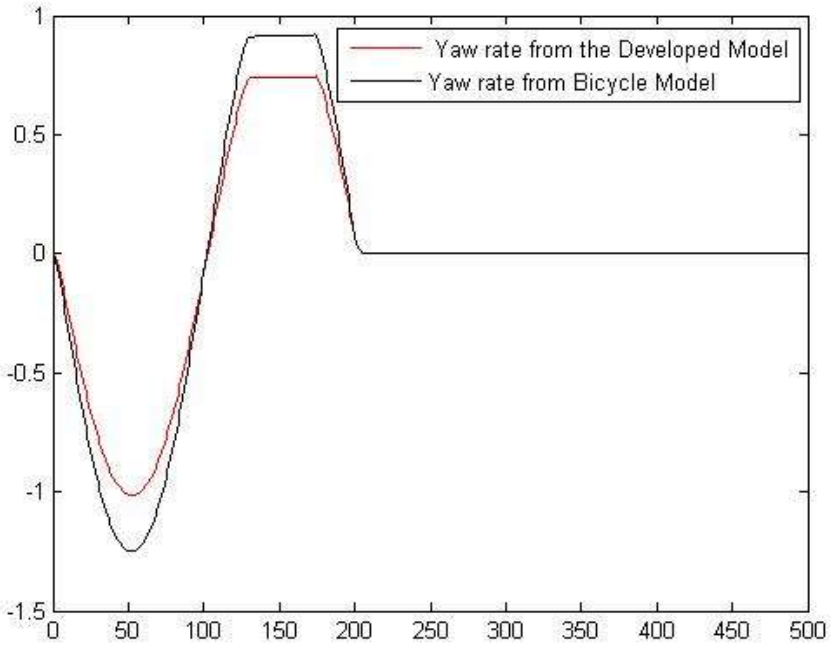

Figure 3.8: Yaw rate (rad/s) vs time (s)

A different steering input from the above scenario leads to the following outputs:

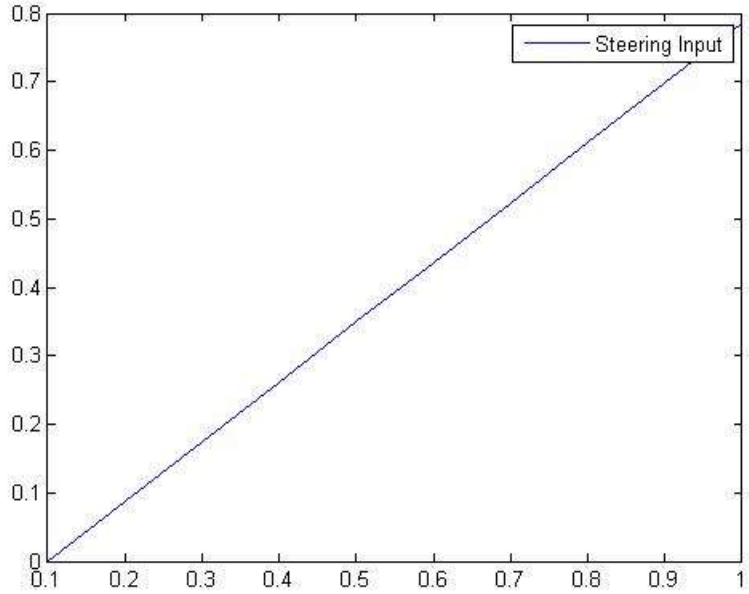

Figure 3.9: Steering input (rad) vs time (s)

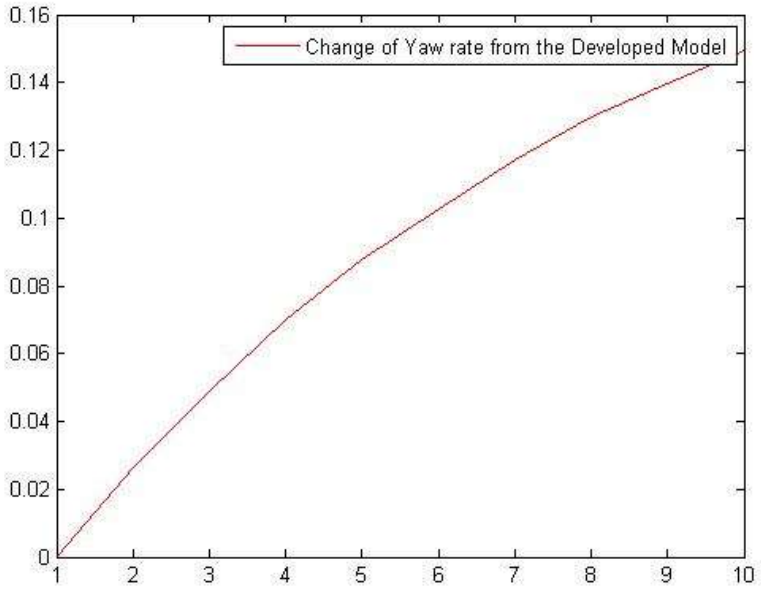

Figure 3.10: Change of Yaw rate (rad/s^2) vs time (s)

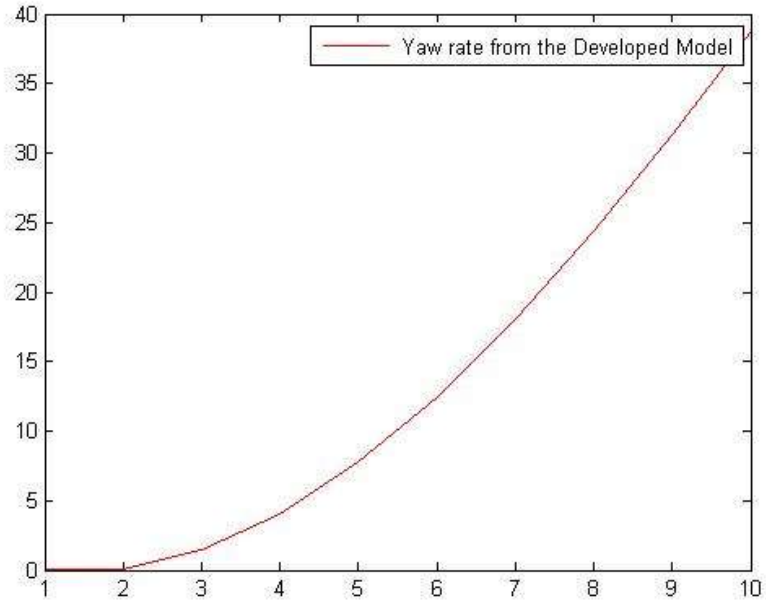

Figure 3.11: Yaw rate (rad/s) vs time (s)

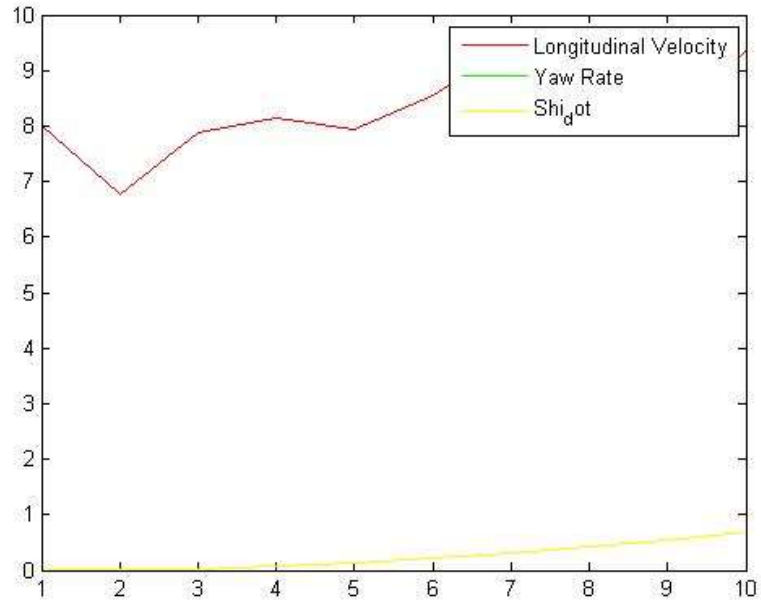

Figure 3.12: Longitudinal velocity (m/s) vs time (s)

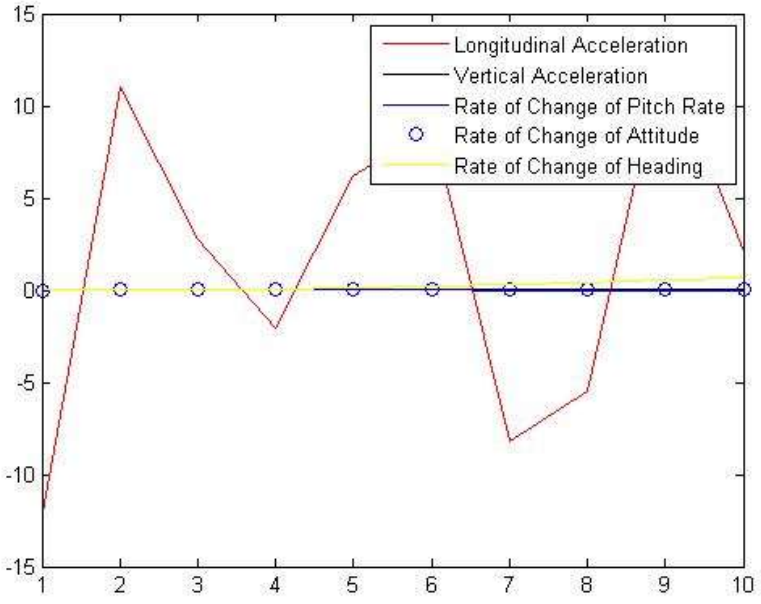

Figure 3.13: Longitudinal acceleration (m/s^2) vs time (s)

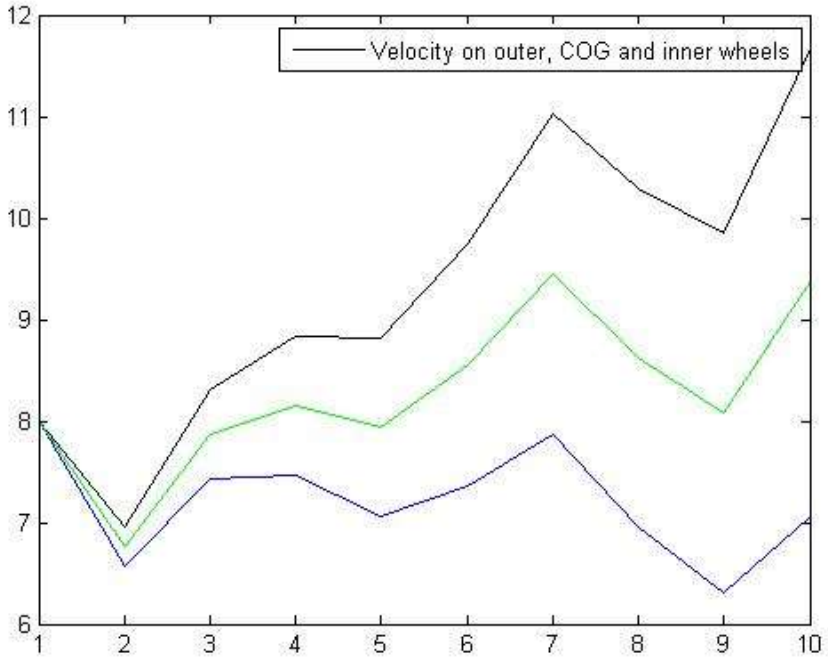

Figure 3.14: Velocity on outer, COG and inner wheels (m/s) vs time (s)

If we give zero acceleration/braking to the car throughout the maneuver the graph would look like below:

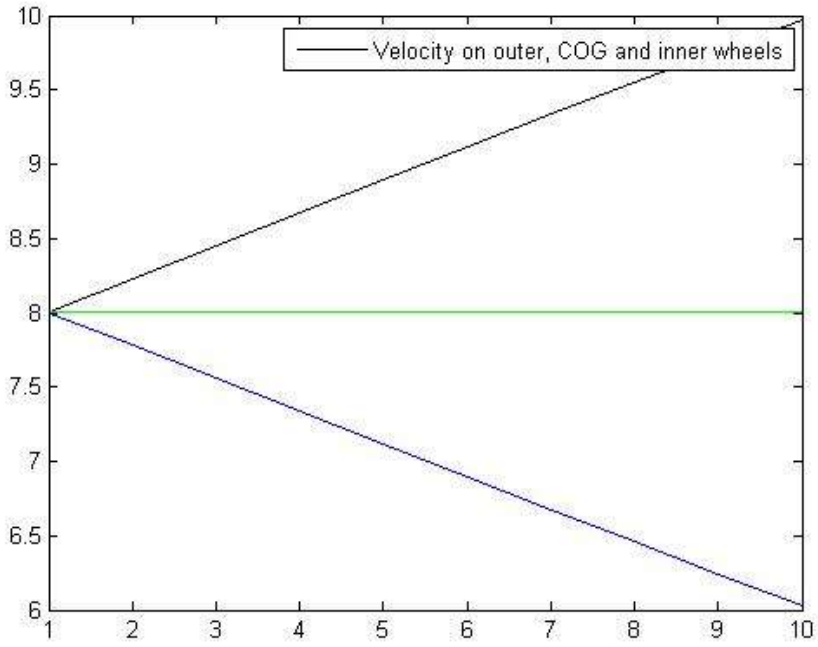

Figure 3.15: Velocity on outer, COG and inner wheels (m/s) without longitudinal input vs time (s)

The first iterative model can estimate the nine states of the vehicle. • Longitudinal Velocity • Lateral Velocity • Vertical Velocity • Roll Rate • Pitch Rate • Yaw Rate • Euler Roll Angle • Euler Pitch Angle • Euler Yaw Angle (Euler angles can be used for navigation calculations, tracking or for various algorithms in connected vehicles). It also considers the dynamic coupling of longitudinal, lateral and vertical parameters and can simulate transient dynamics in comparison to just the steady state dynamics which assumes constant longitudinal velocity while a cornering maneuver in Bicycle Model. The built model also includes the effects of aerodynamics. However, it does not include suspension modelling which is very crucial for understanding dynamics of the vehicle. It also does not address lateral & longitudinal load transfers nor has a robust tire model. The longitudinal and lateral tire stiffness are assumed constant though in real scenario they vary a lot. Another major drawback of this model is that it does not take accelerating/braking inputs and therefore does not calculate longitudinal slip and hence, longitudinal forces accurately.

3.3 ALGORITHM FOR THE SECOND ITERATIVE MODEL

As discussed above, the first iteration of the algorithm has several advantages over the bicycle model. However, it still has many loopholes to counter and this iteration of the algorithm attempts to do so. Since, this model aims to incorporate the physics behind the assumptions taken in the first iteration, we need to include more physical parameters and values. As far as the car dimensions, lengths, inertias and position of COM etcetera were concerned, they were easily available and added to the algorithm. The major additions to the algorithm have been explained below. The first step is to find the longitudinal slip and slip angles for precise calculation of the tire forces. It is these tire forces that move the vehicle and control the states of the vehicles we wish to calculate. First let us try formulating the side slip of the vehicle. Side slip informs us about the deviation of the resultant velocity of the vehicle from the longitudinal x axis. The angle between the resultant velocity vector and the longitudinal velocity gives us the side slip of the angle and the tangent of this angle is simply the ratio of the lateral velocity with the longitudinal velocity of the vehicle COM. For calculating this ratio for the four wheels we would have to first derive the relation between COM velocities and the tire velocities. The X_State_Matrix (i,2) gives lateral velocity of the COM while the X_State_Matrix (i,1) gives its longitudinal velocity. The X_State_Matrix (i,6) denotes the yaw rate of the vehicle. Given these state values one can easily find the velocities at the wheels given that we already know the required distances of the tire centers from the COM.

For example, let us consider the first tire. The COM is at a distance of a/lf units from the tire center. The yaw rate which follows the right hand rule is positive when the Z axis points downward for the given axis system. Thus the contribution of this yaw rate to the lateral velocity at the first tire would be in the negative x direction. Similarly, df/2 is the distance of the COM from the tire in lateral direction

and this again will contribute negatively in case of longitudinal velocity. The velocities of other tire centers are found in the same fashion and are given below:

```
                        Tan(Side_slip_at_tire_1)=                          3.5
                          (X_State_Matrix(i,2)-
          lf*X_State_Matrix(i,6)/2)/(X_State_Matrix(i,1)-
                     df*X_State_Matrix(i,6)/2);

                        Tan(Side_slip_at_tire_2)=
(X_State_Matrix(i,2)  - lf*X_State_Matrix(i,6)/2)/(X_State_Matrix(i,1)+
                     df*X_State_Matrix(i,6)/2);

                        Tan(Side_slip_at_tire_3)=
(X_State_Matrix(i,2)  + lr*X_State_Matrix(i,6)/2)/(X_State_Matrix(i,1)+
                     dr*X_State_Matrix(i,6)/2);

                        Tan(Side_slip_at_tire_4)=
(X_State_Matrix(i,2)  + lr*X_State_Matrix(i,6)/2)/(X_State_Matrix(i,1)-
                     dr*X_State_Matrix(i,6)/2);
```

Since, the car model is front steered we calculate the slip angles at the four wheels as given below. For readers who are confused between side slip and slip angle, the author desires to clarify once more. Side slip is the angle between the longitudinal axis of the vehicle and the resultant velocity of the vehicle. This should ideally be equally to the steer angle given to the wheels. But it is observed that this is not the case. The difference between the steer angle to the wheels and the side slip of the tires therefore gives us the slip angle. Following the same line of thought, the formulations for the slip angles of the wheel are given as:

```
Alpha_1=  atan(Tan(Side_slip_at_tire_1))-Steering_Angle(i,1);      3.6

 Alpha_2=  atan(Tan(Side_slip_at_tire_2))-Steering_Angle(i,1);

           Alpha_3=  atan(Tan(Side_slip_at_tire_3));

           Alpha_4=  atan(Tan(Side_slip_at_tire_4));

            Alpha=[Alpha_1;Alpha_2;Alpha_3;Alpha_4];
```

Considering that the initial yaw rate is zero (The program can handle initial non-zero yaw rate too), the initial longitudinal velocities of the four wheel would be same as the longitudinal velocity of the wheel.

However, after an accelerator or brake pedal input this would change the rotational and hence translational velocities of the wheels.

```
d_Ohmega_R(1:4,i)=
[537.7;537.7;551.6;551.6]*acceleration(i,1)*R*dt*Inertia_Inverse;
```
3.7

Where d_Ohmega_R is the change in the translational velocities caused by the pedal input. The equation is simply the Torque equation given by Torque= Inertia*Angular Acceleration. Now the longitudinal slip at the wheel base is:

```
Longitudinal Slip =
(Angular_velocity of the wheel*Radius of the
wheel/Velocity of the ground or vehicle)-1;
```
3.8

Taking this formulation forward we get:

```
Slip_1= (Angular_velocity1*Radius(1,i+1)/X_State_Matrix(i,1))-1;
```
3.9

```
Slip_2= (Angular_velocity2*Radius(2,i+1)/X_State_Matrix(i,1))-1;
Slip_3= (Angular_velocity3*Radius(3,i+1)/X_State_Matrix(i,1))-1;
Slip_4= (Angular_velocity4*Radius(4,i+1)/X_State_Matrix(i,1))-1;
Slip=[Slip_1; Slip_2; Slip_3; Slip_4];
```

Once we have the longitudinal slip and the slip angles we can calculate the tire forces generated by them provided we know the tires stiffness variations. However, as explained previously this data is hard to get analytically. There are only few analytical models available which don't require any experimental determination of tire forces. However, these models require certain parameters as input to the algorithm which are again hard to obtain especially when there are tons of tire varieties out there in the market. The paper by Salani provides a solution to the above problems by not only formulating the tire mechanics but also providing a detailed list of values of different tire parameters and dimensions. The complete tire model can be found in the appendix and readers who are enthusiastic are urged to have a look if possible. It becomes very important to state here the need of such modeling preferably through a figure which shows the range of variation of both longitudinal and lateral tire stiffness with

slip and slip angles. The experimental variation is shown by the red curve while the blue curve depicts analytical determination of the tire stiffness obtained analytically through the model by Salani.

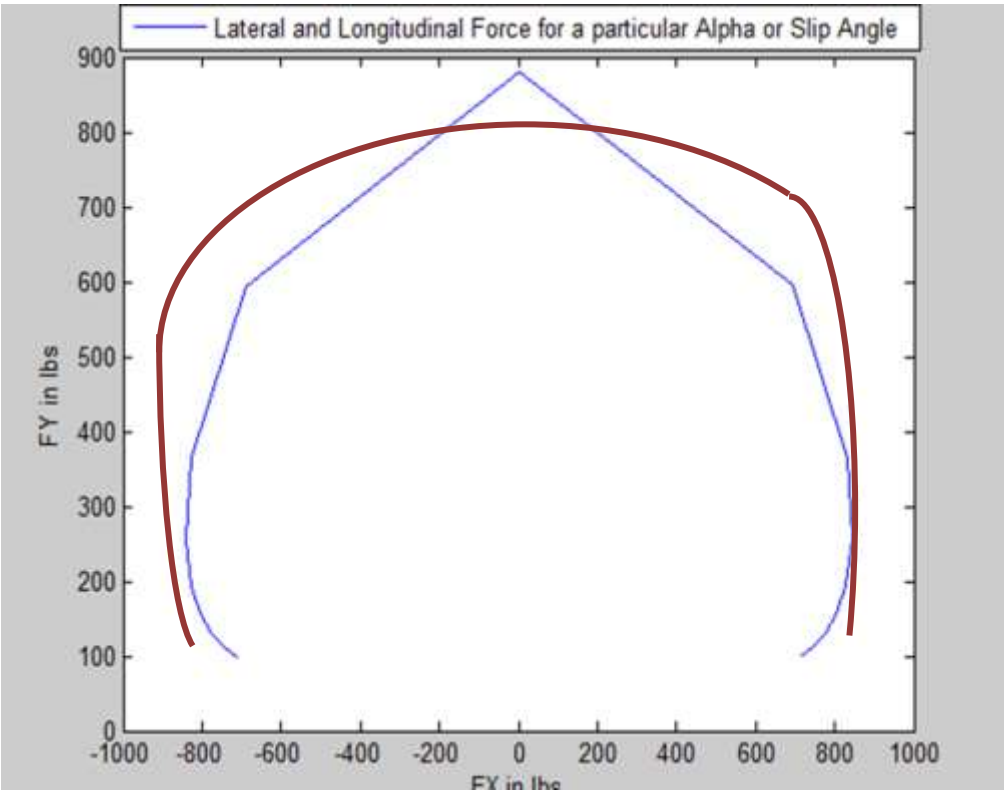

Figure 3.16: Experimental (red) and analytical (blue) tire forces

The tire model gives us the forces originating for the corresponding inputs in pounds which can be conveniently converted to Newton by a multiplication factor of 4.4. Once we have the forces both in X, Y direction we need to find the weight transfer in the Z direction because of lateral and longitudinal load transfer during steering or braking/accelerating inputs respectively as formulated below using moment balance equations. Again, as a reminder, *Delta* is the steering input to the front wheels. Finally, for formulating the forces on the suspensions in the Z direction, the forces along the wheel X and Y axis have to be known. The lateral or Y axis forces at the four centers of the wheel can be mathematically expressed as given. After, quantifying the forces on the X and Y axis, the forces along the Z axis can be modeled conveniently.

```
%Fside1 = Fx1*sin (Delta) + Fy1*cos (Delta)
```

3.10

```
%Fside2 = Fx2*sin (Delta) + Fy2*cos (Delta)

%Fside3 = Fy3

%Fside4 = Fy4

                %%Normal Forces

%Fz_1= (1/2*L)*(mg*lr-h*F_X) + (h/df)*(Fside1 + Fside2)
```

3.11

```
%Fz_2= (1/2*L)*(mg*lr-h*F_X) + (h/df)*(Fside1 + Fside2)

%Fz_3= (1/2*L)*(mg*lf-h*F_X) + (h/df)*(Fside3 + Fside4)

%Fz_4= (1/2*L)*(mg*lf-h*F_X) + (h/df)*(Fside3 + Fside4)
```

3.4 SIMULATION RESULTS FROM THE ALGORITHM OF THE SECOND ITERATIVE MODEL

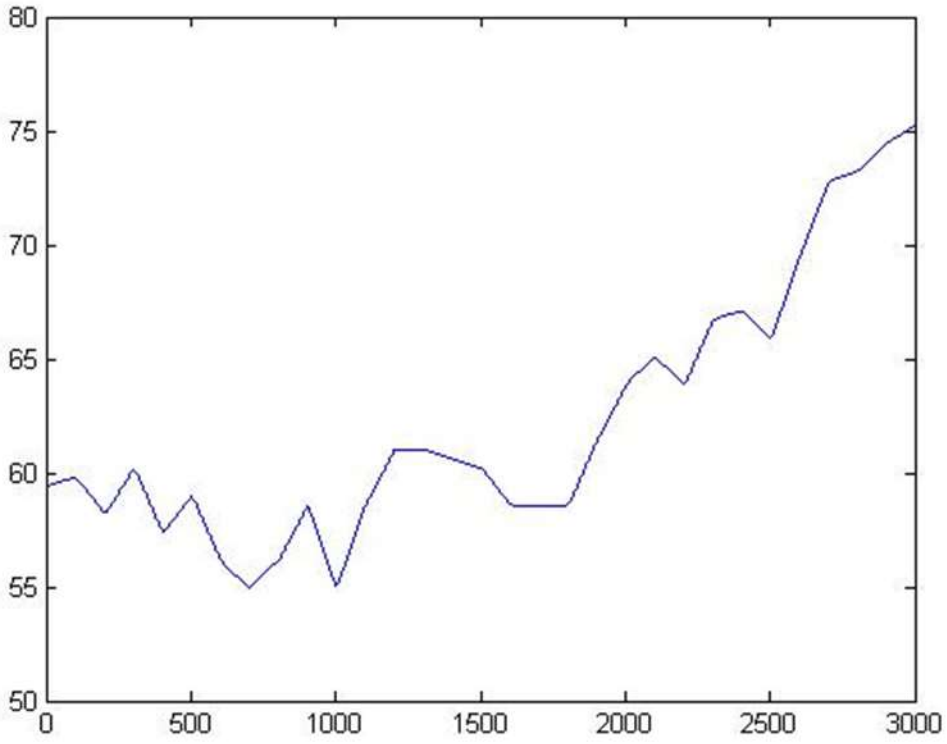

Figure 3.17: Longitudinal velocity (km/hr) vs time (s)

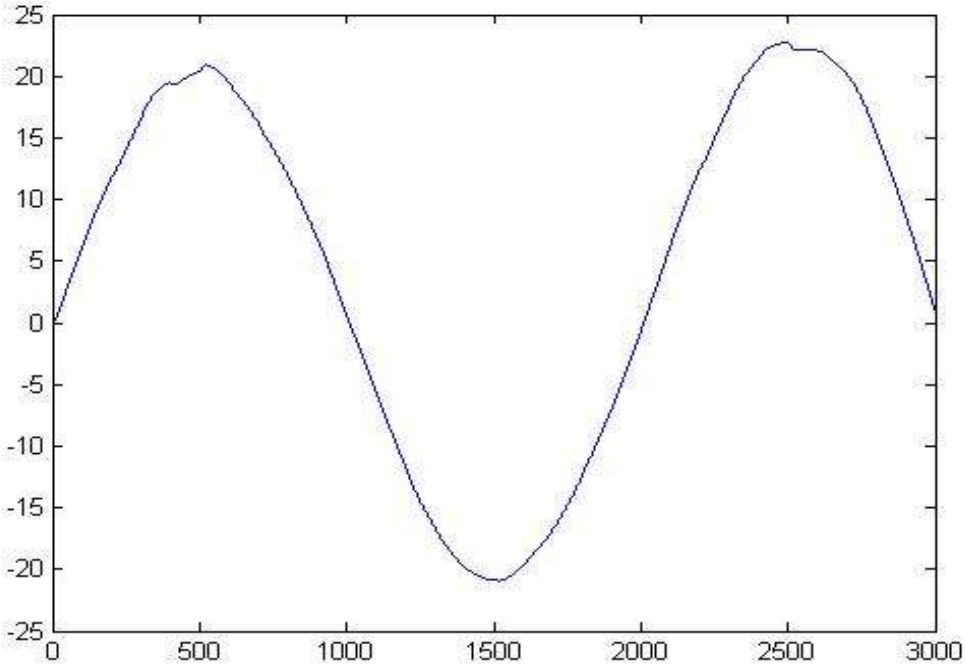

Figure 3.18: Lateral velocity (km/hr) vs time (s)

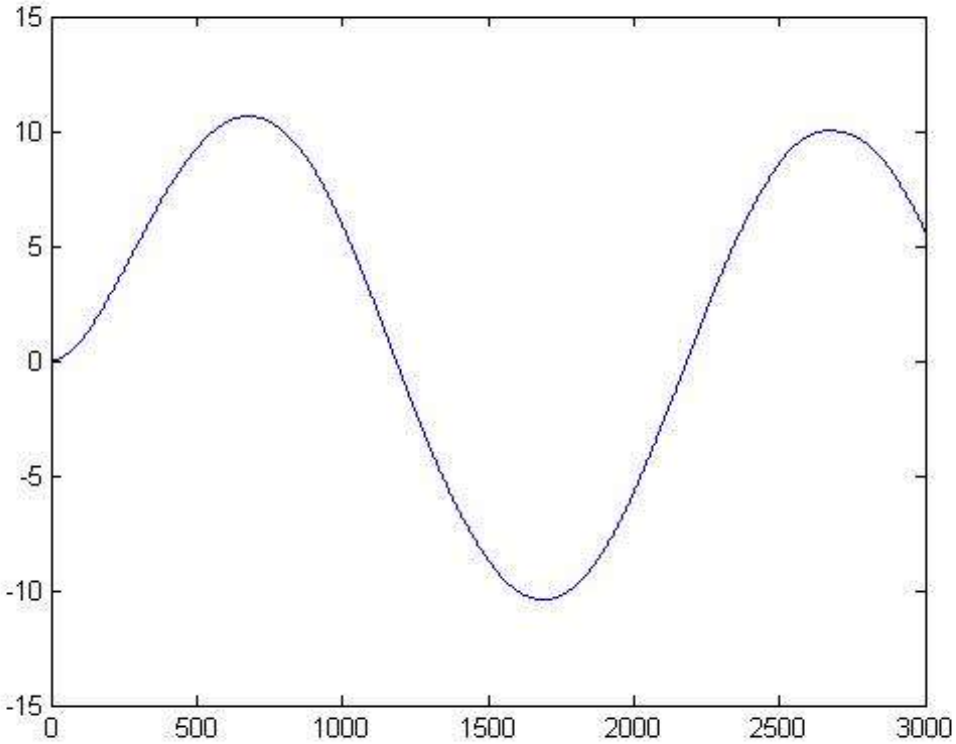

Figure 3.19: Yaw velocity (deg/s) vs time (s)

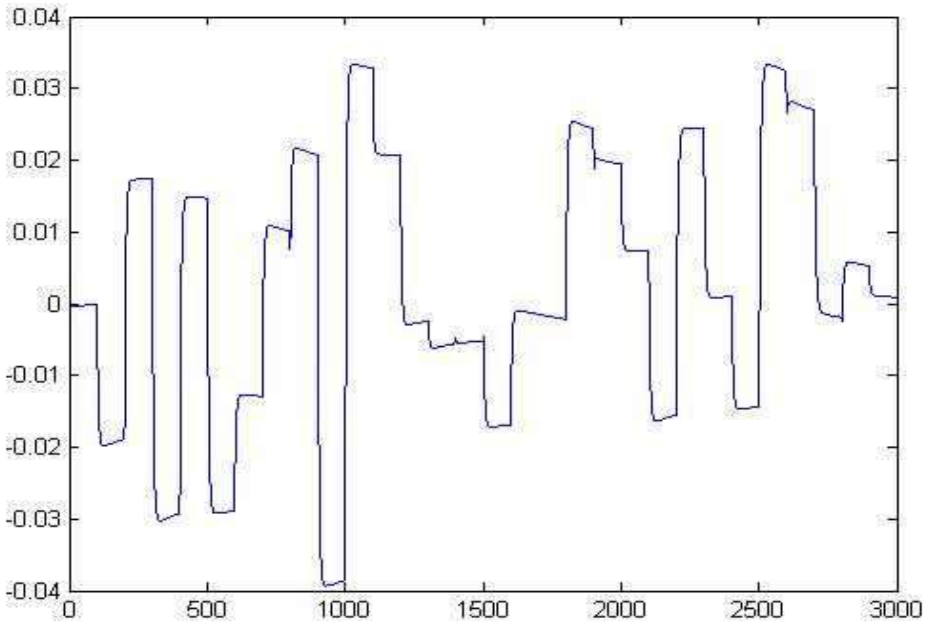

Figure 3.20: Vertical velocity (km/hr) vs time (s)

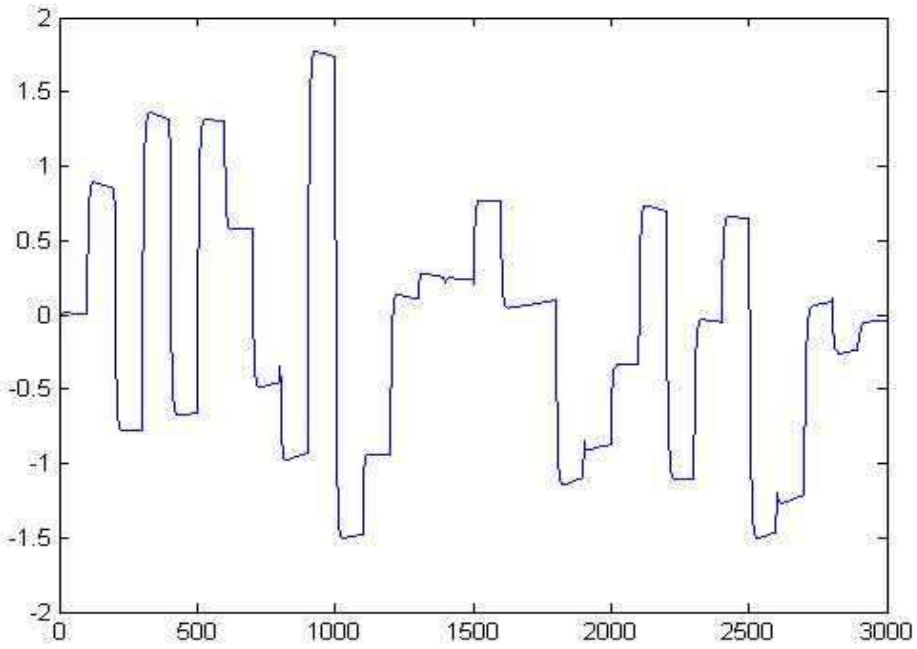

Figure 3.21: Pitch rate (rad/s) vs time (s)

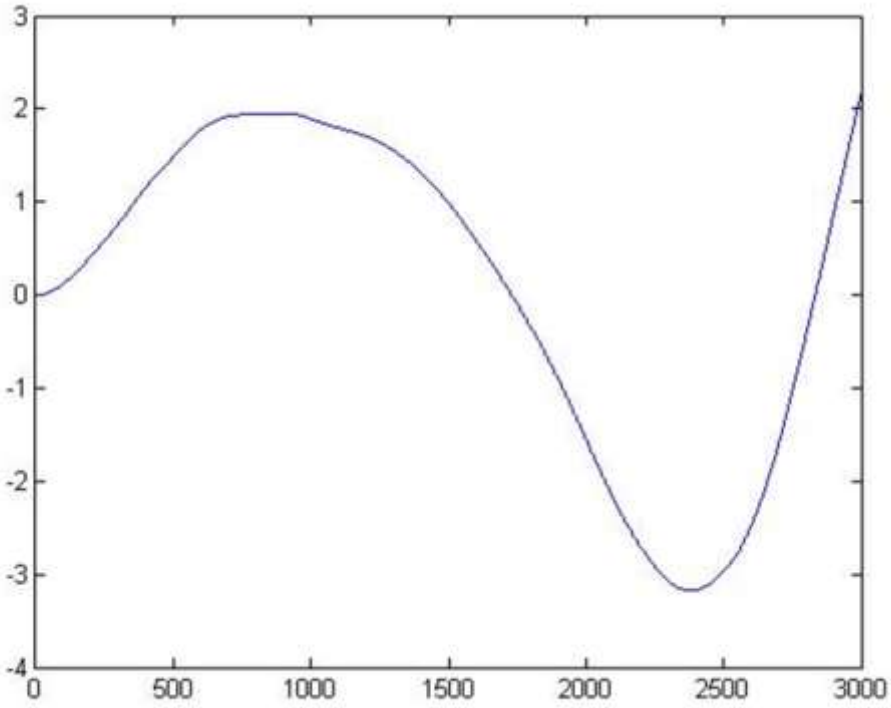

Figure 3.22: Roll rate (rad/s) vs time (s)

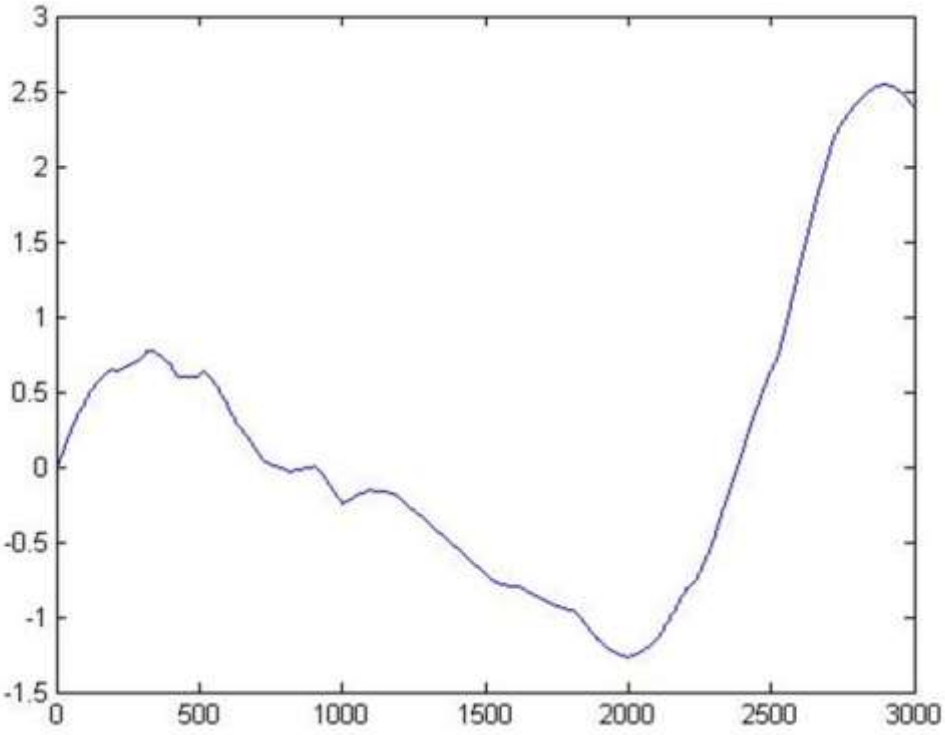

Figure 3.23: Euler roll rate (rad/s) vs time (s)

3.5 VERIFICATION OF THE RESULTS OBTAINED FROM THE ALGORITHM THROUGH CARSIM

CarSim delivers the most accurate, detailed, and efficient methods for simulating the performance of passenger vehicles and light-duty trucks. With twenty years of real-world validation by automotive engineers, CarSim is universally the preferred tool for analyzing vehicle dynamics, developing active controllers, calculating a car's performance characteristics, and engineering next-generation active safety systems.

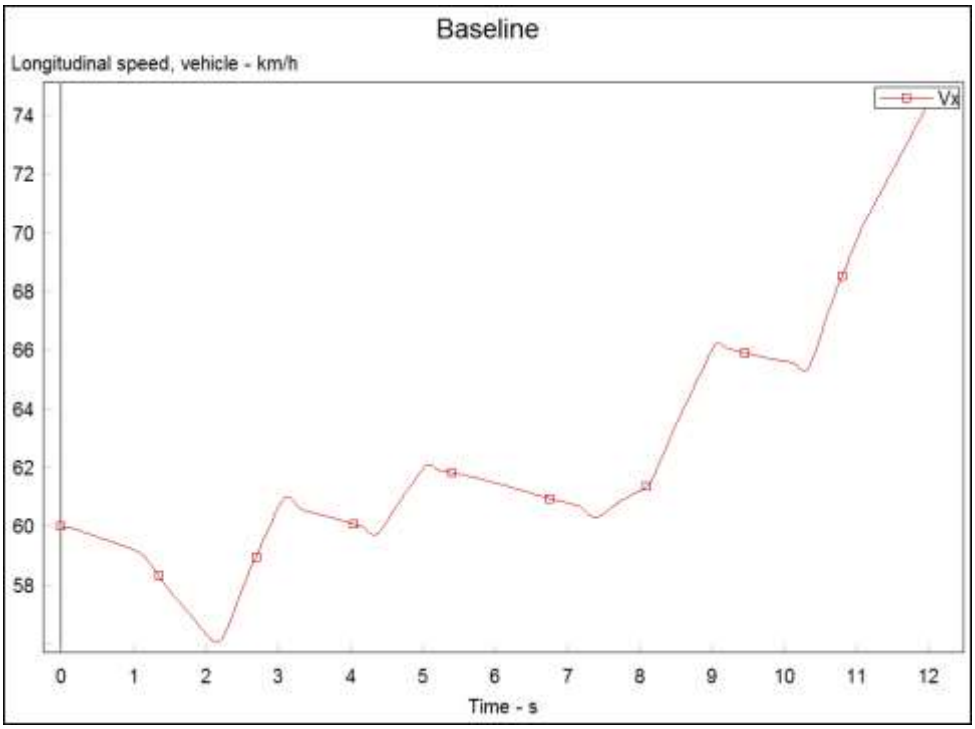

Figure 3.24: Longitudinal velocity (km/hr) vs time (s)

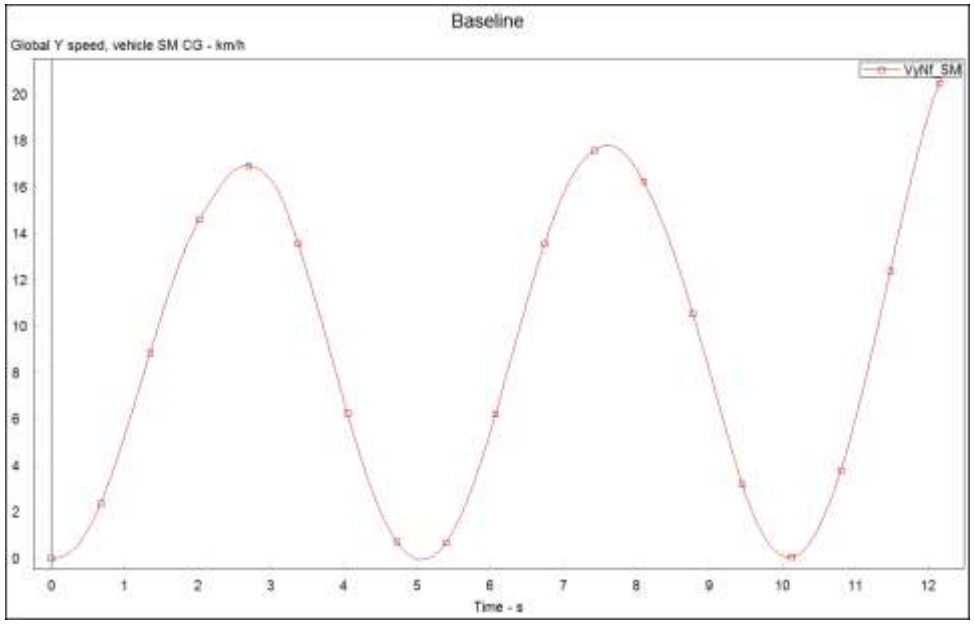

Figure 3.25: Lateral velocity (km/hr) vs time (s)

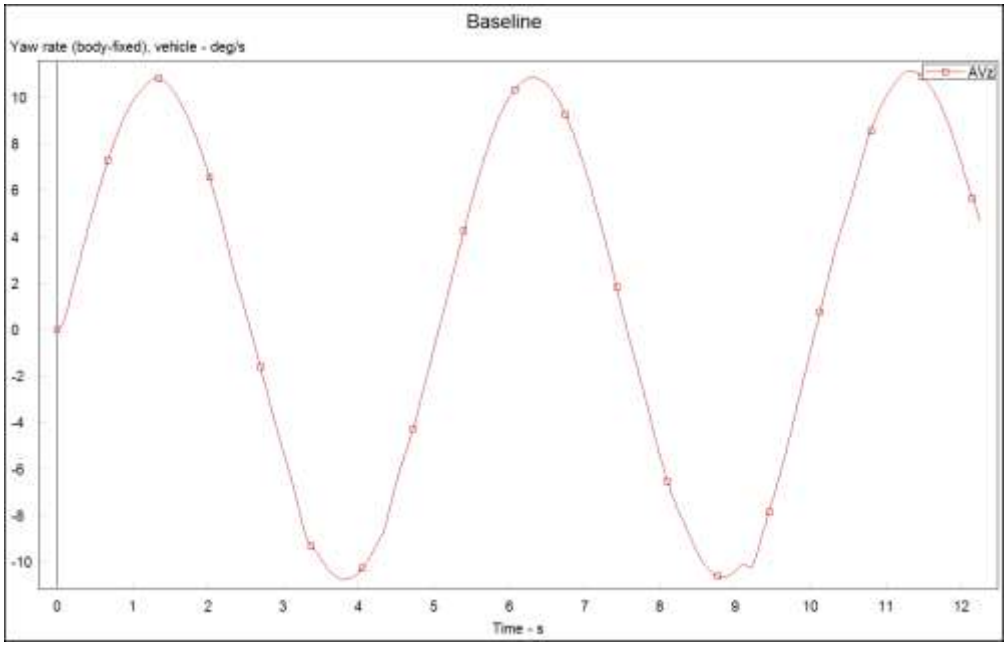

Figure 3.26: Yaw velocity (deg/s) vs time (s)

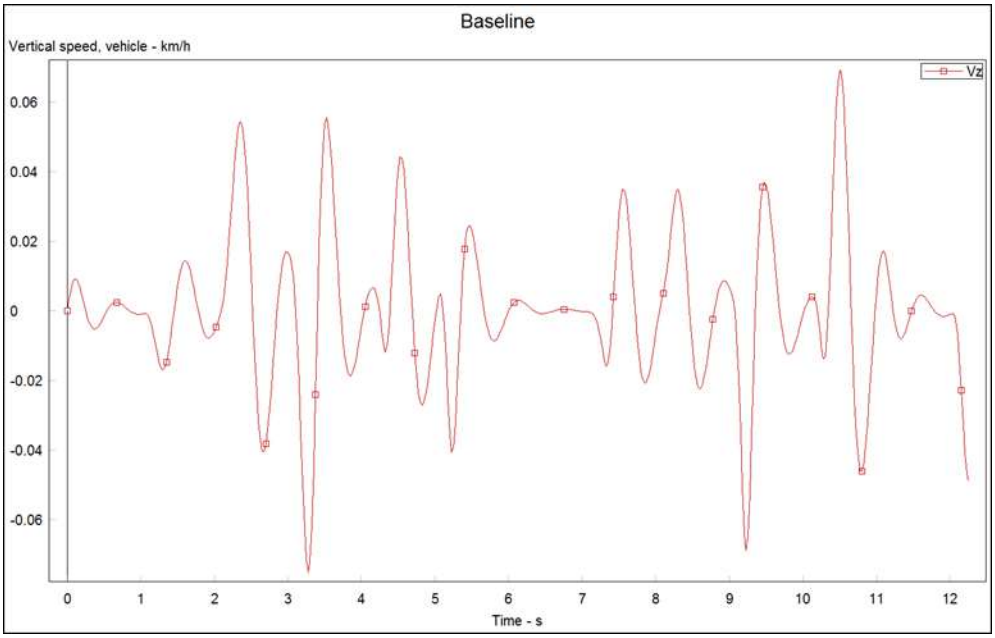

Figure 3.27: Vertical velocity (km/hr) vs time (s)

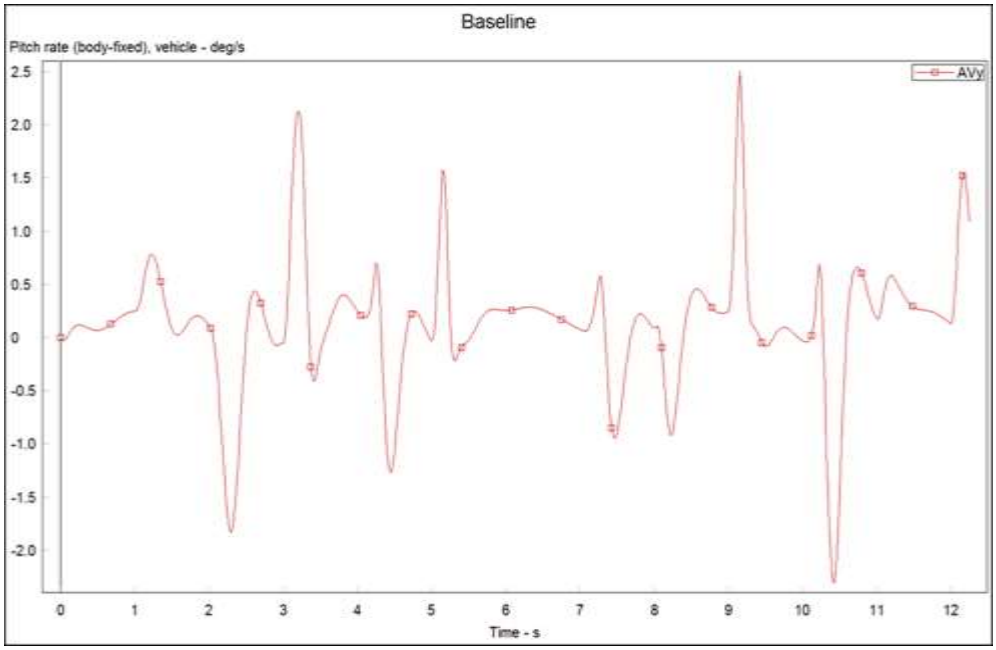

Figure 3.28: Pitch rate (rad/s) vs time (s)

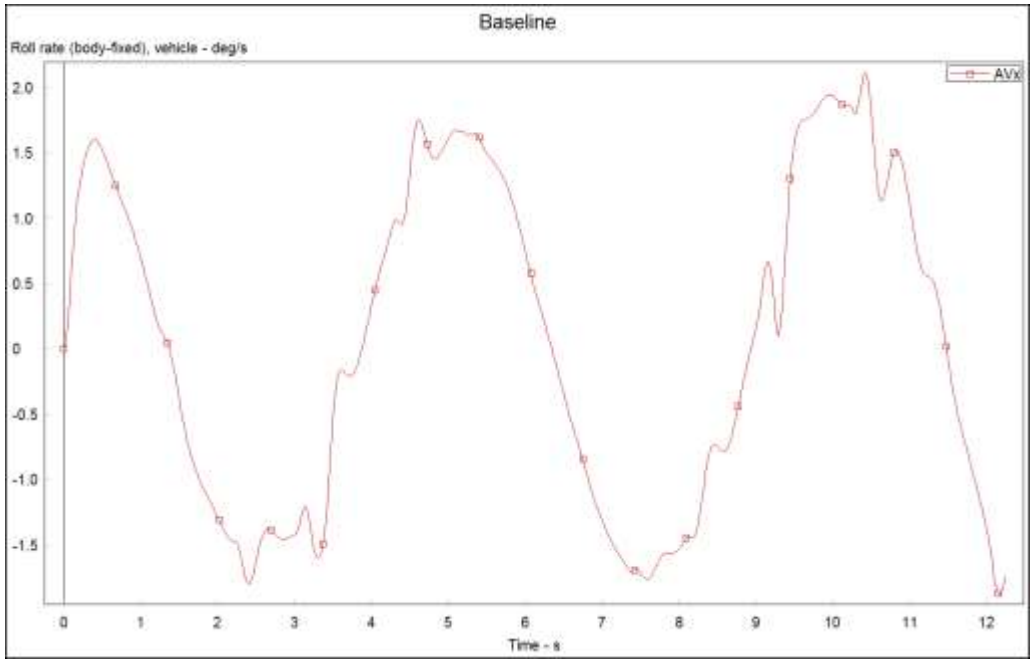

Figure 3.29: Roll rate (rad/s) vs time (s)

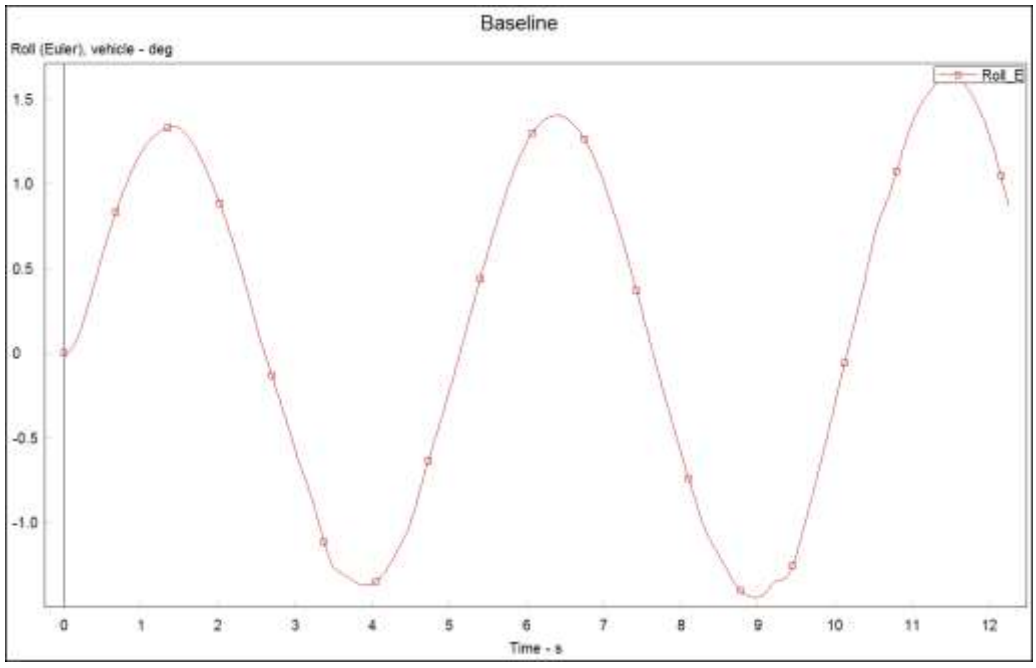

Figure 3.30: Euler roll rate (rad/s) vs time (s)

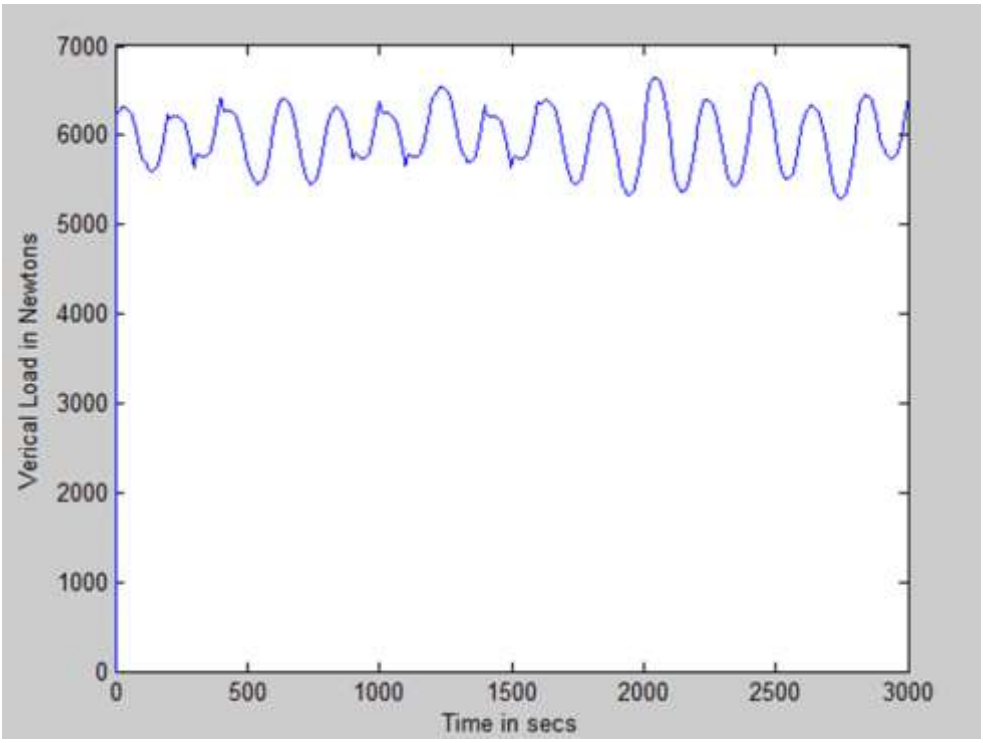

Figure 3.31: Load on suspension (N) vs time (s)

Chapter 4. DISCUSSIONS AND CONCLUSIONS

The thesis target was to build a comprehensive mathematical model which would inform about the six DOF and three Euler angles for a steering or/and acceleration or braking input. There were many assumptions in the previous published models and they need to studied and dealt with. This thesis was in the same direction and efforts were made to make it as comprehensive as possible. Besides, taking these inputs from the driver, the model was built to account for the lateral, longitudinal and vertical coupling of the vehicle dynamics in any condition and maneuver type. The model is able to meet all these requirements and deliverables successfully. It incorporates the effect of aerodynamics, takes account of load transfer both in the longitudinal and lateral direction, models suspension behavior and last but not the least mathematically formulates the effect of changing tire stiffness. However, being such a complex algorithm makes it highly prone to errors and it was imperative to simulate the results for the same input and vehicle on CarSim. When the results were compared they were appreciably same and therefore it can be safely concluded that algorithm and the built program would serve as a great tool for vehicle dynamists both in industry and academia. The focus of this thesis was to mathematically formulate the physics of vehicle dynamics as closely as possible and build a model rather than researching and using mathematical integration tools which would solve the algorithm in the best possible manner. But the author realizes and acknowledges the importance of this step. It is crucial to dwell more on what existing integration techniques would solve the problem more accurately than others. Because the results would depend on the solver used and would play a great part in deciding the use of the built model.

This algorithm can be used on any car controller for designing a control strategy for torque vectoring. This model informs about the speeds of the wheels during a turn and therefore the torque to be

provided. This can be compared to the torque being provided and a simple PID controller can regulate the working of the electronic differential.

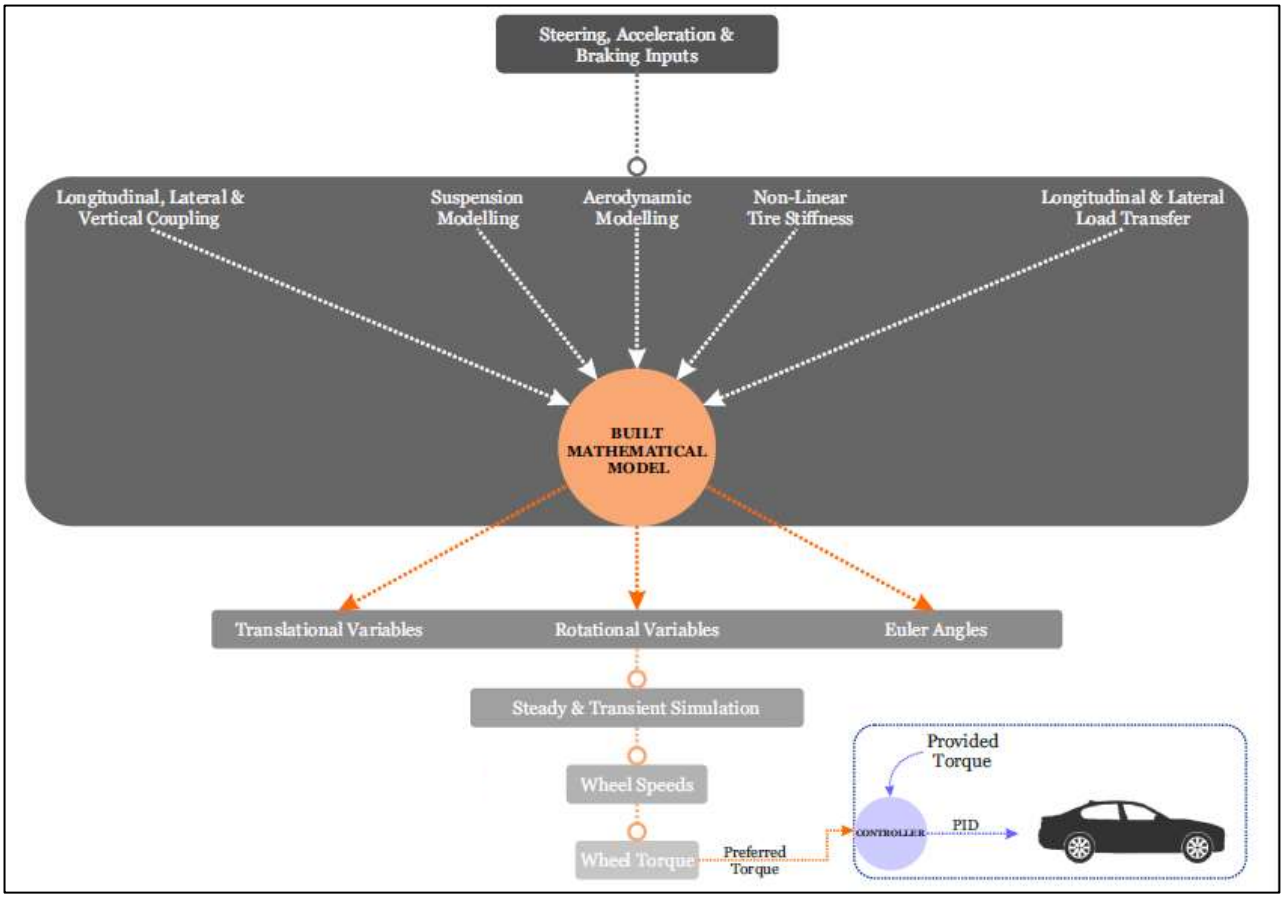

Figure 4.1: Structure of the built algorithm

References

Bastow, Donald. “Car Suspension and Handling.” Edited by Geoffrey P Howard, SAE, 1993.

Blundell, Mike and Damian Harty. “The Multibody Systems Approach to Vehicle Dynamics.” SAE International, 2004.

Campbell, Colin. “New Directions in Suspension Design: Making the Fast Car Faster.” Robert Bentley, Inc, 1981.

Dixon, John C. “Suspension Geometry and Computation.” John Wiley and Sons, 2009.

Dixon, John C. “Tires, Suspension, and Handling, Second Edition.” SAE International, 1996.

Gillespie, Thomas D. “Fundamentals of Vehicle Dynamics.” SAE, 1992.

Hibbeler, R C. “Engineering Mechanics: Dynamics, Thirteenth Edition.” Pearson Prentice Hall, 2013.

Husain, Iqbal. “Electric and Hybrid Vehicles: Design Fundamentals.” CRC Press, 2003.

Irwin, A W. “Perception, Comfort, and Performance Criteria for Human Beings Exposed to Whole Body Pure Yaw Vibration and Vibration Containing Yaw and Translational Components.” Journal of Sound and Vibration, Volume 76, Number 4, 1981, pp. 481-497.

Jazar, Reza N. “Vehicle Dynamics: Theory and Application.” Springer, 2008.

Karnopp, Dean C and Donald L Margolis. “Engineering Applications of Dynamics.” John Wiley and Sons, 2008.

Kato, Tomo and Kaoru Sawase. “Classification and Analysis of Electric-Powered Lateral Torque-Vectoring Differentials.” Journal of Automobile Engineering, 2011.

Kreyszig, Erwin. “Advanced Engineering Mathematics, Tenth Edition.” John Wiley and Sons, 2011.

Martino, Raffaele Di. “Modelling and Simulation of the Dynamic Behaviour of the Automobile.” Université de Haute Alsace - Mulhouse, 2005. English. 96

Milliken, William F and Douglas L Milliken. “Race Car Vehicle Dynamics.” SAE International, 1995.

Rajamani, Rajesh. “Vehicle Dynamics and Control.” Springer, 2006.

Rao, Singiresu S. “Mechanical Vibrations, Fifth Edition.” Pearson Prentice Hall, 2011.

Sakai, H. “Theoretical and Experimental Studies on the Dynamic Properties of Tyres Part 2: Experimental Investigation of Rubber Friction and Deformation of a Tyre.” International Journal of Vehicle Design, Volume 2, Number 2, 1981, pp.182 - 226.

Salaani, Mohamed. “Analytical Tire Forces and Moments Model with Validated Data.” SAE International, 2007.

Schmitz, David. “Modern Flight Dynamics.” McGraw-Hill Higher Education, 2011.

Serway, Raymond A and John W Jewett Jr. “Physics for Scientists and Engineers with Modern Physics, Eighth Edition.” Brooks/Cole Cengage Learning, 2010.

Sleeper, Robert K. “Tire Stiffness and Damping Determined from Static and Free-Vibration Tests.” NASA Scientific and Technical Information Office, 1980.

Society of Automotive Engineering. “Surface Vehicle Recommended Practice J670 R Vehicle Dynamics Terminology.” SAE International, 2008.

Wong, J Y. “Theory of Ground Vehicles.” John Wiley and Sons, 2008.

Appendix

First Iterative Model MATLAB Script

```
symsdt
C_Alpha_F = 3.9e4;
C_Alpha_R = 3.9e4;
m=2200;
U=2;
dt1=1;
h=0.53;
L=2.584;
a=1.446;
b=1.408;
Ixx=63;
Iyy=1049;
Izz=1550;
Ixz=-30.587;
x0=[U;0;0;0; 0; 0; 0; 0;0]
One=(-1.446*C_Alpha_F/(m*U))+(1.408*C_Alpha_R/(m*U))
Two=-(C_Alpha_F +C_Alpha_R)/(U*m)
Three=h*((1/2200)*5030)
Four=1/(1-((Ixz*Ixz)/(Ixx*Izz)));
Five=Four*(Ixz/Ixx);
Six=Four*(Ixz/Izz);
g=10;
Cd=0.31;
Surface=2.2;
Rho=1.225;
Phidot=x0(4,1)+x0(5,1)*sin(x0(7,1))*tan(x0(8,1))+x0(6,1)*cos(x0(7,1))*tan(x0(8,1));
Shidot=(x0(5,1)*sin(x0(7,1))+x0(6,1)*cos(x0(7,1)))*sec(x0(8,1));

A1=[Cd*Surface*U*Rho/m x0(6,1) -x0(5,1) 0 -x0(3,1) x0(2,1) 0 -g*cos(x0(8,1)) 0;
-x0(6,1) Two x0(4,1) x0(3,1) 0 x0(1,1)+One 0 -g*sin(x0(8,1))*sin(x0(7,1)) 0;
x0(5,1) -x0(4,1) 0 -x0(2,1) x0(1,1) 0 -g*cos(x0(8,1))*sin(x0(7,1)) -g*sin(x0(8,1))*cos(x0(7,1)) 0;
0  ((h*Two*Four/Ixx)-(Five*a*C_Alpha_F/(Izz*U))+(b*Five*C_Alpha_R/(Izz*U))) 0 Five*x0(5,1)*((Ixx-
Iyy)/Izz)+Four*Ixz*x0(5,1)/Ixx Four*Ixz*x0(4,1)/Ixx+Four*(Iyy-Izz)*x0(6,1)/Ixx+Five*-Ixz*x0(6,1)/Izz+Five*(Ixx-
Iyy)*x0(4,1)/Ixz Four*(Iyy-Izz)*x0(5,1)/Ixx+(h*One*Four/Ixx)+Five*-Ixz*x0(5,1)/Izz+(a*Five*-a*C_Alpha_F/(Izz*U))+(-
b*b*Five*C_Alpha_R/(Izz*U)) 0 0 0;
Cd*Surface*U*Rho*h/Iyy 0 0 ((Izz-Ixx)/Iyy)*x0(6,1)-2*x0(4,1)*Ixz/Iyy 0 (Izz-Ixx)*x0(4,1)/Iyy+2*Ixz*x0(6,1)/Iyy 0 -
m*h*g*cos(x0(8,1))/Iyy 0 ;
0  ((h*Two*Six/Ixx)-(Four*a*C_Alpha_F/(Izz*U))+(b*Four*C_Alpha_R/(Izz*U)))*0.1 0 Four*x0(5,1)*((Ixx-
Iyy)/Izz)+Six*Ixz*x0(5,1) Six*Ixz*x0(4,1)/Ixx+Six*(Iyy-Izz)*x0(6,1)/Ixx+Four*-Ixz*x0(6,1)/Izz+Four*(Ixx-
Iyy)*x0(4,1)/Ixz Six*(Iyy-Izz)*x0(5,1)/Ixx+(h*One*Six/Ixx)+Four*-Ixz*x0(5,1)/Izz+(a*Four*-a*C_Alpha_F/(Izz*U))+(-
b*b*Four*C_Alpha_R/(Izz*U)) 0 0 0;
0 0 0 1 tan(x0(8,1))*sin(x0(7,1)) tan(x0(8,1))*cos(x0(7,1)) tan(x0(8,1))*cos(x0(7,1))*x0(5,1)-
tan(x0(8,1))*sin(x0(7,1))*x0(6,1) (x0(5,1)*sin(x0(7,1))+ x0(6,1)*cos(x0(7,1))+(x0(7,1)-x0(4,1)))*tan(x0(8,1)) 0 ;
0 0 0 0 cos(x0(7,1)) -sin(x0(7,1)) -(x0(5,1)*sin(x0(7,1))+ x0(6,1)*cos(x0(7,1))) 0 0;
0 0 0 0 sin(x0(7,1))/cos(x0(8,1)) cos(x0(7,1))/cos(x0(8,1)) -(x0(6,1)*sin(x0(7,1))-x0(5,1)*cos(x0(7,1)))/cos(x0(8,1))
x0(9,1)*tan(x0(8,1)) 0]

B1=[5030/2200 5030/2200 5030/2200  5030/2200  0;
   0 0 0 0 C_Alpha_F/m;
   0 0 0 0 0;
   0 0 (Four*Three*h/Ixx)-(b*Five*Three/Izz) (Four*Three*h/Ixx)-(b*Five*Three/Izz) (h*Four*C_Alpha_F/Ixx+
Five*a*C_Alpha_F/Izz);
   Three/Iyy Three/Iyy Three/Iyy Three/Iyy 0;
   0 0 (Six*Three*h/Ixx)-(b*Four*Three/Izz) (Six*Three*h/Ixx)-(b*Four*Three/Izz) h*Six*C_Alpha_F/Ixx+
Four*a*C_Alpha_F/Izz;
   0 0 0 0 0;
   0 0  0  0 0;
   0 0 0 0 0 ];
C1= A1;
D1=B1;
u1=zeros(5,500)
fori=1:100
u1(5,i)= -100*(pi/180)*sin(pi*i/100);
end
fori= 101:200
u1(5,i)= -100*(pi/180)*sin(pi*i/100);
end
u1(5,127:172)=u1(5,126);
u1(5,201:500)=0;
u1(1:4,:)=randi([-10,10],[4,500])*0.09;
t= 0.01:0.01:5;
plot(t,u1(5,:))
legend('Steering Input')
sys= ss(A1,B1,C1,D1)
[y1,t1,x1]=lsim(sys,u1,t,x0)



%%Bicycle Model
C_Alpha_F = 3.9e4   %Cornering Stiffness Front Wheel (N)
C_Alpha_R = 3.9e4   %Cornering Stiffness Rear Wheels (N)
m =2200             %Mass of the vehicle (Kg)
a = 1.446           %Position of COM from Front Axle (m)
b = 1.408           %Position of COM from Rear Axle (m)
Long_Velo = 2     %Initial Longitudinal Velocity (m/sec)
I = 1549.034        %Moment of Inerita about z aixs (Kg.sq(m))
```

```
A2 = [- (C_Alpha_F+ C_Alpha_R)/(m*U) (-a*C_Alpha_F +b*C_Alpha_R)/(m*U)-Long_Velo;...
    - (-a*C_Alpha_F +b*C_Alpha_R)/(I*Long_Velo)  -(a*a*C_Alpha_F +b*b*C_Alpha_R)/(I*Long_Velo)]
B2= [C_Alpha_F/m;a*C_Alpha_F/I]
C2= A2;
D2=B2;

figure()
dt2=0.5;
t=0.01:0.01:5;
u2=u1(5,:);
x0=[0;0]
sys= ss(A2,B2,C2,D2)

[y2,t2,x2]=lsim(sys,u2,t,x0);

plot(0.1*y1(:,2),'r')
holdon
plot(0.1*y2(:,1),'k')
legend('Lateral Acceleration from Developed Model', 'Lateral Acceleration from the Bicycle Model')


figure()
plot(0.1*y1(:,6),'r')
holdon
plot(0.1*y2(:,2),'k')
legend('Change of Yaw rate from the Developed Model','Change of Yaw rate from Bicycle Model')
figure()
plot(x1(:,6),'r')
holdon
plot(x2(:,2),'k')
legend(' Yaw rate from the Developed Model','Yaw rate from Bicycle Model')

figure()
plot(y1(:,1),'r')
holdon
plot(y1(:,3),'k')
holdon
plot(y1(:,5),'b')
holdon
plot(y1(:,8),'o')
holdon
plot(y1(:,9),'y')
legend('Longitudinal Acceleration','VerticalAcceleration','Rate of Change of Pitch Rate','Rate of Change of
Attitude','Rate of Change of Heading')

figure()
plot(x1(:,1),'r')
holdon
plot(x1(:,6),'g')
holdon
plot(y1(:,9),'y')
legend('Longitudinal Velocity','Yaw Rate','Shi_dot')

figure()
plot(x1(:,2),'r')
holdon
plot(x2(:,2),'k')
legend('Lateral Velocity from the Developed Model','Lateral Velocity from Bicycle Model')

%% Torque-Vectoring
Velocity_Outer=zeros(10,1);
Velocity_Inner=zeros(10,1);
Radius=zeros(10,1);

fori=1:10
Radius(i,1)= L/sqrt(2-2*cos(u1(5,i))); % Turning radius in term of Steer Angle of the wheel
end

% Using the fact that outer velocity spans a radius of (R+trackwidth/2) and
% (R-trackwidth/2)for the inner wheel where R is the radius spanned by
% Center line of the wheel track or COM to make it more simpler.

fori=1:10
Velocity_Outer(i,1)=x1(i,1)*(1+(1.66/(2*Radius(i,1))));
Velocity_Inner(i,1)=x1(i,1)*(1-(1.66/(2*Radius(i,1))));
end

% When Radius = Inf then the vehicle is moving in a straight line and hence
% velocity of both the wheel will be equal to the longitudinal velcoity of
% the vehicle.

fori=1:10
ifVelocity_Outer(i,1)==Inf
Velocity_Outer(i,1)=x1(i,1);
end
end

plot(Velocity_Outer,'k')
```

```
holdon
plot(Velocity_Inner,'b')
holdon
plot(x1(:,1),'g')
legend('Velocity on outer, COG and inner wheels')
```

Second Iterative Model MATLAB Script

```
symsdt
m=2200; %mass of the vehicle in Kgs
Longitudinal_Velocity_Initial=16.5; % initial longitudinal velocity of the vehicle in m/sec
h=0.53;  %Height of the centre of mass of the vehicle in meters
L=2.584; % Wheel base in meters
a=1.446; % Distance of front axle from COM in m
b=1.408; % Distance of front axle from COM in m
C_Alpha_F = (3.039e3); % Lateral Stiffness of the front tires
C_Alpha_R = (3.039e3); % Lateral Stiffness of the rear tires
C_Long=(5.03e3); % Longitudinal Stiffness of the front/rear tires
x0=[Longitudinal_Velocity_Initial; 0; 0; 0; 0; 0; 0; 0;0]; %Initial states/reference condition for the vehicle
g=10; % Gravitation Constant
Cd=0.31; % Coefficient of aerodynamic drag
Surface=2.2;   %  Outer Surface Area in m^2
Rho=1.225; % Air density in kg/m^3
Phidot=x0(1,1)+x0(5,1)*sin(x0(7,1))*tan(x0(8,1))+x0(6,1)*cos(x0(7,1))*tan(x0(8,1)); %Inital rate of change of
inertial roll angle
Shidot=(x0(5,1)*sin(x0(7,1))+x0(6,1)*cos(x0(7,1)))*sec(x0(8,1)); %Inital rate of change of inertial yaw angle
r=x0(6,1); % Initial yaw rate
Trackwidth= 1.625092; %Trackwidth in m
df=Trackwidth;
dr=Trackwidth; % Considering same rear and front trackwidth
lf=a;
lr=b;
Inertia_Inverse=0.01; % inv(kg.m^2)%Tire

% Suspension Roll Stiffness and Roll Damping
K_Phi_f= 26018.6;
K_Phi_r= 34702.6;
C_Phi_f= 3450.8;
C_Phi_r= 4091.2;

dt=0.01; %Time step in secs

R=18*2.54/200; %Rolling Radius in m
Ohmega_times_Radius(1:4,1) = [Longitudinal_Velocity_Initial; Longitudinal_Velocity_Initial;
Longitudinal_Velocity_Initial; Longitudinal_Velocity_Initial];

% Steering Input
Steering_Angle=zeros(3000,1);
fori=1:3000
Steering_Angle(i,1)= (30/14)*(pi/180)*sin(pi*i/1000);
end

% Input for simulation
% Inertias
Ixx=63;
Iyy=1049;
Izz=1550;
Ixz=-30.587;
I=(Ixx*Izz-Ixz^2); %Cross intertia term arising in the state space matrix
%acceleration= zeros(3000,1);


%for i=1:100:3000
%acceleration(i:i+98,1)=randi([-10,10])*0.4;  %validate why you took these values
%end
filename='Acceleration_Storage.xlsx';
acceleration=xlsread(filename);



u=zeros(8,3000); %Initiation of the input matrix to the state space system
FZ_initial=[5372.7;5372.7;5516.4;5516.4];
FZ=[5372.7;5372.7;5516.4;5516.4]*.225;

%FZ_Full=zeros(4,100);
%FZ_Full(1:4,1)=Force_Z;
%FZ(1:4,1)=Force_Z;

% Elements of Matrix A

U=Longitudinal_Velocity_Initial;
One=(-1.446*C_Alpha_F/(m*U))+(1.408*C_Alpha_R/(m*U))
Two=-(C_Alpha_F +C_Alpha_R)/(U*m)
Three=h*((1/2200)*5030)
```

```
Four=1/(1-((Ixz*Ixz)/(Ixx*Izz)));
Five=Four*(Ixz/Ixx);
Six=Four*(Ixz/Izz);

O(1:4,1)=Ohmega_times_Radius;
d_Ohmega_R=zeros(4,3000);

V=zeros(3000,4);
V(1,:)=O(:,1)';
slip=zeros(3000,4);
% State Space Form Matrix Declaration
Y_Matrix=zeros(3000,9);
X_State_Matrix=zeros(3000,9);
X_State_Initial_Matrix(1,1:9)=x0';
X_State_Matrix(1,:)=X_State_Initial_Matrix;
alpha=zeros(4,3000);
Fx=zeros(3000,1:4);
Fy=zeros(3000,1:4);

%% Main Program

fori=1:3000
%Slip Ratio
%V_W_X_i is the velocity of the ith wheel center in the wheel heading direction
%Slip is defined as (Ohmega*Radius/V_W_X)-1
%V_WC_i= velocity of ith wheel centre
%v_x, v_y are the velocity componenets of centre of mass
%V_WC_1= (V_x - df*r/2)i + (V_y + lf*r)j
%V_WC_2= (V_x + df*r/2)i + (V_y + lf*r)j
%V_WC_3= (V_x + dr*r/2)i + (V_y - lr*r)j
%V_WC_4= (V_x - dr*r/2)i + (V_y - lr*r)j
%here df, lf, dr, lr and r are front track width, distance of COM from
%front axle, rear track width, distance of COM from
%rear axle and the yaw rate of the vehicle respectively
%V_W_X_1= (V_x - df*r/2)*cos(delta) + (V_y + lf*r)*sin(delta)
%V_W_X_2= (V_x + df*r/2)*cos(delta) + (V_y + lf*r)*sin(delta)
%V_W_X_3= (V_x + dr*r/2)
%V_W_X_4= (V_x - dr*r/2)

Phi=X_State_Matrix(i,7);

e=(X_State_Matrix(i,2)  - lf*X_State_Matrix(i,6)/2)/(X_State_Matrix(i,1)  - df*X_State_Matrix(i,6)/2);
f=(X_State_Matrix(i,2)  - lf*X_State_Matrix(i,6)/2)/(X_State_Matrix(i,1)  + df*X_State_Matrix(i,6)/2);
z=(X_State_Matrix(i,2)  + lr*X_State_Matrix(i,6)/2)/(X_State_Matrix(i,1)  + dr*X_State_Matrix(i,6)/2);
w=(X_State_Matrix(i,2)  + lr*X_State_Matrix(i,6)/2)/(X_State_Matrix(i,1)  - dr*X_State_Matrix(i,6)/2);

Alpha_1=  atan(e)-Steering_Angle(i,1);
Alpha_2=  atan(f)-Steering_Angle(i,1);
Alpha_3=  atan(z);
Alpha_4=  atan(w);

Alpha=[Alpha_1;Alpha_2;Alpha_3;Alpha_4];

V_W_X_1= (X_State_Matrix(i,1)  - df*X_State_Matrix(i,6)/2);
V_W_X_2= (X_State_Matrix(i,1)  + df*X_State_Matrix(i,6)/2);
V_W_X_3= (X_State_Matrix(i,1)  + dr*X_State_Matrix(i,6)/2);
V_W_X_4= (X_State_Matrix(i,1)  - dr*X_State_Matrix(i,6)/2);

d_Ohmega_R(1:4,i)= [537.7;537.7;551.6;551.6]*acceleration(i,1)*R*dt*Inertia_Inverse;
Ohmega_times_Radius=Ohmega_times_Radius+d_Ohmega_R(:,i)*R;
O(1:4,i+1)=Ohmega_times_Radius;
% Have to initialize V
V(i,1:4)=[V_W_X_4 V_W_X_3 V_W_X_2 V_W_X_1];

%Wheel Velocity/Longitudinal Velocity should not be less than zero
if min(O(:,i+1))<=0
O(1:4,i+1)=O(1:4,i);
acceleration(i:i+100,1)=2;
end

ifX_State_Matrix(i,1)<=0
X_State_Matrix(i,1)=X_State_Matrix(i-1,1);
acceleration(i:i+100,1)=2;
end

Slip_1= (O(1,i+1)/X_State_Matrix(i,1))-1;
Slip_2= (O(2,i+1)/X_State_Matrix(i,1))-1;
Slip_3= (O(3,i+1)/X_State_Matrix(i,1))-1;
Slip_4= (O(4,i+1)/X_State_Matrix(i,1))-1;
Slip=[Slip_1; Slip_2; Slip_3; Slip_4];

% Slip Matrix, have to initialize this matrix

slip(i,1:4)=Slip;


%Calculations
```

```
S=zeros(4,1);

for n=1:4
S(n,1) = min(abs(Slip(n,1)),0.99) * sign(Slip(n,1));
end

S %Slip
FZ2 = FZ .* FZ;
CSO= 5.03*10^3;
Eta = 0.978;
FzxO = 1.99e2;
CA1 = -2.587;
CA2 = -1.55;
CAm = 3.03e4;
Fzym = 3000;
GAMMA1 = 1.03;
GAMMA2 = 2.33;
Tz2 = -6.6e-5;
Tz1 = -8.86e-9;
m1=0.6;
mo=pi/4;
Epsx= 0.01;
Tx3 = -0.01;
Tx2 = -3.5e-6;
Tx1 = 1.844e-8;
MURATIO = 0.7/0.85;
MuxO = 1.2;
Mux1 = 0;
Mux2 = -0.04;
MuyO = 1.2;
Muy1 = -0.06;
Muy2 = -0.01;
FzmuO= 401;
DMux3= 0.11;
DMux2 = 3.4e-4;
DMux1 = -1.09e-7;
Eps_sx= 1.05;
DMUy3 = -0.01;
DMUy2 = 0.001;
DMUy1 = -4e-7;
Eps_sy=1.05;
PLYSTEER = [0.0;0.0;0.0;0.0]*pi/180;

% tire longitudinal stiffness : CSO= Tire.CSO; Eta = Tire.Eta; FzxO = Tire.FzxO;
% tire lateral stiffness :CAl = Tire.CA1; CA2 = Tire.CA2; CAm = Tire.CAm; Fzym = Tire.CAFzm;
% inc1ination ang1e 1atera1 force stiffness :GAMMAl = Tire.GAMMA1; GAMMA2 = Tire.GAMMA2;
% aligning moment pneumatic trail : Tz2 = Tire.tz2; Tzl = Tire.tzl;
% aligning moment constants ml = Tire.ml; mO = Tire.mO;
% sliding force eccentricity Epsx = Tire.Epsx;
% overturning moment arm Tx3 = Tire.Tx3; Tx2 = Tire.Tx2; Txl = Tire.Txl;
% road to test friction rate MURATIO = Tire.MUNOM / Tire.MUNTEST;
% longitudinal peak coefficient of friction MuxO = Tire.MuxO; Muxl = Tire.Muxl; Mux2 = Tire.Mux2;
% Lateral peak coefficient of friction MuyO = Tire.MuyO; Muyl = Tire.Muyl; Muy2 = Tire.Muy2;
% minimum load for valid peak friction values FzmuO = Tire.FzO;
% longitudinal sliding coefficient of friction DMUx3 = Tire.KMUx3; DMUx2= Tire.KMUx2; DMUxl = Tire.KMUxl; Eps_sx =
Tire.Lsx;
% lateral sliding coefficient of friction DMUy3 = Tire.KMUy3; DMUy2= Tire.KMUy2; DMUyl = Tire.KMUyl; Eps_sy=
Tire.Lsy;

%%%%%%% Empirical physical properties formulae %%%%%%%%%%%%%%%%%%%%%
% pneumatic trail (Equation 29)

Tz = Tz1.*FZ2 + Tz2.*FZ;

% overturning moment arm (Equation 30)
Tx = Tx1.*FZ2 + Tx2.*FZ + [Tx3; Tx3; Tx3; Tx3];

% lateral stiffness (Equation 26)
CA = CAm.* ([1;1;1;1]-exp(CA1.* (FZ./Fzym).^2 + CA2.*(FZ./Fzym)))

% longitudinal stiffness (Equation 27)
CS = CSO.*(FZ./FzxO).^Eta;

% Inclination angle lateral force stiffness (Equation 31)
FYGAMMA = GAMMA1 .* FZ + GAMMA2 .* FZ2;

% longitudinal peak coefficient of friction (Equation 22)
FZ1=zeros(4,1);
for n=1:4
if FZ(n,1) <FzmuO
FZ1(n,1) = FzmuO;
else
FZ1(n,1)= FZ(n,1);
end
end

MUXp=zeros(4,1);
```

```
for n=1:4
MUXp(n,1)=MURATIO *MuxO* ((FZ1(n,1))/FzmuO) ^(Mux2+Mux1*log((FZ1(n,1))/FzmuO));
end

% lateral peak coefficient of friction (Equation 22)
MUYp=zeros(4,1);

for n=1:4
MUYp(n,1)=MURATIO *MuyO* ((FZ1(n,1))/FzmuO)^(Muy2+Muy1*log((FZ1(n,1))/FzmuO));
end

% longitudinal decay of friction (Equation 23)
DMUx = DMux1.*FZ2 + DMux2.*FZ + [DMux3; DMux3; DMux3; DMux3];

% lateral decay of friction (Equation 23)
DMUy = DMUy1.*FZ2 + DMUy2.*FZ + [DMUy3; DMUy3; DMUy3; DMUy3] ;

% adjust for plysteer

Alpha = Alpha - PLYSTEER;
alpha(:,i)=Alpha;
S1=zeros(4,1);
% sliding coefficient of friction (Equation 24)
for k=1:4
S1(k,1)= min(1,sqrt((sin(Alpha(k,1))))^2+((S(k,1)*cos(Alpha(k,1)))^2));
end
MNUy = (MUYp.* ([1;1;1;1] - (DMUy .* S1)))*Eps_sy;
MNUx = (MUXp.* ([1;1;1;1] - (DMUx .* S1)))*Eps_sx;

% effect of slip on longitudinal stiffness
CSp = CS + (CA - CS).*S1

SIGMA=zeros(4,1);
%adhesion potential rate (Equation 11)
for n=1:4
SIGMA(n,1) = sqrt((CA(n,1)*tan(Alpha(n,1))/(1-S(n,1))/MUYp(n,1)/FZ(n,1))^2+(CS(n,1)*S(n,1)/(1-
S(n,1))/MUXp(n,1)/FZ(n,1))^2);
end

%adhesion and sliding functions (Equations 18 and 19)

SIGMA2 = SIGMA.*SIGMA;
SIGMAU = ([1;1;1;1] - SIGMA2)./([1;1;1;1] + SIGMA2);
F_a = 4/pi.*SIGMA./(SIGMA2 + [1;1;1;1]).^2;
F_s = 1/pi.*([pi/2;pi/2;pi/2;pi/2] - SIGMAU.*sqrt([1;1;1;1]-SIGMAU.^2) - asin(SIGMAU));

SIGMAm= zeros(4,1);
SIGMASm= zeros(4,1);
FY=zeros(4,1);
FX=zeros(4,1);
% lateral and longitudinal forces (Equations 14 and 15)
for n=1:4
SIGMAm(n,1) =  sqrt( (CA(n,1)* tan(Alpha(n,1))/MUYp(n,1))^2 + (CS(n,1) * S(n,1)/MUXp(n,1))^2 );
SIGMASm(n,1) = sqrt( (CA(n,1) * tan(Alpha(n,1))/MNUy(n,1))^2 +(CSp(n,1) * S(n,1)/MNUx(n,1))^2 );
if (SIGMAm(n,1) < 1.0e-6)
FY(n,1)= 0;
FX(n,1)= 0;
else
FY(n,1) = -FZ(n,1)* (CA(n,1)*tan(Alpha(n,1)) *(F_a(n,1)/SIGMAm(n,1) + F_s(n,1)/SIGMASm(n,1)));
FX(n,1) =  FZ(n,1)* (S(n,1) *(CS(n,1)*F_a(n,1)/SIGMAm(n,1) + CSp(n,1)*F_s(n,1)/SIGMASm(n,1)));

end
end

%initialize these two matrix
Fx(i,1:4)= FX;
Fy(i,1:4)= FY;
FX=FX*4.4;
FY=FY*4.4;

%% Longitudinal and Lateral Load Transfers
%Longitudinal Load Transfer
%Ffs=(1/2*L)*mglr
%Frs=(1/2*L)*mglf
%Ff=(1/2*L)*(mglr-h*F_X)
%Fr =(1/2*L)*(mglf-h*F_X)

%Lateral Load Transfer
%DelFf =1/df*(Kf*Phi_ + Cf*Phi + hf (Fside1 + Fside2)
%DelFrf =1/dr*(Kr*Phi_ + Cr*Phi + hr (Fside3 + Fside4)
%Fside1 = Fx1*sin(Delta)+ Fy1*cos(Delta) _
%Fside2 = Fx2*sin(Delta)+ Fy2*cos(Delta) _
%Fside3 = Fy3
%Fside4 = Fy4

%%Normal Forces
```

```
%Fz_1=(1/2*L)*(mglr-h*F_X)+ hf (Fside1 + Fside2)
%Fz_2=(1/2*L)*(mglr-h*F_X)+ hf (Fside1 + Fside2)
%Fz_3=(1/2*L)*(mglf-h*F_X)+ hr (Fside3 + Fside4)
%Fz_4=(1/2*L)*(mglf-h*F_X)+ hr (Fside3 + Fside4)

ifi>1
Fz_1=(1/(2*L))*(m*g*lr-h*(FX(1,1)+FX(2,1)+FX(3,1)+FX(4,1)) +
(h/df)*(FX(1,1)*sin(Steering_Angle(i,1))+FY(1,1)*cos((Steering_Angle(i,1))) +
FX(2,1)*sin(Steering_Angle(i,1))+FY(2,1)*cos(Steering_Angle(i,1))));
Fz_2=(1/(2*L))*(m*g*lr-h*(FX(1,1)+FX(2,1)+FX(3,1)+FX(4,1)) -
(h/df)*(FX(1,1)*sin(Steering_Angle(i,1))+FY(1,1)*cos((Steering_Angle(i,1))) +
FX(2,1)*sin(Steering_Angle(i,1))+FY(2,1)*cos(Steering_Angle(i,1))));
Fz_3=(1/(2*L))*(m*g*lf+h*(FX(1,1)+FX(2,1)+FX(3,1)+FX(4,1)) - (h/df)*(FY(3,1) + FY(4,1)));
Fz_4=(1/(2*L))*(m*g*lf+h*(FX(1,1)+FX(2,1)+FX(3,1)+FX(4,1)) + (h/df)*(FY(3,1) + FY(4,1)));

FZ_Full(1:4,i)=[Fz_1;Fz_2;Fz_3;Fz_4]*.225;
FZ=FZ_Full(1:4,i);
end
FZ_U=FZ*4.4;

%%
g=10;
U=Longitudinal_Velocity_Initial;
A=[Cd*Surface*U*Rho/m x0(6,1) -x0(5,1) 0 -x0(3,1) x0(2,1) 0 -g*cos(x0(8,1)) 0;
-x0(6,1) Two x0(4,1) x0(3,1) 0 x0(1,1)+One g*cos(x0(8,1))*cos(x0(7,1)) -g*sin(x0(8,1))*sin(x0(7,1)) 0;
x0(5,1) -x0(4,1) 0 -x0(2,1) x0(1,1) 0 -g*cos(x0(8,1))*sin(x0(7,1)) -g*sin(x0(8,1))*cos(x0(7,1)) 0;
0  ((h*Two*Four/Ixx)-(Five*a*C_Alpha_F/(Izz*U))+(b*Five*C_Alpha_R/(Izz*U))) 0 Five*x0(5,1)*((Ixx-
Iyy)/Izz)+Four*Ixz*x0(5,1)/Ixx Four*Ixz*x0(4,1)/Ixx+Four*(Iyy-Izz)*x0(6,1)/Ixx+Five*-Ixz*x0(6,1)/Izz+Five*(Ixx-
Iyy)*x0(4,1)/Ixz Four*(Iyy-Izz)*x0(5,1)/Ixx+(h*One*Four/Ixx)+Five*-Ixz*x0(5,1)/Izz+(a*Five*-a*C_Alpha_F/(Izz*U))+(-
b*b*Five*C_Alpha_R/(Izz*U)) 0 0 0;
Cd*Surface*U*Rho*h/Iyy 0 0 ((Izz-Ixx)/Iyy)*x0(6,1)-2*x0(4,1)*Ixz/Iyy 0 (Izz-Ixx)*x0(4,1)/Iyy+2*Ixz*x0(6,1)/Iyy 0 -
m*h*g*cos(x0(8,1))/Iyy 0 ;
0  ((h*Two*Six/Ixx)-(Four*a*C_Alpha_F/(Izz*U))+(b*Four*C_Alpha_R/(Izz*U)))*0.1 0 Four*x0(5,1)*((Ixx-
Iyy)/Izz)+Six*Ixz*x0(5,1) Six*Ixz*x0(4,1)/Ixx+Six*(Iyy-Izz)*x0(6,1)/Ixx+Four*-Ixz*x0(6,1)/Izz+Four*(Ixx-
Iyy)*x0(4,1)/Ixz Six*(Iyy-Izz)*x0(5,1)/Ixx+(h*One*Six/Ixx)+Four*-Ixz*x0(5,1)/Izz+(a*Four*-a*C_Alpha_F/(Izz*U))+(-
b*b*Four*C_Alpha_R/(Izz*U)) 0 0 0;
0 0 0 1 tan(x0(8,1))*sin(x0(7,1)) tan(x0(8,1))*cos(x0(7,1)) tan(x0(8,1))*cos(x0(7,1))*x0(5,1)-
tan(x0(8,1))*sin(x0(7,1))*x0(6,1) (x0(5,1)*sin(x0(7,1))+ x0(6,1)*cos(x0(7,1))+(x0(7,1)-x0(4,1)))*tan(x0(8,1)) 0 ;
0 0 0 0 cos(x0(7,1)) -sin(x0(7,1)) -(x0(5,1)*sin(x0(7,1))+ x0(6,1)*cos(x0(7,1))) 0 0;
0 0 0 0 sin(x0(7,1))/cos(x0(8,1)) cos(x0(7,1))/cos(x0(8,1)) -(x0(6,1)*sin(x0(7,1))-x0(5,1)*cos(x0(7,1)))/cos(x0(8,1))
x0(9,1)*tan(x0(8,1)) 0];

%%

B=(1/m)*[FX(1,1) -FY(1,1)  FX(2,1) -FY(2,1) FX(3,1) -FY(3,1) FX(4,1) -FY(4,1);
   FY(1,1)  FX(1,1)   FY(2,1) FX(2,1)  FY(3,1) FX(3,1) FY(4,1)  FX(4,1) ;
   0         0          0       0        0        0        0        0;
   (1.446*FY(1,1)+0.81*FX(1,1))*Four*Ixz/(Ixx*Izz)+(h*FY(1,1)-FZ_U(1,1)*0.81)*Four/Ixx (1.446*FX(1,1)-
0.81*FY(1,1))*Four*Ixz/(Ixx*Izz)  (1.446*FY(2,1)-0.81*FX(2,1))*Four*Ixz/(Ixx*Izz)+(h*FY(2,1)+FZ_U(2,1)*0.81)*Four/Ixx
(1.446*FX(2,1)+0.81*FY(2,1))*Four*Ixz/(Ixx*Izz) (-1.408*FY(3,1)-
0.81*FX(3,1))*Four*Ixz/(Ixx*Izz)+(h*FY(3,1)+FZ_U(3,1)*0.81)*Four/Ixx (-1.408*FX(3,1)+0.81*FY(3,1))*Four*Ixz/(Ixx*Izz)
(-1.408*FY(4,1)+0.81*FX(4,1))*Four*Ixz/(Ixx*Izz)+(h*FY(4,1)-FZ_U(4,1)*0.81)*Four/Ixx (-1.408*FX(4,1)-
0.81*FY(4,1))*Four*Ixz/(Ixx*Izz);
   0       0         0       0        0         0       0        0;
   (1.446*FY(1,1)+0.81*FX(1,1))*Four/Izz+(h*FY(1,1)-FZ_U(1,1)*0.81)*Four*Ixz/(Izz*Ixx) (1.446*FX(1,1)-
0.81*FY(1,1))*Four/Izz  (1.446*FY(2,1)-0.81*FX(2,1))*Four/Izz+(h*FY(2,1)+FZ_U(2,1)*0.81)*Four*Ixz/(Izz*Ixx)
(1.446*FX(2,1)+0.81*FY(2,1))*Four/Izz (-1.408*FY(3,1)-0.81*FX(3,1))*Four/Izz+(h*FY(3,1)+
FZ_U(3,1)*0.81)*Four*Ixz/(Izz*Ixx) (-1.408*FX(3,1)+0.81*FY(3,1))*Four/Izz (-
1.408*FY(4,1)+0.81*FX(4,1))*Four/Izz+(h*FY(4,1)-FZ_U(4,1)*0.81)*Four*Ixz/(Izz*Ixx) (-1.408*FX(4,1)-
0.81*FY(4,1))*Four/Izz;
   0         0          0       0        0        0        0        0;
   0         0          0       0        0        0        0        0;
   0         0          0       0        0        0        0        0];

u(1:8,i)=[cos(Steering_Angle(i,1)) sin(Steering_Angle(i,1)) cos(Steering_Angle(i,1)) sin(Steering_Angle(i,1)) 1 0 1 0
]';
Y_Matrix(i,1:9)=(A*X_State_Matrix(i,:)'+B*u(1:8,i))';

ifi< 3000
X_State_Matrix(i+1,1)=X_State_Matrix(i,1)+Y_Matrix(i,1)*dt;
X_State_Matrix(i+1,2)=X_State_Matrix(i,2)+Y_Matrix(i,2)*dt;
X_State_Matrix(i+1,4)=X_State_Matrix(i,4)+Y_Matrix(i,4)*dt;
X_State_Matrix(i+1,6)=X_State_Matrix(i,6)+Y_Matrix(i,6)*dt;
X_State_Matrix(i+1,7:9)=X_State_Matrix(i,7:9)+Y_Matrix(i,7:9)*dt;
end
ifi>2 &&i<3000
X_State_Matrix(i+1,3)=X_State_Matrix(i,3)-sum((((FZ_Full(1:2,i)-FZ_Full(1:2,i-1))/(dt*K_Phi_f))+((FZ_Full(3:4,i)-
FZ_Full(3:4,i-1))/(dt*K_Phi_r))));
X_State_Matrix(i+1,5)=(X_State_Matrix(i,5)-(-a*sum((FZ_Full(1:2,i)-FZ_Full(1:2,i-1)))+b*sum((FZ_Full(3:4,i)-
FZ_Full(3:4,i-1))))*dt/Iyy);
end

ifi< 3000
x0(:,1)=X_State_Matrix(i+1,:)';
end


O(1:4,i+1)=O(1:4,i+1)-Fx(i,1:4)'*R*R*dt*0.01;

end
```

Vehicle Parameters

Mercedes CLS 63 AMG

Components	Mass (kg)	Center of gravity (m)			mixi	miyi	mizi	Xi	Yi	Zi	Ixx	Iyy	Izz	Ixz
		xi	yi	zi				xi-xg	yi-yg	zi-zg	mi(Yi²+Zi²)	mi(Xi²+Zi²)	mi(Xi²+Yi²)	miXiZi
Chassis	555	1.35	0.00	0.57	749.3	0	316.35	-0.10	0.00	0.04	0.818	5.909	5.100	-2.036
Engine	200	0.24	0.00	0.58	48.0	0	116	-1.21	0.00	0.05	0.468	291.267	290.802	-11.645
Gearbox	100	0.56	0.00	0.54	56.0	0	54	-0.89	0.00	0.01	0.008	78.475	78.468	-0.734
Driver	75	1.54	-0.38	0.49	115.5	-28.5	36.75	0.09	-0.38	-0.04	11.115	0.796	11.650	-0.295
Front Right passenger	75	1.54	0.38	0.49	115.5	28.5	36.75	0.09	0.38	-0.04	10.807	0.796	11.342	-0.295
Rear left passenger	75	2.30	-0.38	0.51	172.5	-28.5	38.25	0.85	-0.38	-0.02	11.020	54.757	65.706	-1.391
Rear right passenger	75	2.30	0.38	0.51	172.5	28.5	38.25	0.85	0.38	-0.02	10.712	54.757	65.398	-1.391
Tank	80	2.56	0.00	0.32	204.8	0	25.6	1.11	0.00	-0.21	3.586	102.898	99.312	-18.871
Luggages	75	3.28	0.00	0.68	246.0	0	51.15	1.83	0.00	0.15	1.695	254.010	252.317	20.674
Spare wheel	35	3.40	0.00	0.40	119.0	0	14	1.95	0.00	-0.13	0.607	134.266	133.659	-9.009
Battery	10	-0.36	0.60	0.68	-3.6	6	6.8	-1.81	0.60	0.15	3.788	32.830	36.177	-2.678
Driver seat	25	1.59	-0.38	0.49	39.8	-9.5	12.25	0.14	-0.38	-0.04	3.705	0.563	4.181	-0.150
Front rigt passenger seat	25	1.59	0.38	0.49	39.8	9.5	12.25	0.14	0.38	-0.04	3.602	0.563	4.079	-0.150
Rear seats	35	2.37	0.00	0.52	83.0	0	18.2	0.92	0.00	-0.01	0.005	29.899	29.894	-0.379
Misc.	610	1.35	0.00	0.57	823.5	0	347.7	-0.10	0.00	0.04	0.899	6.495	5.605	-2.238
TOTAL SUSPENDED MASS	2050													
FL Wheel	45	0.00	-0.80	0.33	0	-36.0675	14.85	-1.45	-0.80	-0.20			123.171	
FR Wheel	45	0.00	0.80	0.33	0	36.0675	14.85	-1.45	0.80	-0.20			122.781	
RL Wheel	40	2.85	-0.80	0.33	114.16	-31.86	13.2	1.41	-0.80	-0.20			104.868	
RR Wheel	40	2.85	0.80	0.33	114.16	31.86	13.2	1.41	0.79	-0.20			104.523	
TOTAL NON SUSPENDED MASS	170													
TOTAL	2220				3210	6	1180				63	1048	1549	-31

Center of gravity coordinates		
xg (m)	yg (m)	zg (m)
1.45	0.00	0.53

v1	v2	m	M	Ix (kg.m²)	Iy (kg.m²)	Iz (kg.m²)	Ixz (kg.m²)	L (m)	l1 (m)	l2 (m)	h (m)
0.797	0.8015	2050	2220	62.834	1048.280	1549.034	-30.587	2.854	1.446	1.408	0.53
Half-track (m)		Susp Mass. (kg	Total Mass (kg	Inertia				Wheelbase			CG height

Frequency (Hz)	f1	1.2
	f2	1.35
Epsilon (0,35 confort 0,7 sport)	ε	0.5

Front wheel static vertical load (N)	PS1	5372.7
Rear wheel static vertical load (N)	PS2	5516.4
Vertical Wheel Stiffness (N/m)	K1	26018.6
	K2	34702.6
Damping (N/m/s)	R1	3450.8
	R2	4091.2

Mass Bias (Front)	0.493	
m1 (kg)	1095.4	
m2 (kg)	1124.6	
g (m/s²)	9.81	
Aerodynamic	S (m²)	2.2
	Cx	0.31
	S.Cx	0.69

Front axle	ms1 (kg)	457.7
	mns1 (kg)	90.0
Rear axle	ms2 (kg)	482.3
	mns2 (kg)	80